

A MODEL FOR LUMPING ATMOSPHERIC SECONDARY ORGANIC AEROSOL  
AND ITS APPLICATION IN AIR QUALITY MODELING

By

Fei Bian

Dissertation

Submitted to the Faculty of the  
Graduate School of Vanderbilt University  
in partial fulfillment of the requirements

for the degree of

DOCTOR OF PHILOSOPHY

in

Chemical Engineering

August, 2005

Nashville Tennessee

Approved:

Professor Frank M. Bowman

Professor G. Kane Jennings

Professor Robert D. Tanner

Professor Alan R. Bowers

Professor Karl B. Schnelle, Jr.

To my dearest mother,  
for the many years of unconditional love, understanding and support

## ACKNOWLEDGMENTS

I would like to especially express my gratitude to my advisor, Dr. Frank Bowman, for his support, patience, and encouragement. He guided me throughout my doctoral work, encouraged me to develop independent thinking and research skills, and helped me in improving my technical writing and presentation skills. His suggestions and careful reviews of this dissertation have improved it greatly.

I also want to thank all the members in my advisory committee, Dr. Karl Schnelle, Dr. Robert Tanner, Dr. G. Kane Jennings, and Dr. Alan Bowers, for their valuable comments and encouragement during the development of this dissertation.

I would also like to thank the faculty and staff in the Department of Chemical Engineering at Vanderbilt University for their help during my graduate studies at Vanderbilt.

I am also grateful to the financial support from the National Science Foundation under Grant ATM-9985108 for this project, and from the Department of Chemical Engineering.

Finally, and most importantly, I would like to thank my mother, whose constant love and support have sustained me through my life.

## TABLE OF CONTENTS

	Page
DEDICATION .....	ii
ACKNOWLEDGEMENTS .....	iii
LIST OF TABLES .....	vi
LIST OF FIGURES .....	viii
 Chapter	
I. INTRODUCTION .....	1
II. BACKGROUND AND THEORY .....	4
Atmospheric Aerosols .....	4
Secondary Organic Aerosol .....	6
Absorption Partitioning .....	9
Secondary Organic Aerosol Yield .....	12
SOA Precursors and Identified Products .....	14
III. THEORETICAL METHOD FOR LUMPING MULTICOMPONENT SECONDARY ORGANIC AEROSOL MIXTURES .....	18
Abstract .....	18
Introduction .....	19
Theory .....	22
<i>Absorption Partitioning</i> .....	22
<i>Lumping Equations</i> .....	24
Results .....	26
<i>Base Case Mixture</i> .....	26
<i>Random Mixtures</i> .....	32
<i>Temperature Dependence</i> .....	34
<i><math>\alpha</math>-Pinene/O<sub>3</sub> Product Mixture</i> .....	36
IV. A LUMPING MODEL FOR COMPOSITION- AND TEMPERATURE- DEPENDENT PARTITIONING OF SECONDARY ORGANIC AEROSOLS .....	43
Abstract .....	43
Introduction .....	44

Theory .....	46
<i>Absorption Partitioning</i> .....	46
<i>Lumping Procedure</i> .....	48
<i>Lumping Equations</i> .....	49
<i>Lumping Criteria</i> .....	50
Lumping Model Evaluations.....	52
<i>Base Case Mixture</i> .....	52
<i>Random Mixtures</i> .....	57
<i>Absorbing Aerosol Mixtures</i> .....	57
<i><math>\alpha</math>-Pinene/O<sub>3</sub> Product Mixture</i> .....	59
Results.....	61
<i>Base Case Mixture</i> .....	61
<i>Random Mixtures</i> .....	65
<i><math>\alpha</math>-Pinene/O<sub>3</sub> Products</i> .....	66
Conclusions.....	67
V.    DEVELOPING PARTITIONING PARAMETERS OF SOA PRODUCTS FROM MULTIPLE HYDROCARBON PRECURSORS FOR USE IN THE CMAQ AIR QUALITY MODEL .....	69
Introduction.....	69
Current Representation of SOA in CMAQ.....	71
Formulating New SOA Precursors and Products.....	74
<i>Biogenics (TRP1)</i> .....	77
<i>High Yield Aromatics (ARO1)</i> .....	80
<i>Low Yield Aromatics (ARO2)</i> .....	83
<i>Internal Alkenes (OLE2)</i> .....	84
<i>Long Alkanes (ALK5)</i> .....	86
<i>Lumped Groups</i> .....	88
Evaluation of Updated SOA Parameters.....	91
<i>Biogenics (TRP1)</i> .....	92
<i>High Yield Aromatics (ARO1)</i> .....	93
<i>Low Yield Aromatics (ARO2)</i> .....	94
<i>Internal Alkenes (OLE2)</i> .....	95
<i>Long Alkanes (ALK5)</i> .....	97
VI.    SUMMARY AND CONCLUSION .....	99
REFERENCES .....	102

## LIST OF TABLES

Table	Page
2.1 Major SOA products from cyclohexene (Kalberer et al., 2000) .....	18
3.1 Base case mixture properties and lumped group assignments .....	27
3.2 Base case mixture lumped group properties .....	29
3.3 $\alpha$ -Pinene/O <sub>3</sub> product mixture properties and lumped group assignments .....	37
3.4 Experimental and theoretical organic aerosol mass for $\alpha$ -Pinene/O <sub>3</sub> chamber experiments .....	38
3.5 $\alpha$ -Pinene/O <sub>3</sub> product mixture lumped group properties .....	39
3.6 Organic aerosol mass and error for $\alpha$ -Pinene/O <sub>3</sub> product mixture lumped groups .....	40
4.1 Base case mixture component properties and lumped group assignments .....	53
4.2 Base case mixture lumped group properties .....	56
4.3 Absorbing aerosol mixtures .....	58
4.4 $\alpha$ -Pinene/O <sub>3</sub> product mixture properties and lumping assignments .....	60
4.5 RMS errors in aerosol yield for base case mixture and random mixtures .....	64
4.6 Experimental and predicted organic aerosol mass for $\alpha$ -Pinene/O <sub>3</sub> product mixture .....	66
5.1 Current SOA precursors and partitioning parameters in CMAQ (EPA, 2004) .....	74
5.2 SOA products and individual partitioning properties for monoterpenes (TRP1) .....	78
5.3 Chemical structure of individual SOA components for monoterpenes (TRP1) ....	79
5.4 SOA products and individual partitioning properties for high-yield aromatics (ARO1) .....	81
5.5 Chemical structure of individual SOA components for	

	high-yield (ARO1) and low-yield (ARO2) aromatics .....	82
5.6	SOA products and individual partitioning properties for low-yield aromatics (ARO2).....	83
5.7	SOA products and individual partitioning properties for internal alkenes (OLE2).....	85
5.8	Chemical structure of individual SOA components for internal alkenes (OLE2).....	85
5.9	SOA products and individual partitioning properties for long alkanes (ALK5).....	86
5.10	Chemical structure of individual SOA components for long alkanes (ALK5).....	87
5.11	Partitioning properties of lumped groups .....	89
5.12	UNIFAC structural properties of lumped groups .....	90

## LIST OF FIGURES

Figure	Page
2.1	Vapor pressures of volatile, semivolatile, and nonvolatile organic products ..... 8
2.2	Aerosol yield, $Y$ , as a function of absorbing aerosol mass $M_o$ for $\alpha$ -pinene and ozone reaction..... 14
3.1	Base case mixture organic aerosol yield as a function of temperature and organic aerosol mass ..... 28
3.2	Base case mixture organic aerosol yield predictions as a function of organic aerosol mass using 1, 2, 3 and 4 lumped groups. $T = T^* = 25$ °C ..... 29
3.3	Base case mixture organic aerosol yield predictions as a function of temperature using 1, 2, 3 and 4 lumped groups. (a) $M_o = 20$ $\mu\text{g m}^{-3}$ , (b) $M_o = M_o^* = 10$ $\mu\text{g m}^{-3}$ , (c) $M_o = 1$ $\mu\text{g m}^{-3}$ ..... 31
3.4	Recommended $K_i M_o^*$ dividing lines for assigning mixture components to lumped groups..... 33
3.5	Average RMS error in random mixture yield predictions as a function of temperature using 1, 2, 3 and 4 lumped groups. $M_o = 0$ - $20$ $\mu\text{g m}^{-3}$ ..... 34
3.6	$\ln(K)$ as a function of $1/T$ for base case mixture lumped into a single group. $M_o = M_o^* = 10$ $\mu\text{g m}^{-3}$ ..... 35
4.1	Organic aerosol yield predictions as a function of organic aerosol mass for full 16-component base case mixture. Ideal case and absorption into wood smoke and diesel soot at 0% and 80% relative humidity..... 59
4.2	Organic aerosol yield predictions as a function of organic aerosol mass for lumped base case mixture using 1-4 vapor pressure lumped groups: (a) wood smoke at 0% RH, (b) wood smoke at 80% RH, (c) diesel soot at 0% RH, (d) diesel soot at 80% RH ..... 61
4.3	Organic aerosol yield predictions as a function of organic aerosol mass for lumped base case mixture using different lumping criteria: (a) wood smoke at 0% RH, (b) wood smoke at 80% RH, (c) diesel soot at 0% RH, (d) diesel soot at 80% RH ..... 63



5.1	Comparison of predicted and measured organic aerosol yields as a function of organic aerosol mass for biogenic monoterpenes.....	92
5.2	Comparison of predicted and measured organic aerosol yields as a function of organic aerosol mass for high-yield aromatics.....	93
5.3	Comparison of predicted and measured organic aerosol yields as a function of organic aerosol mass for low-yield aromatics.....	95
5.4	Comparison of predicted and measured organic aerosol yields as a function of organic aerosol mass for internal alkenes, at $M_o = 0 - 20 \mu\text{g}/\text{m}^3$ .....	96
5.5	Comparison of predicted and measured organic aerosol yields as a function of organic aerosol mass for internal alkenes, at $M_o = 0 - 140 \mu\text{g}/\text{m}^3$ .....	96
5.6	Comparison of predicted and measured organic aerosol yields as a function of organic aerosol mass for long alkanes.....	97

## CHAPTER I

### INTRODUCTION

Atmospheric aerosols are small solid or liquid particles suspended in the atmosphere. In recent years, the great impacts of these fine particles on atmospheric chemistry, climate change, air pollution, and human health have brought increasing attention and become an important area of study. Atmospheric aerosol can be classified as primary or secondary based on its origin. Primary aerosol is directly emitted into the atmosphere, while secondary aerosol is formed through atmospheric chemical reactions. Secondary organic aerosol (SOA) is produced by atmospheric oxidation of volatile organic compounds (VOC), emitted from both natural and anthropogenic sources. Semivolatile reaction products then partition from the gas phase to the aerosol phase and form secondary organic aerosol. SOA is a major contributor to the fine particulate burden in both urban and rural atmospheres (Castro et al, 1999; Brown et al., 2002; Lim and Turpin, 2002), and contributes to a range of adverse health effects (Pope et al., 1995; Donaldson et al., 1998; Pope, 2000), visibility reduction (Eldering and Cass, 1996; Kleeman et al., 2001), and global climate change (Pilinis et al., 1995; Kanakidou et al., 2004; Maria et al., 2004). Its importance is now well recognized, but many questions remain concerning its formation and processing in the atmosphere.

To understand the sources and formation mechanisms of aerosols, a combination of laboratory studies (e.g., Griffin et al., 1999; Kleindienst et al., 1999; Kalberer et al., 2004), modeling approaches (e.g., Pun et al., 2003; Zhang et al., 2004), and field

measurements (e.g., Leaitch et al., 1999; Edney et al., 2003; Tanner et al., 2004) are necessary. However, the study of particulate matter has been limited by difficulties in identification and characterization of atmospheric aerosols. Therefore, theoretical predictions become particularly useful tools for studying aerosol properties and atmospheric processes. To describe the formation and evolution of air pollutants in the atmosphere on urban and regional scales, air quality models such as EPA's Community Multi-scale Air Quality (CMAQ) model (EPA, 1999) are used.

Incorporating aerosol particles into an air quality model is a big challenge. Ambient atmospheric aerosols are a very complicated system and the aerosol module within an air quality model should be able to appropriately represent aerosol chemistry and dynamics. There are hundreds of different biogenic and anthropogenic aerosol precursors in the atmosphere, each producing dozens of individual aerosol products. To identify and include all SOA precursors and products in air quality models is a nearly impossible task. Therefore, simplification is needed for the representation of SOA in air quality models.

Because SOA formation and gas-aerosol partitioning is very complicated and involves a large quantity of individual organic components, a practical solution is to reduce the multicomponent mixture of hundreds of components to a system of a few lumped compounds that approximates the properties of the detailed mixture. Experimentally derived simplifications are useful for illuminating mixture partitioning behavior in general, but because they provide little insight into the properties of individual mixture components and are only applicable to the specific experimental conditions, they are unlikely to provide a fundamental understanding of partitioning

behavior. Therefore, developing an approach to lumping SOA mixtures from the general theoretical view is of significant importance.

The objective of this research is to gain a more detailed understanding of how the observed partitioning behavior of secondary organic aerosol mixtures is related to the properties of individual organic aerosol components, particularly concerning temperature and composition dependence. The main approach is to develop and apply a detailed theoretical model of partitioning for organic aerosol mixtures that will relate the partitioning properties of the overall mixture to those of individual components.

The dissertation is organized as follows. Chapter II describes in detail the background and significance of this research. Chapter III presents a new theoretical method for lumping SOA mixtures into a small number of model compounds, explores the relationship between the properties of lumped compounds and mixture components, investigates the influence of temperature dependence, and validates the theoretical mixture partitioning predictions with experimental data. Chapter IV describes an improved lumping method that incorporates composition effects, develops a new set of lumping equations, presents several potential new lumping criteria, and compares partitioning predictions with available experimental data. Chapter V investigates the aerosol partitioning properties of aerosol mixtures produced by multiple hydrocarbon precursors, and formulates parameters appropriate for representing biogenic and anthropogenic atmospheric organic aerosols in three-dimensional air quality models. Chapter VI summarizes the results of these studies, presents overall conclusions, and provides suggestions for future work.

## CHAPTER II

### BACKGROUND AND THEORY

#### Atmospheric Aerosols

Aerosol is defined as fine solid or liquid particles suspended in the atmosphere (Seinfeld and Pandis, 1998). These particles can be in either liquid phase, or solid phase, or even a mixture of these two phases. Atmospheric aerosol particles contain a variety of chemical components such as sulfates, nitrates, ammonium, organic material, crustal species, sea salt, hydrogen ions, and water. Aerosols have a number of properties such as size, concentration, hygroscopicity, density and shape that are important for describing their behavior. Among these properties, size is of significant importance. Atmospheric particles range in size from a few nanometers (nm) to a hundred micrometers ( $\mu\text{m}$ ) in diameter. Particle size is normally used to classify atmospheric aerosol because it is most easily measured and is related to almost all other properties (Jacobson, 1998; Seinfeld and Pandis, 1998).

Atmospheric aerosol has a great impact on the environment and people's daily life. That's why it has been studied by researchers and scientists with great interest for the past several decades. Aerosol particles contribute to various environmental problems such as visibility degradation, property damage, acid rain, and global warming (Seinfeld and Pandis, 1998). As a major pollutant in urban atmospheres, aerosol is also harmful to human health. Scientific studies have shown that there is a significant association between exposures to particulate matter and adverse effects on human health (Pope et al., 1995;

Donaldson et al., 1998). Although work is ongoing to determine the exact mechanisms by which particulate matter affects people's health, research has shown that aerosol has both short-term and long-term effects on the respiratory system, pulmonary function and cardiovascular system (Kunzli et al., 2000; Pope, 2000). The composition and nature of aerosols from natural sources and anthropogenic sources vary greatly. But no matter from which sources, all aerosols appear to cause damage when they are inhaled and go deep into the human body (Phalen, 1998). These facts of aerosols make the control and reduction of particulate matter pollution an important issue.

There are two sources for aerosol particles in the atmosphere: natural sources and anthropogenic sources. Natural sources include soil and rock debris (terrestrial dust), volcanic action, sea spray, biomass burning, reactions between natural gaseous emissions, etc. (Jacobson, 1998; Seinfeld and Pandis, 1998). Emissions of particulate matter from anthropogenic activities are primarily from four source categories: fuel combustion, industrial processes, nonindustrial fugitive sources (roadway dust from paved and unpaved roads, wind erosion of cropland, constructions, etc.), and transportation sources (automobiles, etc.) (Seinfeld and Pandis, 1998). Aerosols are generated from all these sources and contribute to the particulate matter levels in the atmospheric pollution of both urban and rural areas. Particles do not stay in the atmosphere indefinitely. Once emitted to the atmosphere, they will be removed through both dry and wet deposition, such as gravitational settling and precipitation. Average lifetimes of aerosols in the atmosphere are a few days to a week, depending on their size and location (Jacobson, 1998).

Aerosol can be classified as primary or secondary. Primary aerosols are particles that are directly emitted into the atmosphere. Secondary aerosols are generated by

physical and chemical processes in the atmosphere. Examples of primary aerosol are soil dust, soot particles from combustion, sea salt particles, volcanic dust and industrial dust (Jacobson, 1998). Secondary aerosols are often produced by condensation processes by gas-to-particle conversion, which is a ubiquitous process in the atmosphere (Seinfeld and Pandis, 1998).

Aerosol material can be either organic or inorganic. The inorganic components are mainly sulphuric acid, ammonium bisulphate, and ammonium nitrate that are formed from the oxidation of sulphur and nitrogen oxides (Seinfeld and Pandis, 1998). A considerable fraction (10%-60%) of atmospheric aerosol consists of organic compounds (Seinfeld and Pandis, 1998). Organic aerosol chemistry, however, is not as well understood as that of the inorganic compounds. Organic aerosol consists largely of organic compounds derived from the oxidation of both natural and anthropogenic hydrocarbons. There are hundreds of individual organic species in atmospheric aerosol that are hard to identify and characterize with current analytical methods (Turpin et al., 2000). This difficulty makes the formation of secondary organic aerosol material only partially understood. Much of the current work in aerosol research is focused on the formation and growth of secondary aerosol particles.

### Secondary Organic Aerosol

Secondary organic aerosol (SOA) is produced by atmospheric oxidation of volatile organic compounds (VOC). VOCs are emitted from both natural and anthropogenic sources and include alkanes, alkenes, aromatics and phenols (Jacobson, 1998). SOA is a major contributor to the fine particulate burden in both urban and rural

atmospheres (Turpin and Huntzicker, 1995). Studies have shown that SOA comprises from 20-70% of fine organic particulate matter, which accounts for approximately 25% of fine particle mass on average in a polluted urban atmosphere (Blando et al., 1998). Even in what are considered as pristine rural locations, SOA is produced from natural organic sources (Day et al., 1997).

SOA is formed when volatile organic compounds (VOC) are oxidized by  $O_3$ ,  $NO_3$  and OH in the atmosphere, creating volatile, semivolatile and nonvolatile organic products. Varied standards are used to define the volatility of a compound for different purposes of applications. A compound can be classified with different volatility for specific environmental standards. For example, one of the VOCs, methanol, is considered as nonvolatile organic compounds in treated waters. In this study, vapor pressure is considered as the determination factor to define the volatility of a compound. There are various definitions of semivolatile organic compounds (SVOC). Usually compounds with a saturated vapor pressure at 25°C between  $10^{-1}$  and  $10^{-7}$  torr are called SVOC (EPA, 1988). Figure 2.1 compares the vapor pressures of the semivolatile products from the reaction of  $\alpha$ -pinene and  $O_3$ , along with a few other organic compounds. The compounds with higher vapor pressures, such as methanol, are considered volatile, while the compounds with lower vapor pressures are considered nonvolatile.

The semivolatile organic compounds then partition from the gas phase to the aerosol phase and form secondary organic aerosol (Odum et al., 1996). To enable them to partition into the aerosol phase, the oxidation products must have sufficiently low vapor pressures. SOA is generally formed only from the oxidation of hydrocarbon molecules



containing seven or more carbon atoms (Odum et al., 1997b). However, recent studies suggest that heterogeneous reactions may increase the partitioning of gas-phase organics

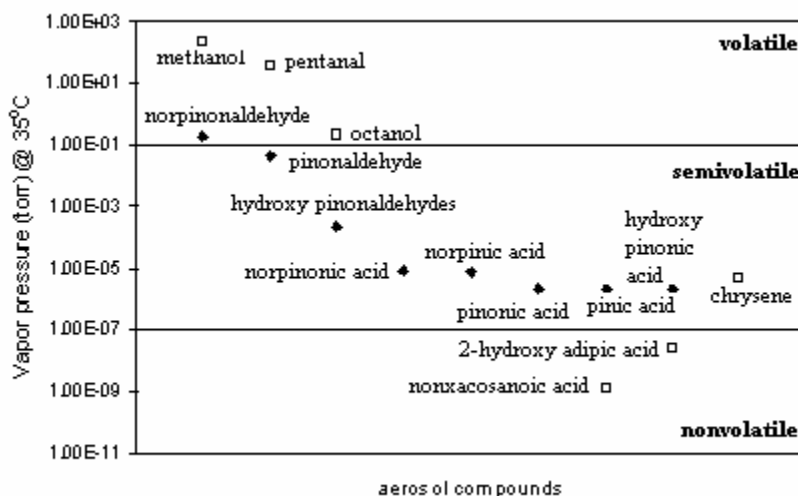


Figure 2.1. Vapor pressures of volatile, semivolatile, and nonvolatile organic products.

into the particle phase, so that even relatively low molecular weight organics may contribute to SOA formation (Jang et al., 2002; Claeys, et al., 2004).

The secondary aerosol formation and partitioning process may involve both adsorption and absorption mechanisms. In adsorption, gas partitions to the surface of a particle already present in the atmosphere. The interactions between adsorbed molecules and the particle surface are complex, involving both physical and chemical forces (Cousins 2001). The adsorption process involves first the partial covering of the particle surface with vapor molecules, leading to the formation of a monolayer, occasionally followed by the formation of additional layers. Mono- and multilayer adsorption processes often have different characteristics, because in the former the adsorbed

molecules interact directly with the particle surface, whereas in the latter they interact mainly with already adsorbed molecules (Goss, 1998; Lazaridis, 1999).

Partitioning also occurs via absorption. In this mechanism, SOA is formed by the absorption of semivolatile products into an existing condensed organic phase, and is governed by the gas-particle equilibrium between the species in the gas phase and the condensed organic phase. The process of gas-particle absorptive partitioning can be represented using the absorption model of Pankow (Pankow, 1994a, 1994b). In urban areas where particulate material generally contains a significant amount of amorphous organic carbon, the absorption mechanism dominates gas-particle partitioning of semivolatile VOCs (Liang et al., 1997; Mader and Pankow, 2002). A great many smog chamber experiments have been performed to study SOA formation and their results also indicate that an absorption partitioning mechanism successfully describes SOA gas/particle equilibrium (e.g., Odum et al., 1996; Hoffmann et al., 1997; Jang et al, 1997; Odum et al., 1997b; Griffin et al., 1999; Cocker III, et al, 2001a). Therefore, the Pankow absorption model is used as the basis of this SOA gas-particle partitioning study.

#### Absorption Partitioning

The gas/particle partitioning process can be described by a characteristic parameter  $K_p$ , the partitioning coefficient (Yamasaki et al., 1982; Pankow, 1991, 1994)

$$K_p = \frac{F / TSP}{A} \quad (2.1)$$

where  $K_p$  ( $\text{m}^3 \mu\text{g}^{-1}$ ) is a temperature-dependent partitioning constant,  $TSP$  ( $\mu\text{g m}^{-3}$ ) is the concentration of total suspended particles, and  $F$  ( $\text{ng m}^{-3}$ ) and  $A$  ( $\text{ng m}^{-3}$ ) are the particulate-phase and gas-phase concentrations of the compound of interest, respectively.

Pankow (1994) was one of the first to suggest that phase partitioning of an absorptive nature also plays an important role for organic aerosols. In presenting a new gas/aerosol absorptive partitioning model, Pankow pointed out that even when the gas-phase partial pressure of an organic compound is less than its saturation vapor pressure, it can still partition into the aerosol phase (Pankow, 1994). An important part of Pankow's work was to derive an expression for the absorption partitioning coefficient

$$K_p = \frac{760 f_{om} 10^{-6} RT}{MW_{om} \zeta_i p_i^o} \quad (2.2)$$

In equation 2.2,  $f_{om}$  is the mass fraction of TSP that is organic matter,  $R$  the ideal gas constant ( $8.206 \times 10^{-5} \text{ m}^3 \text{ atm mol}^{-1} \text{ K}^{-1}$ ),  $T$  the temperature (K),  $MW_{om}$  the molecular weight of the absorbing aerosol ( $\text{g mol}^{-1}$ ),  $\zeta_i$  the activity coefficient of species  $i$ ,  $p_i^o$  the vapor pressure of species  $i$  as a pure liquid (atm), and  $10^{-6}$  is a conversion factor ( $\text{g } \mu\text{g}^{-1}$ ). The absorption partitioning coefficient can be written in a slightly different form as (Bowman et al., 1997)

$$K_i = \frac{10^{-6} RT}{MW \zeta_i p_i^o} \quad (2.3)$$

where  $K_i$  ( $\text{m}^3 \mu\text{g}^{-1}$ ) is defined as the ratio of aerosol-phase concentration  $A_i$  ( $\mu\text{g m}^{-3}$ ) and gas-phase concentration  $G_i$  ( $\mu\text{g m}^{-3}$ ), normalized by the total concentration of absorbing organic material,  $M_o$  ( $\mu\text{g m}^{-3}$ ), present in the aerosol phase (Odum et al., 1996),

$$K_i = \frac{A_i}{G_i M_o} \quad (2.4)$$

As can be seen from equations 2.2 and 2.3, the absorptive partitioning coefficient is predicted to be a function of temperature, vapor pressure, and composition of the absorbing aerosol phase. In addition to the temperature term represented explicitly in equation 2.3, vapor pressure is highly dependent on temperature. According to the Clausius-Clapeyron equation (Atkins, 1990), this dependence is represented by

$$p_i^\circ = C_i \exp\left(\frac{-H_i}{RT}\right) = C_i \exp\left(\frac{-B_i}{T}\right) \quad (2.5)$$

where  $C_i$  (atm) is the pre-exponential constant of product  $i$ ,  $H_i$  (kJ mol<sup>-1</sup>) is the enthalpy of vaporization of product  $i$ , and  $B_i$  (K) is the term  $H_i/R$ . The composition of the absorbing aerosol mixture affects the partitioning coefficient through the activity coefficient and the mean molecular weight.

Numerous laboratory and field studies have confirmed this dependence on temperature and aerosol composition. (Jang et al., 1997; Jang and Kamens, 1998; Kaupp et al., 1999; Leach et al., 1999; Takekawa et al., 2003; Saathoff et al., 2004). For instance, Takekawa et al. (2003) performed smog chamber experiments to investigate the temperature dependence of SOA formation from three aromatic hydrocarbons (toluene, m-xylene and 1,2,4-trimethylbenzene), one biogenic alkene ( $\alpha$ -pinene) and one alkane (n-undecane) at 283 K and 303 K. Results indicate that at a lower temperature, a higher SOA yield was obtained with a higher concentration of SOA generated. Saathoff et al. (2004) investigated SOA formation from the ozonolysis of  $\alpha$ -pinene and limonene at temperatures between 253 and 313 K. The aerosol yields were shown to be a function of temperature and aerosol mass. Jang et al. (1997) studied the effects of vapor pressure and activity coefficient of organic compounds on gas/particle partitioning. Other laboratory and theoretical work (Edney et al., 2000; Ansari and Pandis 2000; Cocker et al., 2001b,

2001c; Tobias 2000) has explored the influence of humidity on SOA partitioning, with discoveries that the presence of water can increase the SOA yield since a high relative humidity increases the amount of absorbing aerosol mass. There is also evidence that the composition of aerosols changes with temperature (Jang and Kamens, 1998).

Recent computer models of organic aerosol partitioning have begun to account for temperature and composition effects (Griffin et al., 2002; Pun et al., 2002; Xia et al., 2004). Griffin et al. (2002) and Pun et al. (2002) developed a model that predicts SOA formation based on the thermodynamic equilibrium partitioning of secondary organic oxidation products, and consists of both hydrophobic and hydrophilic components. Xia et al. (2004) are developing an aerosol module integrated into a Canadian 3D regional air quality model, MC2AQ, that includes the temperature effect for saturation vapor pressure, activity coefficients and the effect of water uptake. The current version of EPA's CMAQ model accounts for temperature effects, however, the activity coefficient for all compounds is assumed to be constant and composition effects on SOA partitioning process are not considered. Moreover, CMAQ uses empirically derived partitioning parameters based on measured laboratory SOA yields. While the empirical representation can successfully fit laboratory data, it is not a suitable method to predict the more complex atmospheric system because it provides limited insight to the properties of the individual SOA products. Moreover, they can only represent the specific mixture and reaction conditions in the experiments they were measured. A representation of SOA partitioning with more accurate parameters for modeling the complicated atmospheric system is needed.

## Secondary Organic Aerosol Yield

Secondary organic aerosol is created when hydrocarbons are oxidized in the atmosphere forming numerous semivolatile products that partition into the aerosol phase. The SOA forming potential of a hydrocarbon is characterized by its aerosol yield,  $Y$ ,

$$Y = \frac{\Delta M_o}{\Delta HC} = \frac{\sum_i A_i}{\Delta HC} \quad (2.6)$$

where  $\Delta HC$  ( $\mu\text{g m}^{-3}$ ) is the amount of hydrocarbon that reacts,  $\Delta M_o$  ( $\mu\text{g m}^{-3}$ ) is the organic aerosol mass produced by the hydrocarbon, and  $A_i$  ( $\mu\text{g m}^{-3}$ ) is the aerosol-phase concentration of semivolatile product  $i$ . Therefore, yield is a measure of the amount of aerosol mass that is formed when a given amount of parent hydrocarbon is oxidized. To measure SOA yields, numerous smog chamber experiments have been conducted in recent years for a variety of hydrocarbon precursors (e.g., Izumi and Fukuyama, 1990; Forstner et al., 1997a, 1997b; Odum et al., 1997; Strader et al., 1999; Yu et al., 1999; Cocker III et al., 2001b, 2001c; Jang and Kamens, 2001; Takekawa et al., 2003; Kalberer et al., 2004).

Based on the theoretical work of Pankow (1994), Odum et al., (1996) developed a gas/particle absorptive partitioning model to explain measured experimental data of aerosol yields

$$Y = M_o \sum_i \frac{\alpha_i K_i}{1 + K_i M_o} \quad (2.7)$$

Equation 2.3 shows that for absorptive partitioning, the yield depends on the amount of absorbing aerosol mass,  $M_o$ , present. This relation between the aerosol yield and the absorbing aerosol mass has been verified by smog chamber experimental data (e.g., Odum, 1996; Hoffmann et al., 1997; Griffin et al., 1999), and is illustrated in Figure 2.2

for the case of the  $\alpha$ -pinene and ozone reaction. Thus, the SOA yield of a given hydrocarbon will vary with  $M_o$ ,  $T$ , and aerosol composition, and will depend on the values of the partitioning parameters of each oxidation product.

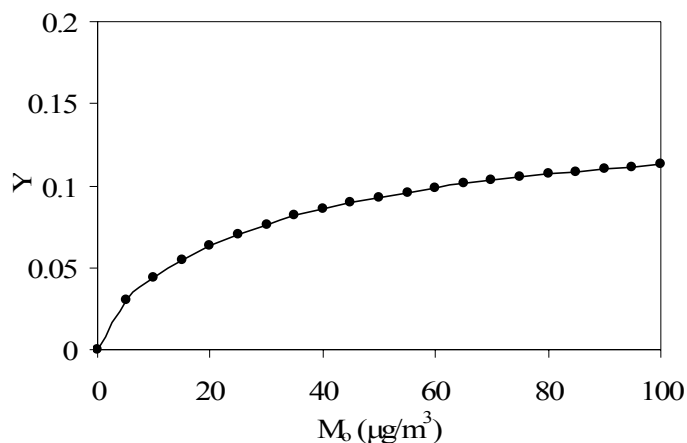


Figure 2.2. Aerosol yield,  $Y$ , as a function of absorbing aerosol mass  $M_o$  for  $\alpha$ -pinene and ozone reaction.

### SOA Precursors and Identified Products

SOA is formed from hydrocarbon precursors from natural or anthropogenic sources, oxidized by photochemical oxidants, such as hydroxyl radicals (OH), ozone ( $\text{O}_3$ ) and nitrate radicals ( $\text{NO}_3$ ). Biogenic emissions are a significant source of secondary organic particulate matter in both rural and urban areas (Sillman, 1999; Guenther et al., 2000). The majority of these emissions are isoprene, monoterpenes, and sesquiterpenes. Isoprene is the biogenic compound emitted in the greatest amounts, but had been shown not to produce organic aerosol under ambient conditions (Pandis et al., 1991). Recent studies, however, suggest that isoprene may form SOA products in the atmosphere via heterogeneous acid-catalyzed oxidation with hydrogen peroxide (Limbeck et al, 2003; Claeys et al., 2004). Monoterpenes,  $\text{C}_{10}\text{H}_{16}$  compounds such as  $\alpha$ -pinene,  $\beta$ -pinene,  $\Delta^3$ -

carene and limonene, and sesquiterpenes, C<sub>15</sub>H<sub>24</sub> compounds including camphene and caryophyllene are some of the major components of biogenic emissions contributing to aerosol formation.

Anthropogenic sources contribute to ambient particulate matter levels more than natural sources in urban areas (Hinds, 1999). Aromatics are the most significant anthropogenic SOA precursors (Grosjean and Seinfeld, 1989; Pandis et al., 1992; Odum et al., 1997; Kalberer et al., 2004). Aromatic hydrocarbons constitute an important fraction of total volatile organic compounds in the urban atmosphere. Compounds like toluene, xylenes, trimethyl-benzenes, etc., are significant SOA precursors in urban areas and have been estimated to be responsible for 50-70% of the organic aerosols in urban areas (Kourtidis and Ziomas, 1999). Other anthropogenic hydrocarbons such as alkanes and alkenes with high carbon numbers have also been estimated to contribute to SOA in urban areas (Schauer et al., 1999).

Experimental work to identify SOA products has been carried out for both biogenic and anthropogenic hydrocarbon precursors (Forstner et al., 1997; Glasius et al., 1999; Yu et al., 1999; Jang and Kamens, 1999; Glasius et al., 2000; Kalberer et al., 2000; Jaoui et al., 2003; etc.). Among smog chamber experiments investigating aerosol forming potentials of oxidized biogenic compounds such as monoterpenes and sesquiterpenes (Pandis et al., 1991; Zhang et al., 1992; Odum et al., 1996; Hoffmann et al., 1997; Griffin et al., 1999; Jaoui and Kamens, 2001; 2003a; 2003b; 2003c; Jaoui et al., 2003),  $\alpha$ -pinene has been the most studied species. There are also numerous experimental studies that investigate the SOA formation potential of aromatic hydrocarbons (Izumi and Fukuyama, 1990; Odum et al., 1997a; Odum et al., 1997b; Kleindienst et al., 1999; Edney et al.,



2000; Hurley et al., 2001; Jang and Kamens, 2001). Other SOA producing anthropogenic hydrocarbons include long-chain olefins and long-chain alkanes (Strader et al., 1999). Various SOA products have been identified, such as multifunctional carboxylic acids, aldehydes, ketones, alcohols, carbonyls, organic nitrates, etc. The low vapor pressure of these products allows the significant existence of these compounds in the particle phase. For example, some of the major SOA products from cyclohexene identified by Kalberer et al. (2000) are shown in Table 2.1.

Table 2.1. Major SOA products from cyclohexene (Kalberer et al., 2000).

SOA products	Structure	SOA products	Structure
2-hydroxy-pentanoic acid		5-oxo-pentanoic acid	
4-hydroxy-butanaldehyde		glutaric acid	
oxalic acid		adipaldehyde	
malonic acid		6-oxo-hexanoic acid	
1,4-butanedial		adipic acid	
4-oxo-butanoic acid		2-hydroxy glutaric acid	
succinic acid		2-hydroxy adipic acid	
glutaraldehyde			

Compared with all the SOA components in the ambient atmosphere, the compounds identified to date in smog chamber experiments are only a very small fraction. All the hydrocarbon precursors and SOA products existing in the atmosphere form an

extremely complicated mixture system. Moreover, each product has its unique temperature- and composition-dependent partitioning properties making it a very challenging task to incorporate SOA into air quality models. Considering computational limitations and lack of experimental and field data, it is impossible to use hundreds of individual gas and aerosol phase chemical species in air quality models. A practical solution is to reduce the multicomponent aerosol mixture to a simplified system of a few lumped compounds that can approximate the properties of the detailed mixture. The following chapters present a theoretical model for defining a set of lumped compounds that accurately represent the complex ambient organic aerosol mixture.

## CHAPTER III

### THEORETICAL METHOD FOR LUMPING MULTICOMPONENT SECONDARY ORGANIC AEROSOL MIXTURES

Published as:

Bian, F. and Bowman, F. M., "Theoretical method for lumping multicomponent secondary organic aerosol mixtures," *Environmental Science & Technology*, 36 (11), 2491 -2497, 2002

#### Abstract

Atmospheric organic aerosol mixtures are composed of hundreds of individual semivolatile organic components, each with its own partitioning properties. In most atmospheric models, these components are grouped together into a few lumped compounds. A theoretical method is described for converting multiple organic aerosol components into one or more lumped groups using a set of equations that calculates the properties of lumped compounds from individual component properties. Expected organic aerosol mass and temperature range values are specified and components are grouped together according to relative volatility. A universal set of volatility dividing lines is presented for dividing components into multiple lumped groups. The lumping method is evaluated with three different mixtures: a base case mixture, a set of 1000 random mixtures with varying properties, and a mixture of products formed from the reaction of  $\alpha$ -pinene and ozone. Modeling results suggest that lumping a multicomponent mixture into two or three groups may be sufficient to represent partitioning behavior over a wide range of temperature and organic aerosol mass. The temperature dependence of lumped groups is predicted to be lower than that of their individual components.

## Introduction

Secondary organic aerosol (SOA) has been identified as an important contributor to fine particulate levels in both urban and rural atmospheres (Schauer et al., 1996; Blando et al., 1998). Secondary organic aerosol formation has been studied in smog chamber experiments (Odum et al., 1996; Griffin et al., 1999; Hallquist et al., 1999; Kamens et al., 1999; Kalberer et al., 2000) and has been shown to occur via an absorptive partitioning mechanism (Pankow, 1994; Odum et al., 1996). Absorptive partitioning is beginning to be incorporated into air quality models, with more recent versions accounting for the temperature dependence of gas-aerosol equilibrium (Meng et al., 1998; Strader et al., 1999; Andersson-Sköld and Simpson, 2001).

A major difficulty in representing organic aerosol partitioning behavior is the extreme complexity of the atmospheric system. Hundreds of different hydrocarbons, both natural and anthropogenic, act as aerosol precursors in the ambient atmosphere, most producing dozens of individual aerosol products (Rogge et al., 1993; Yu et al., 1999; Kalberer et al., 2000). Each product has its own partitioning properties that are dependent on temperature and composition (Bidleman et al., 1986; Leach et al., 1999; Ansari and Pandis, 2000; Pankow et al., 2001). Identifying all of these compounds, determining their exact composition in the organic aerosol mixture, and measuring partitioning properties for each one is a nearly impossible task (Jacobson et al., 2000; Turpin et al., 2000). As an alternative to comprehensive measurements, theoretical and empirical methods are being developed to predict the partitioning properties of individual components (Jang et al., 1997; Pankow, 1998; Cousins and Mackay, 2001; Pankow et al., 2001). Even when these properties can be accurately predicted or measured, the addition to computer air quality

models of several hundred different chemical species in the aerosol phase is computationally prohibitive and of limited utility without similarly detailed ambient measurements.

To be practical, the multicomponent mixture of hundreds of components must be reduced to a system of a few lumped compounds that approximates the properties of the detailed mixture. Smog chamber measurements of partitioning properties have used the approach of fitting experimental results with a two-product model (Odum et al., 1996; Hoffmann et al., 1997; Griffin et al., 1999; Kalberer et al., 2000), where the two products are merely surrogates for the true multicomponent aerosol mixture. Further simplification is possible when aerosol-forming hydrocarbons that form similar products can be treated as a single class of precursor, such as has been shown for the aromatic fraction of gasoline (Odum et al., 1997). Experimentally derived lumped parameters, however, provide little insight into the underlying properties of individual mixture components. Furthermore, they are only applicable to the specific overall mixture and reaction conditions for which they were measured. Experimentally determined parameters are tremendously useful for illuminating partitioning behavior in general, are the most accurate means of determining overall parameters for specific mixtures, and are the dataset on which theoretical and empirical predictions are based, but alone they are unlikely to provide a fundamental understanding of mixture partitioning behavior.

In this paper, we present a theoretical method for defining lumped compounds to represent an organic aerosol mixture. Unlike an experimental approach, where partitioning parameters are determined from fits to data, in this method, lumped parameters are calculated directly from the properties of the individual mixture

components. While overall partitioning behavior will vary under different conditions as reaction kinetics, individual semivolatile production rates, and aerosol-phase composition vary, the partitioning properties of individual components do not change.

This method provides additional insight beyond experimental measurements, by explaining how surrogate compound properties are related to those of the individual components. It also provides a theoretical framework that can be used in the future both for extending experimental measurements to other  $T$  and  $M_o$  conditions and for creating lumped groups from the products of several different SOA precursors. Using this method as a basis for developing appropriate surrogate groups, absorption partitioning can be more easily incorporated into large-scale atmospheric models.

The basis of this theoretical method is a set of equations for calculating the properties of lumped compounds from individual component properties. These lumping equations are applied to three different mixtures of semivolatile organics: a base case mixture, a set of 1000 random mixtures, and a mixture of products observed in chamber studies of the reaction of  $\alpha$ -pinene and ozone. For each mixture, multiple semivolatile components are converted into one or more lumped compounds using the lumping equations. Modeling results demonstrate that this method is effective at approximating partitioning behavior over a range of temperature and organic aerosol mass conditions.

## Theory

### *Absorptive Partitioning*

Secondary organic aerosol is created when hydrocarbons are oxidized in the atmosphere forming semivolatile products, which can then partition into the aerosol phase via absorption into an existing condensed organic phase. The SOA forming potential of a hydrocarbon is characterized by its aerosol yield

$$Y = \frac{\Delta M_o}{\Delta HC} = \frac{\sum_i A_i}{\Delta HC} \quad (3.1)$$

where  $\Delta HC$  ( $\mu\text{g m}^{-3}$ ) is the amount of hydrocarbon that reacts,  $\Delta M_o$  ( $\mu\text{g m}^{-3}$ ) is the organic aerosol mass produced by the hydrocarbon, and  $A_i$  ( $\mu\text{g m}^{-3}$ ) is the aerosol-phase concentration of semivolatile product  $i$ . For absorptive partitioning, the yield depends on the amount of absorbing aerosol present,  $M_o$ , according to the equation

$$Y = M_o \sum_i \frac{\alpha_i K_i}{1 + K_i M_o} \quad (3.2)$$

where  $\alpha_i$  is the dimensionless mass stoichiometric product coefficient, and  $K_i$  ( $\text{m}^3 \mu\text{g}^{-1}$ ) is the absorptive partitioning coefficient of semivolatile product  $i$  (Odum et al., 1996).

The absorptive partitioning coefficient can be expressed as a function of physical and thermodynamic properties of the semivolatile compound (Bowman et al., 1997)

$$K_i = \frac{10^{-6} RT}{MW \zeta_i p_i^\circ} \quad (3.3)$$

where  $R$  is the ideal gas constant ( $8.206 \times 10^{-5} \text{ m}^3 \text{ atm mol}^{-1} \text{ K}^{-1}$ ),  $T$  is temperature (K),  $MW$  is the mean molecular weight of the organic aerosol phase ( $\text{g mol}^{-1}$ ),  $\zeta_i$  is the activity

coefficient of species  $i$  in this phase,  $p_i^o$  is the vapor pressure of product  $i$  as a pure liquid (atm), and  $10^{-6}$  is a conversion factor ( $\text{g } \mu\text{g}^{-1}$ ).

$K_i$  values are not constant, but vary with temperature and aerosol composition (Bidleman et al., 1986; Leach et al., 1999; Ansari and Pandis, 2000; Pankow et al., 2001). In addition to the temperature term represented explicitly in equation 3.3, vapor pressure is highly dependent on temperature. According to the Clausius-Clapeyron equation (Atkins, 1990), this dependence is represented by

$$p_i^o = C_i \exp\left(\frac{-H_i}{RT}\right) = C_i \exp\left(\frac{-B_i}{T}\right) \quad (3.4)$$

where  $C_i$  (Pa) is the pre-exponential constant of product  $i$ ,  $H_i$  ( $\text{kJ mol}^{-1}$ ) is the enthalpy of vaporization of product  $i$ , and  $B_i$  (K) is the term  $H_i/R$ .  $B_i$  values are assumed constant over moderate temperature ranges based on previous findings that available  $H_i$  data for SOA components show variations of less than 3% between 15 and 35 °C (Sheehan and Bowman, 2001).

The composition of the absorbing aerosol mixture affects the partitioning coefficient through the activity coefficient and the mean molecular weight. In this work we focus solely on temperature effects and have assumed that  $\zeta$  and  $MW$  terms are constant. This is clearly a major simplification that will generally not hold true in the atmosphere where aerosol mixtures include a variety of organic and inorganic components as well as water. While compositional dependence is beyond the scope of this initial study, it is clearly important and will be accounted for in future work.

Given an experimentally determined partitioning coefficient,  $K_i^*$ , at a reference temperature,  $T^*$ , and assuming a constant activity coefficient and mean molecular weight,



an equation for a temperature-dependent partitioning coefficient,  $K_i(T)$ , can be developed based on equations 3.3 and 3.4 (27)

$$K_i(T) = K_i^* \frac{T}{T^*} \exp\left[B_i\left(\frac{1}{T} - \frac{1}{T^*}\right)\right] \quad (3.5)$$

Equation 3.5 can be combined with equation 3.2 to show that yield is a function of the amount of available absorbing organic material and temperature

$$Y(M_o, T) = M_o \sum_i \frac{\alpha_i K_i^* \frac{T}{T^*} \exp\left[B_i\left(\frac{1}{T} - \frac{1}{T^*}\right)\right]}{1 + K_i^* \frac{T}{T^*} \exp\left[B_i\left(\frac{1}{T} - \frac{1}{T^*}\right)\right]} M_o \quad (3.6)$$

Thus, the SOA yield of a given hydrocarbon will vary with both  $M_o$  and  $T$ , and will depend on the values of the parameters  $\alpha_i$ ,  $K_i^*$ , and  $B_i$  for each oxidation product.

### *Lumping Equations*

To simplify the system we would like to group these multiple individual components together into a few lumped compounds such that the lumped system approximates the partitioning behavior of the detailed mixture, as expressed by  $Y(M_o, T)$

$$Y(M_o, T)_{\text{detailed}} \approx Y(M_o, T)_{\text{lumped}} \quad (3.7)$$

For a single lumped compound, all of the individual components are grouped together into one compound. For two or more lumped compounds, components are divided into the appropriate number of groups, each of which is lumped into a single compound.

The goal then is to develop a set of equations that expresses the lumped parameters  $\alpha$ ,  $K^*$ , and  $B$  as functions of the component parameters  $\alpha_i$ ,  $K_i^*$ , and  $B_i$ . To

maintain conservation of mass, the stoichiometric product coefficient of the lumped group,  $\alpha$ , is defined to be the sum of the individual coefficients,  $\alpha_i$ ,

$$\alpha = \sum_i \alpha_i \quad (3.8)$$

Deriving expressions for  $K^*$  and  $B$  is more complicated. Exact equations will not provide constant values of  $K^*$  and  $B$ , but will be dependent on  $M_o$  and  $T$ .

An appropriate value of  $K^*$  can be approximated by using an average mass of absorbing material,  $M_o^*$ , and  $T=T^*$  when substituting equation 3.6 into equation 3.7

$$\sum_i \frac{\alpha_i K_i^*}{1 + K_i^* M_o^*} \approx \frac{\alpha K^*}{1 + K^* M_o^*} \quad (3.9)$$

which can then be solved for  $K^*$

$$K^* = \frac{\sum_i \frac{\alpha_i K_i^*}{1 + K_i^* M_o^*}}{\sum_i \frac{\alpha_i}{1 + K_i^* M_o^*}} \quad (3.10)$$

Note that  $M_o$  is a variable, whereas  $M_o^*$  is a constant used to represent a range of  $M_o$  values. When  $M_o=M_o^*$ , this equation is exactly correct. For yield predictions over a range of  $M_o$ , a value of  $M_o^*$  equal to the midpoint of the desired  $M_o$  range was found to provide the most accurate results.

The average temperature dependence of a lumped group can be approximated by using equation 3.10 to calculate lumped  $K$  values,  $K(T_{\text{high}})$  and  $K(T_{\text{low}})$ , corresponding to the extremes of a desired temperature range,  $T_{\text{high}}$  and  $T_{\text{low}}$ , respectively.

$$K(T_{\text{high}}) = \frac{\sum_i \frac{\alpha_i K_i(T_{\text{high}})}{1 + K_i(T_{\text{high}}) M_o^*}}{\sum_i \frac{\alpha_i}{1 + K_i(T_{\text{high}}) M_o^*}} \quad (3.11)$$

These data points,  $K(T_{\text{high}})$ ,  $K(T_{\text{low}})$ ,  $T_{\text{high}}$ ,  $T_{\text{low}}$ , are then used to fit equation 3.5 and determine a lumped  $B$  value

$$B = \frac{\ln\left(\frac{K(T_{\text{low}}) T_{\text{high}}}{K(T_{\text{high}}) T_{\text{low}}}\right)}{\left[\frac{1}{T_{\text{low}}} - \frac{1}{T_{\text{high}}}\right]} \quad (3.12)$$

A weighted average of individual temperature dependence parameters,  $B_i$ ,

$$B = \frac{\sum_i \alpha_i B_i}{\sum_i \alpha_i} \quad (3.13)$$

was also considered, but significant errors resulted.

Thus, equations 3.8, 3.10, and 3.12 can be used to determine the appropriate lumped parameters  $\alpha$ ,  $K^*$ , and  $B$  from the individual parameters  $\alpha_i$ ,  $K_i^*$ , and  $B_i$  for a given range of absorbing organic mass, defined by  $M_o^*$ , and range of temperature,  $T_{\text{low}}-T_{\text{high}}$ .

## Results

### *Base Case Mixture*

Three sets of lumping trials were performed to test the lumping methodology. For the first set, a base case mixture containing 9 individual components was used. Table 3.1 summarizes the base case component properties. Each component has the same concentration with an  $\alpha_i$  value of 0.1, such that the maximum possible yield for the mixture is 0.9.  $K_i^*$  values cover a wide range of volatility, varying from 0.0001 to 1.0 m<sup>3</sup> μg<sup>-1</sup>, with approximately even spacing on a logarithmic scale. All components in the base

case have the same temperature dependence, with  $B_i=20,000$  K. This represents a large temperature dependence and is the maximum expected value based on estimated heats of vaporization (Sheehan and Bowman, 2001). It provides an extreme case for testing the lumping method's ability to approximate temperature dependence.

Table 3.1. Base case mixture properties and lumped group assignments.

$K_i^*$ ( $\text{m}^3 \mu\text{g}^{-1}$ )	$\alpha_i$	$B_i$ (K)	Lumped Groups*			
			1	2	3	4
0.0001	0.1	20000	a	a	a	a
0.0003	0.1	20000	a	a	a	a
0.001	0.1	20000	a	a	a	a
0.003	0.1	20000	a	a	a	a
0.01	0.1	20000	a	a	a	b
0.03	0.1	20000	a	a	b	b
0.1	0.1	20000	a	b	b	c
0.3	0.1	20000	a	b	c	c
1.0	0.1	20000	a	b	c	d

\* a, b, c, d represent the lumped group to which a component is assigned.

Organic aerosol yield,  $Y$ , for the base case mixture was calculated as a function of temperature,  $T$ , and absorbing aerosol mass,  $M_o$ , as shown in Figure 3.1.  $T$  and  $M_o$  ranges of 0-40 °C and 0-25  $\mu\text{g m}^{-3}$ , respectively, mimic expected atmospheric conditions. The data presented in Figure 3.1 were calculated using all of the individual components and represents the detailed mixture yield against which lumped mixtures will be compared.

Figure 3.1 shows that yield is strongly dependent on both  $T$  and  $M_o$ . Holding temperature constant, the yield vs.  $M_o$  curves have the shape predicted by previous descriptions of absorptive partitioning (Odum et al., 1996; Hoffmann et al., 1997; Griffin et al., 1999; Kalberer et al., 2000) - linear at low  $M_o$ , and approaching a constant maximum yield at large  $M_o$ . At constant  $M_o$ , the influence of temperature can be seen. For

high temperatures, yield approaches zero. For low temperatures, it approaches the maximum yield. At intermediate temperatures, yield is linear with  $T$ . The linear dependence on  $T$  is partly a result of the evenly spaced  $K_i$  and equal  $\alpha_i$  values of the base case, but even for much less uniform mixtures, approximately linear behavior is observed.

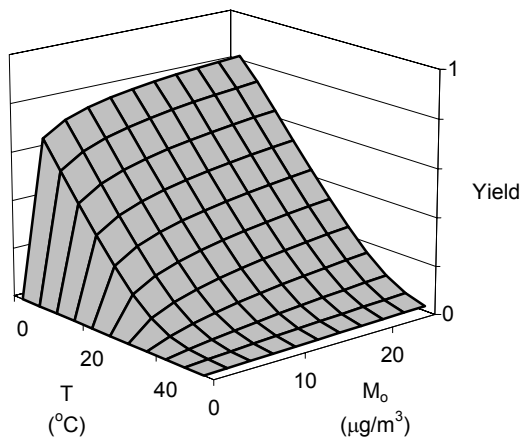


Figure 3.1. Base case mixture organic aerosol yield as a function of temperature and organic aerosol mass.

The base case mixture was lumped into 1-4 group mixtures, according to the group assignments listed in Table 3.1. For example, when two lumped groups are formed, the first six components are lumped together into group 2a, and the last three components are lumped to form group 2b. The resulting properties for the lumped groups are shown in Table 3.2. Figure 3.2 compares the yield predictions of these lumped groups to the detailed result of Figure 3.1 for the case where  $T = T^* = 25$  °C,  $M_o$  ranges from 0-20  $\mu\text{g m}^{-3}$  and  $M_o^*$  is 10  $\mu\text{g m}^{-3}$ . The lumped group approximations are all exactly correct at  $M_o = M_o^*$  and  $M_o = 0$ , but they overpredict yield when  $M_o > M_o^*$ , and underpredict yield when  $M_o < M_o^*$ . The magnitude of these errors is lowest near  $M_o^*$  and 0 and increases when  $M_o$  is further away from  $M_o^*$  and 0. Overall accuracy is relatively insensitive to the

exact  $M_o^*$  value used, and by selecting the midpoint of the  $M_o$  range, over- and under-predictions are approximately equal. An overall error in yield for the entire  $M_o$  range can be calculated using the root mean square (RMS) error.

Table 3.2. Base case mixture lumped group properties.

Lumped Groups	$K^*$ ( $\text{m}^3 \mu\text{g}^{-1}$ )	$\alpha$	$B$ (K)
1a	0.0390	0.9	10050
2a	0.00647	0.6	15110
2b	0.257	0.3	18520
3a	0.00275	0.5	16610
3b	0.0576	0.2	19290
3c	0.487	0.2	19410
4a	0.00109	0.4	18010
4b	0.0192	0.2	19400
4c	0.167	0.2	19430
4d	1	0.1	20000

$$M_o^* = 10 \mu\text{g m}^{-3}, T^* = 25 \text{ }^\circ\text{C}, T_{\text{hi}} = 40 \text{ }^\circ\text{C}, T_{\text{low}} = 0 \text{ }^\circ\text{C}$$

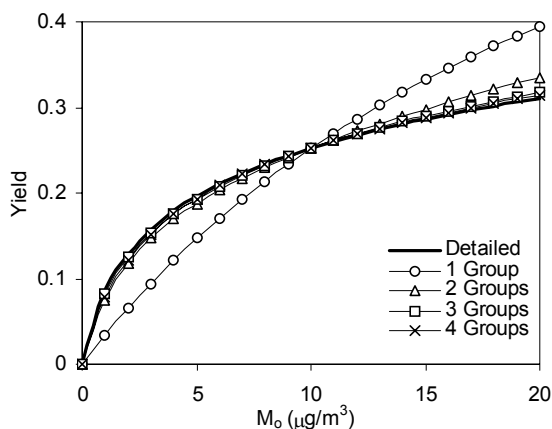
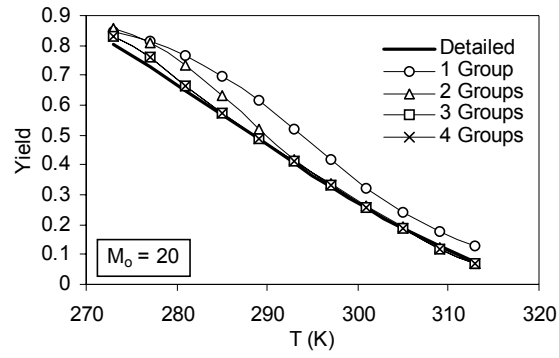


Figure 3.2. Base case mixture organic aerosol yield predictions as a function of organic aerosol mass using 1, 2, 3 and 4 lumped groups.  $T = T^* = 25 \text{ }^\circ\text{C}$ .

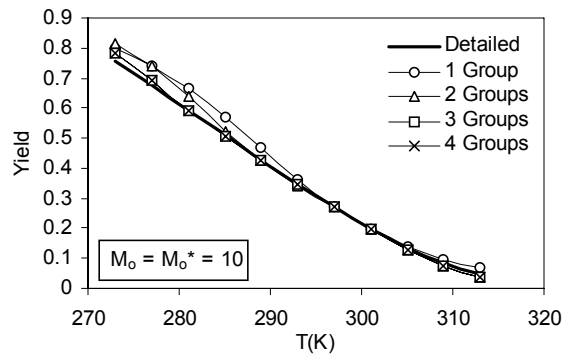
When only one lumped group is used, the resulting yield curve (circles in Figure 3.2) is significantly different from the detailed case, and a large RMS error of 0.0485 results. As the number of lumped groups increases, accuracy improves and the curves get closer to the detailed yield curve, with both absolute and RMS errors decreasing. 2, 3, and 4 lumped groups all approximate the detailed yield curve well with RMS errors of 0.0120, 0.0040, and 0.0037, respectively, that are well within experimental uncertainties.

Variable temperature yield predictions for 1-4 lumped groups were calculated using the base case mixture at high, medium, and low  $M_o$  as shown in Figure 3.3. Consistent with results at constant temperature, yields tend to be overpredicted at high  $M_o$  and underpredicted at low  $M_o$ . Lumping into a single group results in large errors, particularly at high and low  $M_o$ , while accuracy improves when additional groups are used. When the uncertainty associated with individual component partitioning properties is considered, two or, at most, three groups should be sufficient to adequately represent partitioning behavior for this base case mixture over a wide range of temperature and organic aerosol mass. Simulations of mixtures containing 20 components showed similar results, indicating that the required number of lumped groups does not depend on the number of mixture components. It is important to note, of course, that the optimum number of lumped groups for a given application will ultimately be governed by the degree of model accuracy and complexity desired.

(a)



(b)



(c)

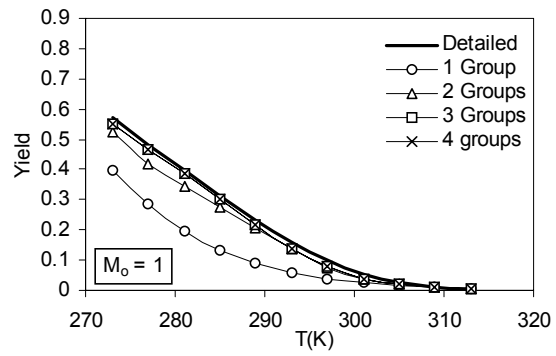


Figure 3.3. Base case mixture organic aerosol yield predictions as a function of temperature using 1, 2, 3 and 4 lumped groups. (a)  $M_o = 20 \mu\text{g m}^{-3}$ , (b)  $M_o = M_o^* = 10 \mu\text{g m}^{-3}$ , (c)  $M_o = 1 \mu\text{g m}^{-3}$ .



### *Random Mixtures*

When lumping individual components into multiple groups, specific criteria need to be defined for how to group the components. To lump together components of similar volatility, components are divided between groups based on their  $K_i$  values. A set of 1000 random mixtures patterned after the base case mixture was used to determine optimum  $K_i$  dividing lines for defining lumped groups. Each mixture contained eight components with random  $\alpha_i$  values that were normalized so that  $\sum \alpha_i = 1$ . The  $\log(K_i^*)$  for each component was randomly chosen in the range of -4.0 to 1.0.  $B_i$  values were also randomly selected over the range of 0 to 20,000 K. The  $\log(K_i^*)$  for each component was randomly chosen in the range of -4.0 to 1.0.  $B_i$  values were also randomly selected over the range of 0-20,000 K. All random values were generated using a pseudorandom number function employing a shuffled multiplicative congruential method (IMSL, 1997). The reference temperature,  $T^*$ , was defined as 25 °C, and the temperature and  $M_o$  ranges used were, respectively, 0-40 °C and 0-20  $\mu\text{g m}^{-3}$ .

Values for dividing lines vary depending on the range of organic aerosol mass considered but are essentially constant when expressed as the product of  $K_i$  and  $M_o^*$ . The term  $K_i M_o^*$  is a normalized measure of volatility that provides dividing lines that can be used under all  $M_o$  conditions. Recommended dividing lines, based on  $K_i M_o^*$ , for various numbers of lumped groups are shown in Figure 3.4 and are those used for all lumping trials reported in this paper. When  $K_i M_o^* < 0.001$ , a component is quite volatile and will reside almost entirely in the gas phase. It can be considered a gas-phase product and need not be included as part of the semivolatile mixture. At the other extreme, when  $K_i M_o^* > 100$ , a component is nonvolatile and will partition almost completely into the aerosol

phase. These components can be considered purely aerosol-phase products that contribute directly to organic aerosol mass but do not need to be lumped into the semivolatile mixture. Lumping performance is relatively insensitive to the dividing line used, so the exact values listed in Figure 3.4 should be treated as general guidelines only.

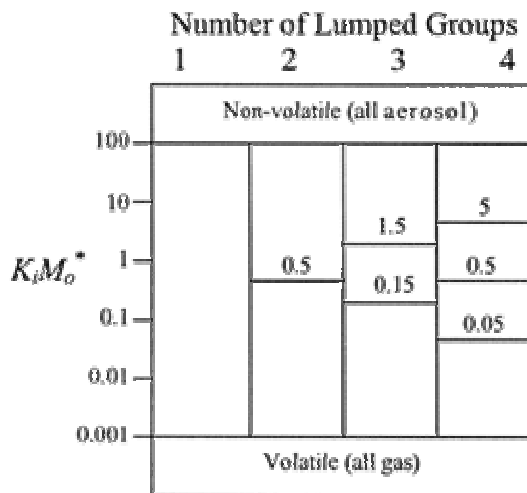


Figure 3.4. Recommended  $K_i M_o^*$  dividing lines for assigning mixture components to lumped groups.

The average RMS error in yield predictions for the set of 1000 random mixtures was determined at different temperatures for different numbers of lumped groups, as shown in Figure 3.5. Similar to the base case mixture, accuracy improves as more groups are used to approximate the full mixture. Again, error with one group is considerably higher than that for multiple groups. With the exception of a single group, error is lowest at the reference temperature and increases when temperature is further away from  $T^*$ . As compared to the base case, numerical values of average RMS error at  $T^*$  for the random

mixtures are similar, suggesting that, in general, two or three groups may be sufficient to represent mixture partitioning behavior.

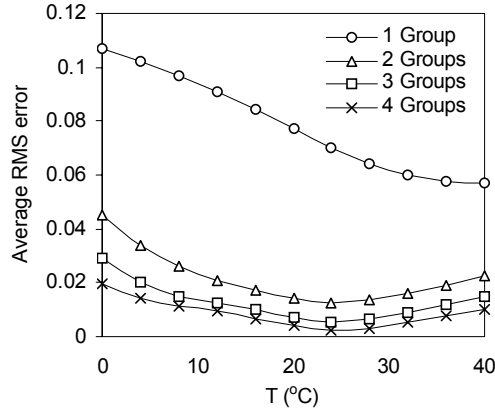


Figure 3.5. Average RMS error in random mixture yield predictions as a function of temperature using 1, 2, 3 and 4 lumped groups.  $M_o = 0\text{-}20 \mu\text{g m}^{-3}$ .

### *Temperature Dependence*

The temperature dependence of a lumped mixture can be seen on a plot of  $\ln(K)$  vs.  $1/T$  where  $K$  is the lumped partitioning coefficient at the given temperature. Figure 3.6 shows this plot for the base case mixture with temperature ranging from 0 to 40 °C and  $M_o^* = 10 \mu\text{g m}^{-3}$ . The thick solid line represents the exact values of  $K$  calculated using equations 3.8, 3.10, and 3.12 to lump all eight components into a single group. For a single component a linear relationship results, but when a mixture of components is used linearity is not ensured. Typically, however, as seen in Figure 3.6, a linear approximation for mixture temperature dependence is valid. The solid line represents the approximated mixture temperature dependence based on the lumped  $B$  value of 10,050 K calculated

using equation 3.12. It intersects the exact data points at the reference temperature  $T^*$ , and provides a good fit with minimal error over the entire temperature range.

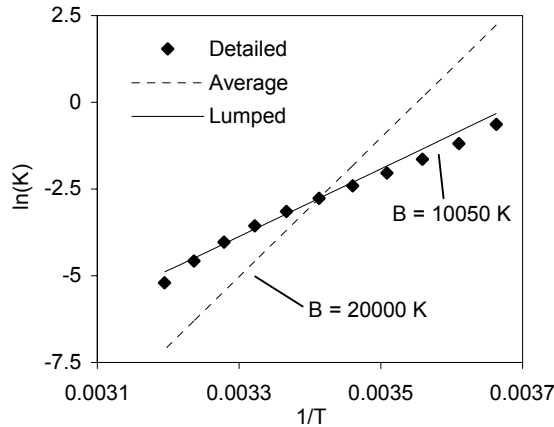


Figure 3.6.  $\ln(K)$  as a function of  $1/T$  for base case mixture lumped into a single group.  $M_o = M_o^* = 10 \mu\text{g m}^{-3}$ .

It is important to note that the lumped  $B$  value, representing the overall mixture, is much lower than that of the individual components. In the base case mixture, all components have  $B_i = 20,000$  K, but the lumped mixture  $B$  value is only 10,050 K. This occurs as a result of the wide volatility range of the mixture components. Components with very high  $K_i$  reside primarily in the aerosol phase, while those with very low  $K_i$  are found mostly in the gas phase. Even when temperature changes, these components at the extremes of volatility remain almost entirely in one phase or the other. Components with moderate volatility, however, shift between gas and aerosol phases and account for the majority of mixture temperature dependence. Thus, high and low volatility components tend to moderate overall mixture temperature dependence when lumped together.

The magnitude of this effect depends on the degree of dissimilarity between components. When multiple lumped groups are used, each group contains components of relatively similar volatility and lumped temperature dependences will be more reflective of the individual values. This effect has important implications for estimating the temperature dependence of semivolatile products used in air quality models. Because model compounds typically represent a variety of different products, measured or estimated temperature dependence of individual components may not provide an accurate prediction of actual mixture behavior.

#### *$\alpha$ -Pinene/O<sub>3</sub> Product Mixture*

A third set of lumping trials was performed using an organic aerosol mixture composed of products formed from the reaction of  $\alpha$ -pinene and ozone. This aerosol-forming reaction has been widely studied and experimental partitioning parameter and concentration data exist for most of the individual semivolatile components. Table 3.3 lists the mixture components and their properties.  $K_i$  and  $\alpha_i$  data are based on measured values from Yu et al. (Yu et al., 1999). Following the work of Pankow et al. (Pankow et al., 2001), product  $X$  is used to represent unidentified aerosol mass and is assigned a very large partitioning coefficient such that it partitions almost entirely into the aerosol phase.  $B_i$  values have been experimentally determined for pinonaldehyde (9080 K) (Hallquist et al., 1997) and have been derived from vapor pressure estimates for pinic acid (11 200 K) (Kamens et al., 1999; Sheehan and Bowman, 2001), but similar temperature dependence data for the other components is unavailable. Theoretical predictions, using boiling point estimates (Yu et al., 1999) and the method of Schwarzenbach et al. (Schwarzenbach et al.,

1993) as described in Sheehan and Bowman (Sheehan and Bowman, 2001) suggest  $B_i$  values in the range of 8400-10,000 K. Because these experimental and theoretical values are relatively similar and have a high degree of uncertainty, all components were assumed to have a  $B_i$  value of 10,000 K.

Table 3.3.  $\alpha$ -Pinene/ $O_3$  product mixture properties and lumped group assignments.

Condensable Component	$K_i^*$	$\alpha_i$	$B_i$	Lumped Groups			
	( $m^3 \mu g^{-1}$ )			(K)	1	2	3
pinic acid	0.00121	0.1458	10000	a	a	a	a
norpinic acid	0.00196	0.0208	10000	a	a	a	a
hydroxy pinonaldehydes	0.0129	0.1129	10000	a	a	b	b
pinonic acid	0.0195	0.0762	10000	a	a	b	b
norpinonic acid + isomers	0.0276	0.0661	10000	a	a	b	b
pinonaldehyde	0.0284	0.0568	10000	a	a	b	b
norpinonaldehyde	0.0384	0.0012	10000	a	b	b	c
hydroxy pinonic acid	0.0607	0.0397	10000	a	b	b	c
product X	10000	0.0167	10000	a	b	c	d

This nine-component mixture can be used to predict the amount of organic aerosol mass,  $M_{otheor}$ , that was produced in three different sets of smog chamber experiments. The temperature,  $T$ , amount of  $\alpha$ -pinene reacted,  $\Delta HC$ , and organic aerosol mass formed,  $M_{oexp}$ , for each experiment are shown in Table 3.4. Most of the experiments were performed at 30-37 °C and included 2-butanol as an OH scavenger to ensure that reaction with  $O_3$  was the only degradation pathway for  $\alpha$ -pinene. The other two experiments shown in Table 3.4 were conducted at 49 and 16 °C, providing high and low temperature data points for comparison. These data are from a set of experiments that did not include an OH scavenger, but were included because the  $O_3$  reaction was shown to be

the dominant degradation pathway, accounting for 85 and 94% of  $\alpha$ -pinene reacting (Hoffmann et al., 1997).

Table 3.4. Experimental and theoretical organic aerosol mass for  $\alpha$ -pinene/O<sub>3</sub> chamber experiments.

Chamber Experiment	$T$ (K)	$\Delta\text{HC}$ ( $\mu\text{g m}^{-3}$ )	$M_{o\text{ exp}}$ ( $\mu\text{g m}^{-3}$ )	$M_{o\text{ theor}}$ ( $\mu\text{g m}^{-3}$ )	Error (%)
Griffin-99 (4)	310	89.5	7.4	3.4	-54
	310	97.5	8.5	4.1	-52
	303	170	30.3	37.3	23
	303	249	46	68.9	50
Yu-99 (13)	308	350	65.1	89.7	38
	308	307	54.2	72.6	34
	306	245	38.8	57.0	47
Hoffmann-97 (23)	322	196	29.9	5.4	-82
	289	508	341	240.8	-29

$M_{o\text{ exp}}$  and  $M_{o\text{ theor}}$  values show general agreement, with aerosol mass increasing with the amount of hydrocarbon reacted, and varying inversely with temperature, as predicted by absorption partitioning theory. Discrepancies between experiment and theory, with errors ranging from 50% overprediction to 80% underprediction, are likely a result of uncertainties in both the properties of the mixture components and the measured  $M_o$  data. The theory underpredicts aerosol formation for both the high and low temperature experiments. One possible explanation is that gas-phase chemistry is dependent on temperature, causing production rates of condensable components ( $\alpha_i$ ) to vary with temperature. Additional experimental measurements are needed to confirm individual component production rates and properties, particularly as a function of temperature. As this data becomes available, it should be possible to more closely predict organic aerosol formation.

For the present study of lumping methods, perfect agreement between experimental and theoretical  $M_o$  values is not necessary. The component property data listed in Table 3.3 provide a realistic multicomponent mixture to use as a base case against which lumped groups are compared.

Equations 3.8, 3.10, and 3.12, using  $M_o^*=30 \mu\text{g m}^{-3}$ ,  $T_{\text{high}}=49 \text{ }^\circ\text{C}$ , and  $T_{\text{low}}=16 \text{ }^\circ\text{C}$ , and the previously recommended dividing lines, were applied to the nine-component mixture to form the lumped groups listed in Table 3.5.

Table 3.5.  $\alpha$ -Pinene/ $\text{O}_3$  product mixture lumped group properties.

Lumped Groups	$K^*$ ( $\text{m}^3 \mu\text{g}^{-1}$ )	$\alpha$	$B$ (K)
1a	0.0148	0.5362	7300
2a	0.0114	0.4786	8200
2b	0.0979	0.0576	8550
3a	0.00130	0.1666	9980
3b	0.0224	0.3529	9570
3c	10000	0.0167	10000
4a	0.00130	0.1666	9980
4b	0.0197	0.312	9790
4c	0.0599	0.0409	9990
4d	10000	0.0167	10000

$M_o^*=30 \mu\text{g m}^{-3}$ ,  $T^*=34 \text{ }^\circ\text{C}$ ,  $T_{\text{hi}}=49 \text{ }^\circ\text{C}$ ,  $T_{\text{low}}=16 \text{ }^\circ\text{C}$

For the case of a single group, where all components have been lumped together,  $\alpha=0.5362$ . When two groups are used, most condensable mass is still lumped together into a single group with  $\alpha=0.4786$ . With three or four groups, there is a more even distribution of condensable mass between groups of varying volatility. The temperature



dependence parameter,  $B$ , also varies with the number of lumped groups. For a single group, where high and low volatility compounds are grouped together, the overall temperature dependence is  $B=7,300$ , which is considerably lower than that for the individual components ( $B_i=10,000$  K). When more groups are used, components within a group are closer in volatility and as a result lumped  $B$  values are much closer to those of the individual components.

These lumped  $K$ ,  $\alpha$ , and  $B$  values were then used to predict the amount of organic aerosol formed under conditions of the smog chamber experiments. Results for 1, 2, 3, and 4 lumped groups are compared to those for the full 9-component mixture in Table 3.6. In general, the greater the number of lumped groups, the closer predictions are to the full mixture. Lumped groups underpredict aerosol mass when  $M_o < M_o^*$  and overpredict aerosol mass when  $M_o > M_o^*$ .

Table 3.6. Organic aerosol mass and error for  $\alpha$ -pinene/ $O_3$  product mixture lumped groups.

Detailed Mixture $M_o$ ( $\mu\text{g m}^{-3}$ )	Lumped Group $M_o$ ( $\mu\text{g m}^{-3}$ )				Lumping Error (%)			
	1	2	3	4	1	2	3	4
3.4	0.0	0.0	3.1	3.3	-100	-100	-7.7	-2.3
4.1	0.0	0.0	3.7	4.0	-100	-100	-8.4	-2.5
37.3	39.8	38.9	37.6	37.4	6.9	4.4	1.0	0.5
68.9	82.4	78.9	70.1	69.5	19.7	14.6	1.8	0.9
89.7	115.2	106.9	92.2	90.9	28.4	19.2	2.8	1.3
72.6	92.0	84.9	74.6	73.6	26.7	16.9	2.8	1.3
57.0	68.5	64.2	58.2	57.6	20.2	12.6	2.2	1.0
5.4	0.0	0.0	5.3	5.4	-100	-100	-2.0	-0.2
240.8	256.1	256.5	241.2	241.2	6.4	6.5	0.2	0.2

When only 1 or 2 lumped groups are used, the underprediction at low  $M_o$ , is such that no organic aerosol is predicted to form. Absorption partitioning theory implies a

threshold amount of parent organic that must react before sufficient condensable products build up in the gas-phase and aerosol formation can begin (Bowman et al., 1997). In the full mixture, this threshold is quite low due to low volatility product *X*, which partitions to the aerosol phase almost immediately forming a condensed organic phase into which other components can absorb.

For the one and two group cases, product *X* is grouped with more volatile components, and the resulting average partitioning coefficient is considerably lower than for product *X* alone. This causes an artificial increase in the threshold for aerosol formation such that no aerosol is predicted to form. Alternatively, for the three and four group cases, product *X* forms its own group, a more realistic threshold results and aerosol formation, while still underpredicted, can occur. To overcome this problem, very low volatility products should be treated as purely aerosol-phase compounds and not be included in the lumping of semivolatiles. In the ambient atmosphere, however, there will likely always be some absorbing aerosol mass present so that the threshold constraint is not a concern.

Contrary to results from the base case and random mixtures, there is relatively little improvement gained using two groups instead of one. This is the result of most of the condensable mass remaining together in a single group, even when a second group is formed. When three groups are used, condensable mass is more evenly distributed, and performance improves significantly. This suggests that better results could be obtained by setting dividing lines based on the specific mixture being analyzed. For universal application to a variety of mixtures, however, a single set of fixed dividing lines is

desirable. In these cases, it may be more practical to use a larger number of lumped groups to ensure that condensable mass is well-distributed among groups.

## CHAPTER IV

### A LUMPING MODEL FOR COMPOSITION- AND TEMPERATURE-DEPENDENT PARTITIONING OF SECONDARY ORGANIC AEROSOLS

Published as:

Bian, F. and Bowman, F. M., "A lumping model for composition-and temperature-dependent partitioning of secondary organic aerosols," *Atmospheric Environment*, 39, 1263-1274, 2005

#### Abstract

An improved lumping model is described for converting multiple semivolatile organic aerosol components into one or more lumped groups that can represent the organic aerosol mixture in atmospheric models. Lumping equations to calculate temperature- and composition-dependent absorption partitioning parameters are presented, together with lumping criteria for dividing components into groups based on component vapor pressure, chemical structure, and activity coefficient in water. Lumping performance of the model is evaluated using a base case mixture of organic aerosol components, random mixtures selected from a set of identified semivolatile organic compounds, and products from the  $\alpha$ -pinene/ozone reaction. Modeling results show that aerosol composition has a strong influence on SOA partitioning and lumping accuracy. Comparisons of different lumping criteria suggest that lumping components by a combination of vapor pressure and water interactions or by vapor pressure alone will produce optimum results.

*Keywords:* secondary organic aerosol; partitioning; lumping; composition dependence; modeling

## Introduction

Secondary organic aerosol (SOA) is a significant contributor to the fine particulate burden in both urban and rural atmospheres (Schauer et al., 1996; Blando et al., 1998; Strader et al., 1999). SOA is created by atmospheric oxidation of gas-phase hydrocarbons to form semivolatile products that partition to the aerosol phase via an absorptive partitioning mechanism (Pankow et al., 1994; Odum et al., 1996). In recent years, SOA absorptive partitioning has begun to be included in air quality models (Strader et al., 1999; Andersson-Sköld and Simpson, 2001), with more recent versions accounting for the temperature and composition dependence of gas-aerosol equilibrium (Pun et al., 2002; Binkowski and Roselle, 2003).

A major difficulty of modeling organic aerosol partitioning behavior is the extreme complexity of the multicomponent aerosol mixture which contains hundreds of individual components, each with its own unique partitioning properties. A practical solution is to approximate the detailed mixture with a few representative SOA compounds. Experimental studies of SOA partitioning have used this approach by fitting experimental results with a 2-product model (Odum et al., 1996; Griffin et al., 1999; Kalberer et al., 2000). The two products are not real compounds, but simply a numerical representation of the actual aerosol components. Some models have used a surrogate approach where specific individual components are used to represent all other components of a similar class (Griffin et al., 2003). An alternate strategy is to lump

components together and create a hypothetical compound that is an “average” of the components. This lumped compound approach is similar to that used in some gas-phase atmospheric chemistry mechanisms (Stockwell et al., 1997; Carter, 2000).

In our previous work, a method was described for defining lumped semivolatile compounds to represent an organic aerosol mixture (Bian and Bowman, 2002). Lumped parameters are calculated directly from individual component properties. Modeling results demonstrated that this method is effective at approximating partitioning behavior over a range of temperature and organic aerosol mass conditions. This original lumping method, however, accounted only for the temperature dependence of partitioning, neglecting the influence of composition.

In this paper we present an improved model with new parameters to account for aerosol mixture chemical composition. The basis of this theoretical model is a set of equations for calculating the properties of lumped compounds from individual component properties. These lumping equations are applied to three different systems of semivolatile organics: a base case mixture of 16 known aerosol components, a set of random mixtures selected from a database of identified aerosol components, and products from the  $\alpha$ -pinene/ozone reaction. For each mixture, multiple semivolatile components are converted into one or more lumped compounds using the lumping equations and various lumping criteria. The total SOA yield predicted by the lumped groups is compared with the yield of the full, unlumped, mixture. Results are used to demonstrate lumping model performance and to suggest optimum lumping criteria.

This lumping model provides a method to convert multiple organic aerosols to a few lumped groups with properties that can approximate the partitioning behavior of the

detailed mixture. It will be used to generate partitioning parameters for air quality models, reflecting more detailed information about SOA products and providing a better representation of SOA in air quality models.

## Theory

### *Absorptive Partitioning*

Secondary organic aerosol is created when hydrocarbons are oxidized in the atmosphere forming semivolatile products that partition into the aerosol phase via absorption into an existing condensed organic phase. The gas/particle partitioning of a semivolatile product  $i$  is described by the partitioning coefficient  $K_i$  ( $\text{m}^3 \mu\text{g}^{-1}$ ), which is the ratio of aerosol-phase concentration  $A_i$  ( $\mu\text{g m}^{-3}$ ) and gas-phase concentration  $G_i$  ( $\mu\text{g m}^{-3}$ ), normalized by the total concentration of absorbing organic material,  $M_o$  ( $\mu\text{g m}^{-3}$ ), present in the aerosol phase (Odum et al., 1996),

$$K_i = \frac{A_i}{G_i M_o} \quad (4.1)$$

Following the work of Pankow (1994), the absorptive partitioning coefficient can be expressed as a function of physical and thermodynamic properties of the semivolatile compound

$$K_i = \frac{10^{-6} RT}{MW \zeta_i p_i^\circ} \quad (4.2)$$

where  $R$  is the ideal gas constant ( $8.314 \text{ J mol}^{-1} \text{ K}^{-1}$ ),  $T$  is temperature (K),  $MW$  is the mean molecular weight of the organic aerosol phase ( $\text{g mol}^{-1}$ ),  $\zeta_i$  is the activity

coefficient of species  $i$  in this phase,  $p_i^o$  is the vapor pressure of product  $i$  as a pure liquid (Pa), and  $10^{-6}$  is a conversion factor ( $\text{g } \mu\text{g}^{-1}$ ).

$K_i$  values vary with temperature and aerosol composition (Bidleman et al., 1986; Ansari and Pandis, 2000; Pankow et al., 2001; Takekawa et al., 2003). Vapor pressure is highly dependent on temperature, and can be represented by the Clausius-Clapeyron equation

$$p_i^o = C_i \exp\left(\frac{-H_i}{RT}\right) = C_i \exp\left(\frac{-B_i}{T}\right) \quad (4.3)$$

where  $C_i$  (Pa) is the pre-exponential constant,  $H_i$  ( $\text{J mol}^{-1}$ ) is the enthalpy of vaporization, and  $B_i$  (K) is the term  $H_i/R$ .  $B_i$  values are assumed constant over moderate temperature ranges based on previous findings that available  $H_i$  data for SOA components show variations of less than 3% between 15 and 35°C (Sheehan and Bowman, 2001).

Given a vapor pressure,  $p_i^{o*}$  at a reference temperature,  $T^*$ , an equation for a temperature-dependent vapor pressure,  $p_i^o(T)$ , can be developed based on equation 4.3

$$p_i^o(T) = p_i^{o*} \exp\left[B_i\left(\frac{1}{T} - \frac{1}{T^*}\right)\right] \quad (4.4)$$

Aerosol mixture composition, and to a lesser extent temperature, influence activity coefficient values. In this study, activity coefficients are parameterized using the UNIFAC group contribution method (Fredenslund et al., 1975). Each component is represented as a collection of different functional groups according to its molecular structure, and the interaction between components is assumed to be the sum of interactions between their functional groups. Activity coefficients are calculated as a function of  $x_i$ , the aerosol-phase mole fraction of product  $i$ ,  $s_{ji}$ , the number of groups  $j$  in molecule  $i$ , and temperature.



$$\zeta_i = f(x_i, s_{ji}, T) \quad (4.5)$$

The SOA forming potential of a hydrocarbon can be characterized by its aerosol yield, which is defined as the ratio of the organic aerosol mass produced to the amount of hydrocarbon that reacts. For absorptive partitioning, the yield depends on the amount of absorbing aerosol present,  $M_o$ , according to the equation (Odum et al., 1996)

$$Y = M_o \sum_i \frac{\alpha_i K_i}{1 + K_i M_o} \quad (4.6)$$

where  $\alpha_i$  is the mass stoichiometric product coefficient. Note that the resulting yield in equation 4.6 is dimensionless. Equations 4.2, 4.4 and 4.5 can be substituted into equation 4.6 to form an expression for SOA yield that is a function of individual component properties, aerosol phase composition, absorbing aerosol mass, and temperature.

$$Y = f(\alpha_i, MW_i, s_{ji}, p_i^{\circ*}, B_i, x_i, M_o, T) \quad (4.7)$$

### *Lumping Procedure*

The objective in lumping multiple individual components together into a few lumped compounds is to create a lumped system that approximates the partitioning behavior of the detailed mixture. Where partitioning behavior is represented by the aerosol yield in a given system,  $Y(x_i, M_o, T)$ , the desired relationship takes the form

$$Y(x_i, M_o, T)_{\text{detailed}} \approx Y(x_i, M_o, T)_{\text{lumped}} \quad (4.8)$$

A complete lumping procedure needs to include 1) a set of equations expressing the parameters of a lumped group ( $\alpha$ , MW,  $s_j$ ,  $p^{\circ*}$ ,  $B$ ) as functions of the component parameters ( $\alpha_i$ ,  $MW_i$ ,  $s_{ji}$ ,  $p_i^{\circ*}$ ,  $B_i$ ), and 2) criteria for dividing mixture components into lumped groups.

### *Lumping Equations*

To maintain conservation of mass, the stoichiometric product coefficient of the lumped compound,  $\alpha$ , is defined to be the sum of the individual component coefficients,  $\alpha_i$ ,

$$\alpha = \sum_i \alpha_i \quad (4.9)$$

$MW$  is calculated as a weighted average of the molecular weight of each individual product,

$$MW = \frac{\sum_i \alpha_i MW_i}{\alpha} \quad (4.10)$$

Chemical structure parameter  $s_j$  represents the number of UNIFAC functional groups  $j$  in a lumped compound. It is estimated as a weighted average of component structure parameters,  $s_{ji}$ ,

$$s_j = \frac{\sum_i \alpha_i s_{ji}}{\alpha} \quad (4.11)$$

It is important to note that this lumped compound is a hypothetical molecule. Its chemical structure, as defined by  $s_j$ , may not correspond to any real molecule, but its molecular interactions with other compounds should be similar to those of the individual components.

Expressions for  $p^{o*}$  and  $B$  depend on  $M_o$  and  $T$ . An appropriate value of  $p^{o*}$  can be estimated by using average values,  $M_o^*$ ,  $T^*$  and  $MW^*$ , assuming  $\zeta_i=1$ , and combining equations 4.2, 4.6 and 4.8

$$p^{\circ*} = \frac{\sum_i \frac{\alpha_i}{1 + \frac{RT^* M_o^*}{MW^* p_i^{\circ*}}}}{\sum_i \frac{\alpha_i / p_i^{\circ*}}{1 + \frac{RT^* M_o^*}{MW^* p_i^{\circ*}}}} \quad (4.12)$$

The average temperature dependence of a lumped group can be approximated by using equation 4.12 to calculate lumped  $p^{\circ}$  values corresponding to the extremes of a desired temperature range,  $T_{\text{high}}$  and  $T_{\text{low}}$ . These data points,  $p^{\circ}(T_{\text{high}})$ ,  $p^{\circ}(T_{\text{low}})$ ,  $T_{\text{high}}$ , and  $T_{\text{low}}$ , are then used in equation 4.4 to determine a lumped  $B$  value

$$B = \frac{\ln \left( \frac{p^{\circ}(T_{\text{high}})}{p^{\circ}(T_{\text{low}})} \right)}{\left[ \frac{1}{T_{\text{low}}} - \frac{1}{T_{\text{high}}} \right]} \quad (4.13)$$

Thus, equations 4.9-4.13 can be used to calculate the lumped parameters  $\alpha$ ,  $MW$ ,  $s_j$ ,  $p^{\circ*}$ , and  $B$  from the individual parameters  $\alpha_i$ ,  $MW_i$ ,  $s_{ji}$ ,  $p_i^{\circ*}$ , and  $B_i$  for expected ranges of absorbing organic mass, defined by  $M_o^*$ , temperature,  $T_{\text{low}} - T_{\text{high}}$ , and mean molecular weight,  $MW^*$ . Testing with the current and previous version of the lumping method has shown that the exact values of  $M_o^*$ ,  $T^*$  and  $MW^*$  have little influence on overall performance of the lumping model.

### *Lumping Criteria*

Three different parameters were considered as criteria for dividing components into lumped groups - vapor pressure, chemical structure, and activity coefficient in water. Lumping by vapor pressure divides components into groups of similar volatility. A set of dividing lines between groups was specified based on the term  $p_i^{\circ*} MW^* / M_o^*$ , which is a

normalized measure of volatility applicable under different  $M_o$  conditions. Numerical values of  $p_i^{o*}$ -based dividing lines used in this study were adapted from  $K_i^*$ -based dividing lines determined previously (Bian and Bowman, 2002). Values of the dividing lines (in units of  $\text{Pa m}^3 \mu\text{g}^{-1}$ ) are 0.01 for 2-group lumping, 0.001 and 0.1 for 3-group lumping, and 0.001, 0.01 and 0.1 for 4-group lumping. Different SOA mixtures will have specific dividing lines that provide optimum results, but in general lumping performance is relatively insensitive to the dividing line used.

A second possible criterion for lumping is chemical structure, where compounds with similar functional groups are grouped together. In this study, components were assigned to four different chemical categories: aromatics, long-chained acids, short-chained acids, and aldehydes or ketones. For 2-group lumping, components were divided into groups as aromatics and non-aromatics. For 3-group lumping, the non-aromatic compounds were further divided, with long-chained acids in one group, and short-chained acids, aldehydes and ketones in another. Other category definitions were also tried, but none of the alternatives provided a significant improvement in lumping results on average. SOA precursor species can also be a useful lumping criterion and would allow SOA mass to be attributed to specific precursor sources. Future work will focus on lumping aerosols formed from multiple hydrocarbon precursors based on their precursor types.

A third lumping criterion groups components by their activity coefficients in water. The activity coefficient of a compound in an equimolar mixture with water,  $\zeta_{w,i}$ , was estimated by UNIFAC and used as a measure of hydrophobicity. Dividing lines

based on  $\zeta_{w,i}$  were 1.1 for 2-group lumping, 1.0 and 1.3 for 3-group lumping, and 1.0, 1.1 and 1.3 for 4-group lumping.

Lumping by a combination of both vapor pressure and chemical structure was also investigated. Components were initially assigned to three groups according to vapor pressure. Components in the middle volatility group were then divided by chemical structure into two groups with aromatics in one group and non-aromatics in another. Lumping by both vapor pressure and activity coefficient in water was performed in a similar way. The intermediate volatility group was subdivided into a group with  $\zeta_{w,i} < 1.1$  and another with  $\zeta_{w,i} > 1.1$ .

### Lumping Model Evaluations

Lumping model performance was evaluated with three different organic aerosol systems. The first two compare yield predictions for mixtures of semivolatile components partitioning into an existing aerosol phase. A base case mixture of SOA products with various chemical structures and a set of random mixtures selected from identified aerosol products were used as semivolatile organic mixtures. Wood smoke and diesel soot mixtures at 0% and 80% relative humidity (RH) were used as absorbing aerosols. A third evaluation predicted the amount of organic aerosol mass formed from the reaction of  $\alpha$ -pinene and ozone in several smog chamber experiments.

#### *Base Case Mixture*

The lumping model was first tested with the base case mixture shown in Table 4.1.

Table 4.1. Base case mixture component properties and lumped group assignments

Component <sup>a</sup>	MW <sub>i</sub>	p <sub>i</sub> <sup>o*</sup> (torr)	Type <sup>k</sup>	ζ <sub>w,i</sub>	Activity Coefficient			
					wood 0%	smoke 80%	diesel 0%	soot 80%
fluoranthene <sup>b</sup>	202	1.20x10 <sup>-4 i</sup>	ARO	2.78	3.93	38.3	3.92	4.06
caronaldehyde <sup>c</sup>	168	9.15x10 <sup>-5 j</sup>	ALD	1.48	0.40	0.74	4.89	4.68
1,4-butanediol <sup>d</sup>	86	5.35x10 <sup>-5 e</sup>	ALD	1.57	0.71	0.90	10.9	10.5
glutaraldehyde <sup>e</sup>	100	2.72x10 <sup>-5 e</sup>	ALD	1.60	0.61	0.84	8.29	7.95
keto-limonic acid <sup>f</sup>	188	2.18x10 <sup>-5 i</sup>	SCA	0.94	2.32	0.84	122	99.4
heptadecanoic acid <sup>g</sup>	270	2.05x10 <sup>-5 i</sup>	LCA	1.29	4.45	12.4	1.22	1.16
6-oxo-hexanoic acid <sup>g</sup>	130	1.23x10 <sup>-5 e</sup>	SCA	1.06	0.93	0.78	10.4	9.33
stearic acid <sup>d</sup>	284	9.26x10 <sup>-6 i</sup>	LCA	1.30	4.94	14.8	1.19	1.13
norpinonic acid <sup>c</sup>	170	8.17x10 <sup>-6 e</sup>	SCA	1.11	0.90	0.91	7.15	6.48
norsabinic acid <sup>c</sup>	172	7.50x10 <sup>-6 e</sup>	SCA	1.01	2.14	1.24	12.3	10.6
3,4-dimethoxybenzoic acid <sup>h</sup>	182	6.90x10 <sup>-6 i</sup>	ARO	0.84	1.29	0.88	33.8	23.9
chrysene <sup>b</sup>	228	4.57x10 <sup>-6 i</sup>	ARO	2.63	4.13	47.9	4.33	4.48
pinic acid <sup>c</sup>	186	2.10x10 <sup>-6 e</sup>	SCA	1.02	2.03	1.41	6.41	5.49
docosanoic acid	340	3.15x10 <sup>-7 i</sup>	LCA	1.30	7.53	30.4	1.07	1.01
2-hydroxy-glutaric acid <sup>d</sup>	148	4.87x10 <sup>-8 e</sup>	SCA	0.90	3.13	0.88	454	353
hexacosanoic acid	396	8.02x10 <sup>-9 i</sup>	LCA	1.31	11.4	62.0	0.95	0.91

<sup>a</sup> α<sub>i</sub> = 0.06, B<sub>i</sub> = 10,000 K, T\* = 35 °C for all components.

<sup>b</sup> Harner and Bidleman, 1998

<sup>c</sup> Yu et al., 1999

<sup>d</sup> Kalberer et al., 2000

<sup>e</sup> Pankow et al., 2001

<sup>f</sup> Glasius et al., 2000

<sup>g</sup> Hemming and Seinfeld, 2001

<sup>h</sup> Forstner et al., 1997

<sup>i</sup> Joback and Reid, 1987; Myrdal and Yalkowsky, 1997

<sup>j</sup> Hallquist et al., 1997.

<sup>k</sup> Chemical structure type: ARO=aromatics, ALD=aldehydes or ketones, SCA=short-chained acids, LCA=long-chained acids.

Table 4.1. (continued)

Component <sup>a</sup>	Lumping Criteria <sup>1</sup>							
	VP				CH	VP+	WT	VP+
	1	2	3	4	4	CH	4	WT
fluoranthene <sup>b</sup>	a	a	a	a	a	a	b	a
caronaldehyde <sup>c</sup>	a	a	a	a	b	a	d	a
1,4-butanedial <sup>d</sup>	a	a	b	b	b	b	d	c
glutaraldehyde <sup>e</sup>	a	a	b	b	b	b	d	c
keto-limonic acid <sup>f</sup>	a	a	b	b	c	b	a	b
heptadecanoic acid <sup>g</sup>	a	a	b	b	d	b	c	c
6-oxo-hexanoic acid <sup>g</sup>	a	a	b	b	c	b	b	b
stearic acid <sup>d</sup>	a	a	b	b	d	b	c	c
norpinonic acid <sup>c</sup>	a	a	b	b	c	b	c	c
norsabinic acid <sup>c</sup>	a	a	b	b	c	b	b	b
3,4-dimethoxybenzoic acid <sup>h</sup>	a	b	b	c	a	c	a	b
chrysene <sup>b</sup>	a	b	b	c	a	c	d	c
pinic acid <sup>c</sup>	a	b	b	c	c	b	b	b
docosanoic acid	a	b	c	d	d	d	d	d
2-hydroxy-glutaric acid <sup>d</sup>	a	b	c	d	c	d	a	d
hexacosanoic acid	a	b	c	d	d	d	d	d

<sup>a</sup>  $\alpha_i = 0.06$ ,  $B_i = 10,000$  K,  $T^* = 35$  °C for all components.

<sup>b</sup> Harner and Bidleman, 1998

<sup>c</sup> Yu et al., 1999

<sup>d</sup> Kalberer et al., 2000

<sup>e</sup> Pankow et al., 2001

<sup>f</sup> Glasius et al., 2000

<sup>g</sup> Hemming and Seinfeld, 2001

<sup>1</sup> VP = Vapor pressure, CH = Chemical structure, WT = Activity coefficient in water.

The mixture contains 16 SOA compounds with various chemical structures. Each component is assigned an  $\alpha_i$  value of 0.06 such that the maximum possible yield for the mixture is 0.96. Component molecular weights,  $MW_i$ , range from 86 to 396. All components are assumed to have the same  $B_i = 10,000$  K, based on previous results (Bian and Bowman, 2002), representing a relatively large temperature dependence.  $p_i^{o*}$  values vary from  $1.20 \times 10^{-4}$  to  $8.02 \times 10^{-9}$  torr at 35°C. Base case components also vary in polarity, with  $\zeta_{w,i}$  values ranging from 0.84 to 2.78. Activity coefficients were calculated for the individual components at infinite dilution in wood smoke and diesel soot particles. Relatively non-polar components such as the long-chained acids have smaller  $\zeta_i$  values in diesel soot, while the more polar components prefer wood smoke particles. Lumped group assignments are also presented in Table 4.1 for each of the different lumping criteria. The letters a, b, c, or d denote the group to which a component has been assigned. 1, 2, 3, and 4 groups were tested for the vapor pressure lumping criteria. The other criteria all used 4 lumped groups.

Partitioning properties for each of the lumped compounds are listed in Table 4.2. For groups lumped by vapor pressure,  $p^{o*}$  values range from low to high volatility, but for groups lumped solely by chemical structure or water activity coefficient, components of high and low volatility are relatively evenly distributed among lumped groups, resulting in similar  $p^*$  values for all groups. Most lumped group activity coefficients are considerably larger in diesel soot than in wood smoke, except for chemical structure group 4d and water interaction group 4c, which are composed mostly of long-chained acids. Lumped  $B$  values are smaller than the individual  $B_i$  values because temperature



dependence of the lumped compound is moderated when components with high and low volatility are lumped together (Bian and Bowman, 2002).

Table 4.2. Base case mixture lumped group properties<sup>a</sup>

Lumped Group	$\alpha$	$p^{0*}$ (torr)	MW	B (K)	$\zeta_w$	Activity Coefficient			
						wood 0%	smoke 80%	diesel 0%	soot 80%
<i>Lumped by Vapor Pressure</i>									
1	0.96	4.41x10 <sup>-6</sup>	203	6008	1.11	0.98	1.55	3.60	3.26
2a	0.60	1.72x10 <sup>-5</sup>	177	8959	1.20	0.87	1.27	4.01	3.71
2b	0.36	1.09x10 <sup>-6</sup>	247	7362	1.03	1.24	2.20	3.09	2.70
3a	0.12	1.04x10 <sup>-4</sup>	185	9984	2.03	1.04	4.40	3.63	3.61
3b	0.66	8.84x10 <sup>-6</sup>	181	8964	1.07	0.98	1.23	4.91	4.39
3c	0.18	1.15x10 <sup>-7</sup>	295	9542	1.09	1.96	3.59	2.34	2.09
4a	0.12	1.04x10 <sup>-4</sup>	185	9984	2.03	1.04	4.40	3.63	3.61
4b	0.48	1.39x10 <sup>-5</sup>	175	9942	1.12	0.95	1.07	4.70	4.27
4c	0.18	3.89x10 <sup>-6</sup>	199	9646	1.01	1.26	2.14	6.50	5.56
4d	0.18	1.15x10 <sup>-7</sup>	295	9542	1.09	1.96	3.59	2.34	2.09
<i>Lumped by Chemical Structure</i>									
4a	0.18	8.95x10 <sup>-6</sup>	204	7819	1.22	1.57	6.68	4.73	4.31
4b	0.18	4.56x10 <sup>-5</sup>	118	9714	1.53	0.52	0.77	7.09	6.80
4c	0.36	3.64x10 <sup>-6</sup>	166	7215	0.99	1.56	0.88	25.7	21.8
4d	0.24	1.70x10 <sup>-6</sup>	322	5793	1.30	6.61	24.3	1.10	1.05
<i>Lumped by Vapor Pressure &amp; Chemical Structure</i>									
4a	0.12	1.04x10 <sup>-4</sup>	185	9984	2.03	1.04	4.40	3.63	3.61
4b	0.54	1.00x10 <sup>-5</sup>	176	8904	1.10	1.02	1.08	5.07	4.58
4c	0.12	5.56x10 <sup>-6</sup>	205	9935	1.06	1.23	3.47	6.45	5.51
4d	0.18	1.15x10 <sup>-7</sup>	295	9542	1.09	1.96	3.59	2.34	2.09
<i>Lumped by Water Interaction</i>									
4a	0.18	2.58x10 <sup>-6</sup>	173	5970	0.86	1.89	0.78	110	84.4
4b	0.24	7.29x10 <sup>-6</sup>	172	7645	1.15	1.29	1.69	5.48	4.97
4c	0.18	1.09x10 <sup>-5</sup>	241	9756	1.23	2.06	4.19	1.66	1.55
4d	0.36	3.12x10 <sup>-6</sup>	220	4723	1.50	1.10	3.37	1.96	1.90
<i>Lumped by Vapor Pressure &amp; Water Interaction</i>									
4a	0.12	1.04x10 <sup>-4</sup>	185	9984	2.03	1.04	4.40	3.63	3.61
4b	0.3	6.68x10 <sup>-6</sup>	172	9135	0.93	1.58	0.94	21.2	17.5
4c	0.36	1.17x10 <sup>-5</sup>	190	9084	1.40	1.01	2.38	2.23	2.14
4d	0.18	1.15x10 <sup>-7</sup>	295	9542	1.09	1.96	3.59	2.34	2.09

<sup>a</sup>  $T^* = 35$  °C,  $MW^* = 203$ ,  $M_o^* = 20$   $\mu\text{g m}^{-3}$ ,  $T_{high} = 50$  °C,  $T_{low} = 0$  °C

### *Random Mixtures*

The lumping model was also tested on mixtures composed of 16 aerosol components, randomly chosen from a set of 64 semivolatile organic aerosol compounds. Most of the dataset compounds are oxygenated organics or of high molecular weight. SOA products from compound classes without appropriate UNIFAC interaction parameters, such as organic nitrates, were not included.  $p_i^{o*}$  values were obtained from published predictions or were calculated based on the thermodynamic and chemical structural properties of the compound (Joback and Reid, 1987; Myrdal and Yalkowsky, 1997). All compounds were assumed to have  $B_i = 10,000$  K.  $\alpha_i$  values for each component were randomly chosen and normalized so that  $\sum \alpha_i = 1$ . As with the base case mixture, these random mixtures were divided into groups according to the lumping criteria discussed above.

### *Absorbing Aerosol Mixtures*

In model tests the base case and random mixtures of semivolatile components partition into an existing organic aerosol phase. The composition of this absorbing particulate mass significantly affects the partitioning process. Table 4.3 lists the absorbing aerosol mixtures used in this study - diesel soot and wood smoke at 0% and 80% RH. These mixtures are treated as nonvolatile and thus reside entirely in the aerosol phase. The composition of diesel soot uses the representative set of compounds suggested by Jang et al. (1997) and is relatively nonpolar. Wood smoke uses the model compositions from Chandramouli et al. (2003) and is much more polar. Aerosol water content was estimated from absorption partitioning theory using UNIFAC to calculate

aerosol phase activity coefficients. At 80% RH hydrophobic diesel soot absorbs only a small amount of water and its overall composition changes little, while more hydrophilic wood smoke absorbs a large amount of water that changes its composition dramatically.

Table 4.3. Absorbing aerosol mixtures

Component	MW <sub>i</sub>	$x_i$ (RH=0%)	$x_i$ (RH=80%) <sup>c</sup>
<i>Wood smoke</i> <sup>a</sup>			
hexadecanoic acid	256	0.19	0.0783
pentanedioic acid	132	0.07	0.0286
homovanillic acid	182	0.18	0.074
4-propylbenzenediol	152	0.28	0.1154
1-gualacylpropane	166	0.17	0.07
3,4-dimethoxybenzaldehyde	166	0.11	0.0455
water	18	0	0.5881
<i>Diesel soot</i> <sup>b</sup>			
heneicosane	296	0.45	0.4376
tetracosane	338	0.14	0.1358
hexanoic acid	116	0.11	0.1066
undecanoic acid	186	0.17	0.1654
hexadecanoic acid	256	0.06	0.0674
benzoic acid	122	0.07	0.0587
water	18	0	0.0285

<sup>a</sup>Jang et al., 1997

<sup>b</sup>Chandramouli et al., 2003

<sup>c</sup>Water content estimated based on UNIFAC predictions.

Compositional effects are most significant when the absorbing aerosol is highly dissimilar from the partitioning compounds. Yield curves for the detailed base case mixture in the different absorbing aerosols are shown in Figure 4.1. Compared to the yield predicted when composition effects are neglected (denoted by the solid line in Figure 4.1), the yield at 0% RH is considerably reduced for both wood smoke and diesel soot, indicating that neither system behaves ideally. Yields for diesel soot are much lower

than those for wood smoke because the relatively polar base case components partition into nonpolar diesel soot less readily than into more polar wood smoke. When RH increases from 0 to 80%, the organic aerosol yield increases approximately 20% for wood smoke, but changes little for hydrophobic diesel soot.

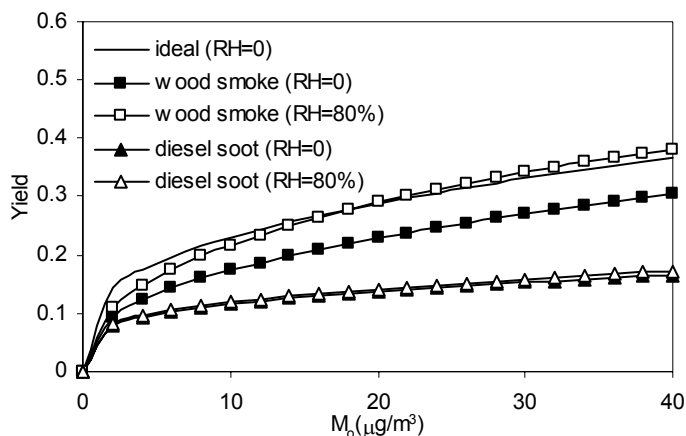


Figure 4.1. Organic aerosol yield predictions as a function of organic aerosol mass for full 16-component base case mixture. Ideal case and absorption into wood smoke and diesel soot at 0% and 80% relative humidity.

#### *$\alpha$ -Pinene/ $O_3$ Product Mixture*

A third set of trials tested the lumping model in simulations of several  $\alpha$ -pinene/ozone SOA experiments. Table 4.4 lists the individual semivolatile products, their partitioning properties, and lumping assignments. Product X represents unidentified aerosol mass and is treated as nonvolatile (Pankow et al., 2001).  $\alpha_i$  values are those measured by Yu et al. (1999), and  $p_i^{o*}$  values are those predicted by Pankow et al. (2001). A temperature dependence of  $B_i = 10,000$  K was assumed for all components. Following the lumping guidelines described previously, using  $T^* = 35$  °C,  $MW^* = 178$ , and  $M_o^* = 30$   $\mu\text{g m}^{-3}$ , components were divided into groups. For this mixture, lumping by vapor

pressure results in the same group assignments when using 3 or 4 groups. Chemical structure lumping divided the components into 3 groups: aldehydes, acids, and diacids. Lumping by any of the other criteria produces the same groups as lumping by vapor pressure alone, so these lumping assignments are not presented in Table 4.4. The full 9-component mixture and the lumped group mixtures were then used to predict the amount of organic aerosol mass,  $M_o$ , produced in six smog chamber experiments (Yu et al., 1999; Griffin et al., 1999).  $M_o$  was also predicted for each experiment using a 9-component mixture where  $\zeta_i = 1$ .

Table 4.4.  $\alpha$ -Pinene/ $O_3$  product mixture properties and lumping assignments

Component <sup>a</sup>	$\alpha_i$	$p_i^{o*}$ (torr)	$MW_i$	Lumping Criteria <sup>b</sup>			
				VP			CHEM
				1	2	3	3
norpinonaldehyde	0.0208	$1.74 \times 10^{-1}$	154	a	a	a	a
pinonaldehyde	0.1458	$4.63 \times 10^{-2}$	168	a	a	a	a
hydroxy pinonaldehydes	0.0762	$2.29 \times 10^{-4}$	184	a	a	a	a
norpinonic acid & isomers	0.1129	$8.17 \times 10^{-6}$	170	a	b	b	b
norpinic acid	0.0012	$7.50 \times 10^{-6}$	172	a	b	b	c
pinonic acid	0.0568	$2.22 \times 10^{-6}$	184	a	b	b	b
pinic acid	0.0661	$2.10 \times 10^{-6}$	186	a	b	b	c
hydroxy pinonic acid	0.0397	$2.03 \times 10^{-6}$	200	a	b	b	b
X (unidentified)	0.0167	$1.00 \times 10^{-12}$	184	a	b	c	b

<sup>a</sup> Yu et al., 1999; Pankow et al., 2001

<sup>b</sup> VP = vapor pressure, CHEM = chemical structure

## Results

### Base Case Mixture

Yield results for the base case mixture partitioning into each of the absorbing aerosol mixtures are shown in Figures 4.2 and 4.3.

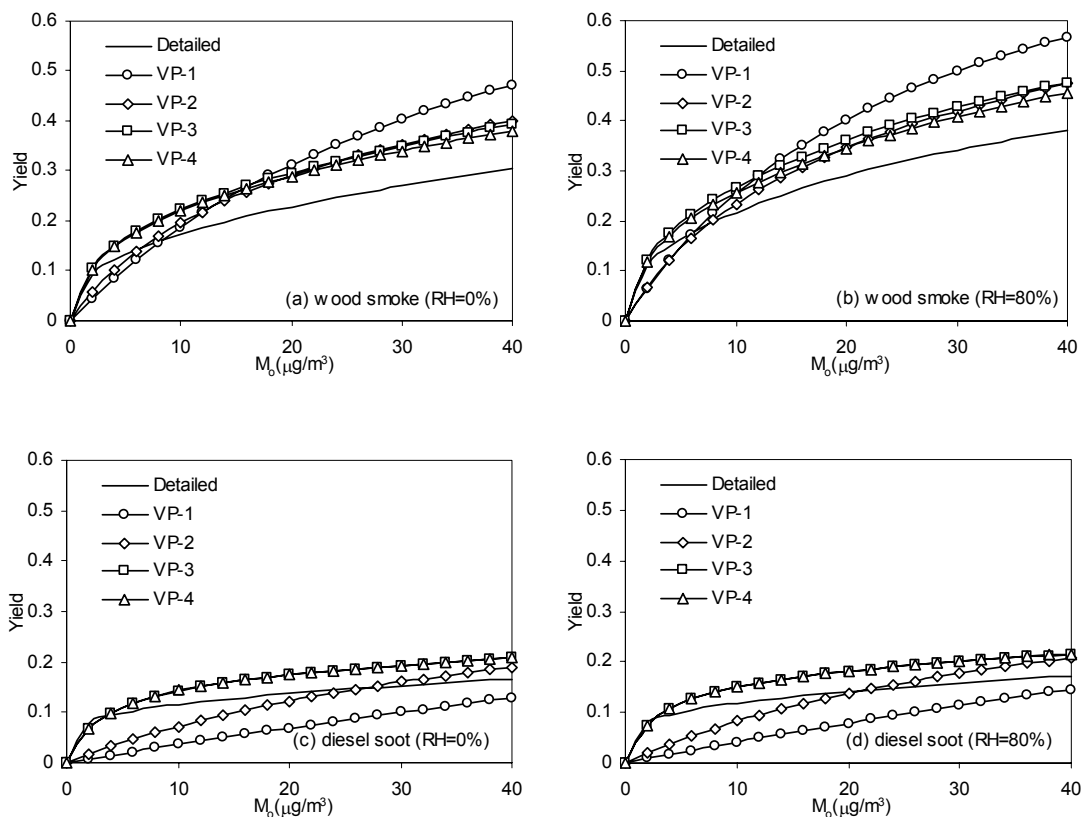


Figure 4.2. Organic aerosol yield predictions as a function of organic aerosol mass for lumped base case mixture using 1-4 vapor pressure lumped groups: (a) wood smoke at 0% RH, (b) wood smoke at 80% RH, (c) diesel soot at 0% RH, (d) diesel soot at 80% RH.

Figure 4.2 compares yield predictions using vapor pressure groups with the detailed mixture yield at  $T = T^* = 35^\circ\text{C}$ . When components are lumped into only one group, the yield curve is significantly different from the detailed yield for all absorbing

aerosol types. Even considering the large uncertainties that currently exist in our understanding of SOA formation, using a single lumped group produces unacceptable results. Diesel soot yields, for example, are underpredicted by over a factor of five at  $M_o \leq 4 \mu\text{g m}^{-3}$ . Additionally, for each case shown in Figure 4.2 the general shape of the yield curve is much different when only one lumped group is used. As the number of lumped groups increases, predictions get closer to the detailed yield, but even with 4 groups nonnegligible errors occur. For wood smoke (Figures 4.2a and 4.2b), 1- and 2-group lumping underpredict the yield at small  $M_o$  and overpredict it at large  $M_o$ , while 3- and 4-group lumping tend to overpredict the yield over most of the  $M_o$  range. For diesel soot (Figures 4.2c and 4.2d), 3- and 4-group lumping also overpredict the yield over most of the  $M_o$  range. Increasing relative humidity from 0% to 80% results in larger aerosol yields due to the presence of water in the absorbing aerosols, but it has no significant effect on lumping accuracy.

Errors seen with the current lumping model are in contrast to results from the earlier version, which did not include composition effects, where 3- or 4-group lumping approximated full mixture predictions extremely well (Bian and Bowman, 2002). By ignoring composition, however, the full mixture predictions themselves are in error as seen by the differences between yield curves in Figure 4.1. Accounting for composition makes the lumping challenge more difficult, but lumped predictions will still be more accurate than if composition were neglected. Yield predictions for vapor pressure lumped groups were also calculated as a function of temperature while holding  $M_o$  constant at 2, 20, and  $40 \mu\text{g m}^{-3}$ . The results are similar to findings in the previous study (Bian and Bowman, 2002). As temperature increases, vapor pressures rise, leading to a lower yield.

Consistent with results at constant temperature, lumping into 1 or 2 groups causes relatively large errors, while accuracy improves somewhat when more groups are used.

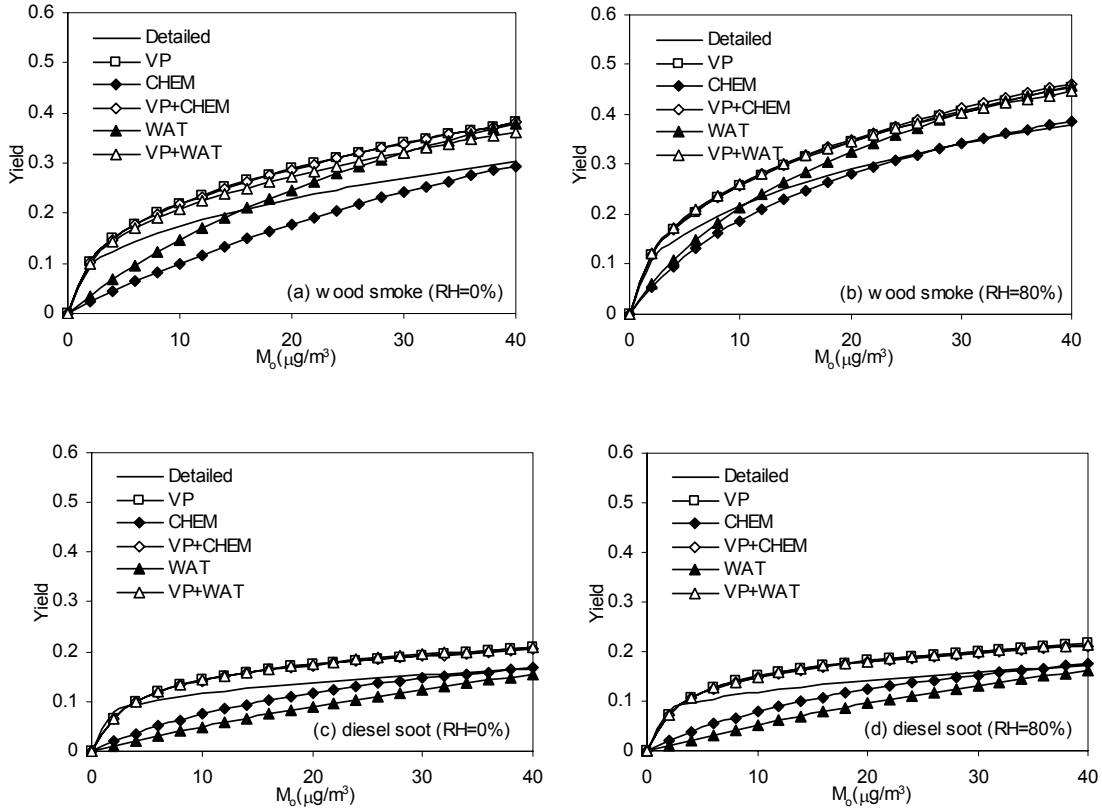


Figure 4.3. Organic aerosol yield predictions as a function of organic aerosol mass for lumped base case mixture using different lumping criteria: (a) wood smoke at 0% RH, (b) wood smoke at 80% RH, (c) diesel soot at 0% RH, (d) diesel soot at 80% RH.

Figure 4.3 compares the yield predicted using different lumping criteria. For all absorbing aerosol types, dividing the mixture according to chemical structure alone underpredicts the yield over most of the  $M_o$  range. When lumping by  $\zeta_{w,i}$ , yield is underpredicted at smaller  $M_o$  and overpredicted at larger  $M_o$  for wood smoke particles, and underpredicted over the entire  $M_o$  range for diesel soot particles. Lumping by vapor pressure and chemical structure together or vapor pressure and water activity coefficient



together produces yields similar to those obtained when lumping by vapor pressure alone, with overpredictions at most  $M_o$  values.

Root-mean-square (RMS) errors in the dimensionless aerosol yield over the entire  $M_o$  range at  $T = 35^\circ\text{C}$  are shown in Table 4.5 for different lumping criteria. With vapor pressure lumping, error decreases about 50% as the number of lumped groups increases from 1 to 2. However, 3-group lumping has larger RMS errors than 2-group lumping for all types of absorbing aerosol, and for diesel soot, 4-group lumping performs no better. Although 3- and 4-group lumping overpredict yield at all  $M_o$  values for this mixture, they fit the overall shape of the detailed yield curve better. With other mixtures, lumping accuracy should generally improve as more groups are used. There are no consistent trends in how water uptake influences lumping accuracy for the base case mixture, with errors changing little when RH varies from 0% to 80%.

Table 4.5. RMS errors in aerosol yield for base case mixture and random mixtures

Lumping Criteria <sup>a</sup>	Number of Groups	RMS Errors							
		Base Case Mixture				Random Mixtures			
		wood smoke		diesel soot		wood smoke		diesel soot	
		0%	80%	0%	80%	0%	80%	0%	80%
VP	1	0.100	0.119	0.063	0.059	0.112	0.154	0.196	0.187
VP	2	0.064	0.060	0.031	0.031	0.051	0.055	0.108	0.100
VP	3	0.066	0.069	0.035	0.037	0.027	0.047	0.030	0.028
VP	4	0.058	0.054	0.034	0.036	0.023	0.033	0.028	0.026
CHEM	4	0.051	0.023	0.030	0.029	0.093	0.104	0.031	0.031
VP + CHEM	4	0.057	0.058	0.032	0.034	0.027	0.048	0.015	0.015
WAT	4	0.045	0.047	0.048	0.047	0.105	0.190	0.045	0.044
VP + WAT	4	0.043	0.053	0.035	0.035	0.021	0.034	0.014	0.014

<sup>a</sup> VP = vapor pressure, CHEM = chemical structure, WAT = activity coefficient in water

With the base case mixture, lumping by chemical structure alone generally produces the smallest RMS errors. Since the 16 base case components have distinctly different chemical structures but many have similar vapor pressures, categorizing them by structure instead of by vapor pressure provides better results in this specific case. As will be seen with the random mixture results, chemical structure alone is typically not the best lumping criteria.

### *Random Mixtures*

Yield predictions for 200 random sets of 16-component aerosol mixtures were calculated similarly. Average RMS errors in yield for these 200 mixtures are also listed in Table 4.5. Unlike base case mixture results, accuracy steadily improves as additional  $p^{0*}$ -based lumped are used. Lumping solely by chemical structure or water interaction produces relatively large errors, especially for wood smoke. Lumping a mixture of diverse components based on similar functional groups or water interaction alone, while neglecting vapor pressure entirely, does not accurately predict the yield. For wood smoke, the most accurate lumping criteria are vapor pressure alone (average error of 0.023 at 0% RH and 0.033 at 80% RH) or a combination of vapor pressure and activity coefficient in water (0.021 at 0% RH and 0.34 at 80% RH). For diesel soot, lumping by  $p^{0*}$  and  $\zeta_{w,i}$  together produces the smallest average error of 0.014, and lumping by both vapor pressure and chemical structure has a slightly larger error of 0.015. Overall, these results suggest that a combination of vapor pressure and water interaction works best as a lumping criterion.

### *$\alpha$ -Pinene/O<sub>3</sub> Products*

Table 4.6 shows experimental conditions for the seven  $\alpha$ -pinene/O<sub>3</sub> experiments together with predicted aerosol mass,  $M_o$ , using various lumping criteria. Detailed  $M_o$  is the aerosol mass predicted using the full 9-component mixture described in Table 4.4. It shows good agreement with the experimentally determined aerosol mass,  $M_{o,exp}$ , for all experiments except the two with low  $\Delta HC$  and  $M_o$ . Ideal  $M_o$  predictions are also based on the detailed mixture, but neglect composition dependence, setting  $\zeta_i=1$ . The difference between ideal predictions and experimental values is much larger, indicating that taking composition effects into account provides a much better approximation.

Table 4.6. Experimental and predicted organic aerosol mass for  $\alpha$ -pinene/O<sub>3</sub> product mixture.

$T$ (K)	$\Delta HC$ ( $\mu\text{g m}^{-3}$ )	$M_{o,exp}$ ( $\mu\text{g m}^{-3}$ )	Predicted $M_o$ ( $\mu\text{g m}^{-3}$ )					
			Detailed (ideal)	Detailed	Lumping Criteria <sup>a</sup>			
					VP-1	VP-2	VP-3	CHEM
308	350	65.1	87.0	65.6	95.5	68.2	67.1	79.8
308	308	54.2	70.6	54.0	72.9	55.5	54.8	59.8
306	244	38.8	55.2	42.3	47.0	42.9	42.6	46.6
310	89	7.4	3.08	3.25	0.0	0.0	3.12	0.0
310	98	8.5	3.71	3.92	0.0	0.0	3.67	0.0
303	169	30.3	37.2	28.6	18.2	28.3	28.5	31.3
303	250	46	69.2	51.3	61.5	52.7	52.3	55.1

<sup>a</sup> VP = Vapor pressure, CHEM = Chemical structure.

$M_o$  predictions improve as the number of vapor pressure groups increases, in agreement with random mixture test results. With a single vapor pressure group,  $M_o$  is significantly overpredicted when  $M_o > M_o^*$ , and underpredicted when  $M_o < M_o^*$ . For low  $M_o$  experiments, the underprediction is such that no organic aerosol is predicted to form.

With two lumped groups,  $M_o$  predictions are close to detailed  $M_o$  for all but the low  $M_o$  experiments, which continue to show no aerosol formation. Three lumped groups predicts organic aerosol levels similar to those obtained with the detailed mixture for both the low and high  $M_o$  experiments. Lumping into 3 groups by chemical structure results in much larger errors, indicating that vapor pressure provides the best lumping criteria for the  $\alpha$ -pinene/ $O_3$  experimental system.

### Conclusions

An improved lumping model was developed for converting multiple semivolatile organic aerosol components into lumped groups. Lumping equations to calculate temperature and composition dependent partitioning parameters were presented, as well as lumping criteria based on component vapor pressure, chemical structure, and activity coefficient in water. Trials were performed on several SOA systems: base case and random mixtures of semivolatile organics partitioning into wood smoke and diesel soot absorbing aerosols, and organic products from the reaction of  $\alpha$ -pinene and  $O_3$  in smog chamber experiments.

Evaluation results show that aerosol mixture composition has a strong influence on gas/particle partitioning and lumping performance of the model. When composition effects are integrated into the lumping model, predicted SOA yields are more accurate and lower than when an ideal solution is assumed. In the previous model, where composition is not considered, 3- and 4-group lumping approximated the partitioning behavior of the full mixture very well, but in the new model even 4-group lumping produces nonnegligible lumping errors. It is important to emphasize, however, that while

incorporating composition makes the aerosol system more complex and the lumping challenge more difficult, lumped predictions are still likely to be more accurate than if composition were neglected.

Comparisons of different lumping criteria show that lumping performance generally improves as the number of groups increases. Criteria that neglect component vapor pressure entirely produce relatively large errors. Results suggest that forming lumped groups based on a combination of vapor pressure and water interaction will produce the best results on average for all types of absorbing aerosols. Lumping by vapor pressure alone also works reasonably well, however, and since it requires fewer calculations, may be a more reasonable alternative. Further refinement of lumping criteria could also lead to improved lumping performance. For current atmospheric modeling applications, where uncertainties in SOA formation remain quite large, the selection of an appropriate number of lumped groups will likely be governed by computational limitations. This work provides guidance on the optimum criteria for lumping and helps define the additional uncertainty introduced when using a simplified lumped approximation of the detailed organic aerosol mixture.

## CHAPTER V

### DEVELOPING PARTITIONING PARAMETERS OF SOA PRODUCTS FROM MULTIPLE HYDROCARBON PRECURSORS FOR USE IN THE CMAQ AIR QUALITY MODEL

#### Introduction

In Chapter III and Chapter IV, a theoretical model was developed that can successfully convert multiple secondary organic aerosol components into lumped compounds and effectively represent the whole aerosol mixture and relate the partitioning properties of lumped compounds to those of individual aerosol components. For simplification purpose in developing the lumping method, the initial evaluations described in the previous chapters assume that the secondary organic aerosol components to be lumped are generated from a single hydrocarbon precursor or are part of a single mixture. But the real atmospheric condition is much more complicated than this theoretical simplification. In the atmosphere, hundreds of hydrocarbons from many different sources form secondary organic aerosol. Air quality models that simulate these processes try to describe the connection between hydrocarbon emission sources and observed aerosol component concentrations. For a single hydrocarbon precursor, the resulting products are relatively similar physically and chemically, providing a reasonable basis for lumping them together. With multiple hydrocarbon precursors, however, SOA components will have a much wider range of chemical structures and properties. To develop a meaningful lumping scheme for use in air quality modeling, it is necessary to move forward and apply the model to investigate the partitioning behavior of aerosol mixtures produced by multiple hydrocarbon precursors from multiple sources.

As described previously, secondary organic aerosols are formed when volatile hydrocarbons are oxidized in the atmosphere. Hundreds of different hydrocarbons from both anthropogenic and biogenic sources act as aerosol precursors in the ambient atmosphere, most producing dozens of individual aerosol products. The semivolatile products from the oxidation will then partition between gas and aerosol phases. It is nearly impossible to identify and quantify each of the semivolatile products formed from these precursors and their physical or chemical properties. To appropriately represent this complicated dynamic system, simplified approaches are necessary to incorporate aerosol formation and partitioning process into air quality models.

The general approach is to use a small number of model compounds to represent these hundreds of different organic species. One common approach is to use a 2-product model to fit smog chamber experimental results (Odum et al., 1996; Hoffmann et al., 1997; Griffin et al., 1999; Kalberer et al., 2000), where the two products represent the real multicomponent aerosol mixture. This 2-product fitting approach is applied in air quality models such as CMAQ (Binkowski, 1999) and PMCAMx (Environ, 2003). Further simplification is possible when aerosol-forming hydrocarbons that form similar products can be treated as a single class of precursor, such as has been shown for the aromatic fraction of gasoline (Odum et al., 1997). Another approach is to choose a few specific aerosol products to represent the whole mixture as surrogate compounds for the other individual aerosol products. The Caltech Atmospheric Chemistry Mechanism (CACM) (Griffin et al, 2002; Seinfeld et al., 2002) is one application of this approach.

These approaches greatly simplify the work of integrating SOA into air quality models, but they do not provide a fundamental understanding of the detailed chemical

structure and other partitioning properties of the individual components in the detailed aerosol mixture. The lumped method described in the above chapters is an original approach to this problem and has been shown to approximate the detailed SOA mixture quite well. In this method, lumped parameters are calculated directly from the properties of the individual mixture components. It provides a theoretical framework that can be expanded in the future to include more SOA products and partitioning conditions.

In this chapter, the lumping method is applied to study representative atmospheric mixtures of SOA products from multiple hydrocarbon precursors. A detailed set of SOA products is compiled based on experimentally identified and theoretically predicted reaction products. The properties of each individual SOA component are determined from published experimental data or by theoretical estimation. The lumping method described in Chapter IV is used to lump the individual components into a small number of representative SOA products, suitable for inclusion in an updated aerosol module for the CMAQ air quality model.

### Current Representation of SOA in CMAQ

The Community Multi-scale Air Quality (CMAQ) modeling system is an air quality model developed by the U.S. EPA. The system has three major components, meteorology, emissions, and chemical transport model, along with several interface processors. With a flexible structure, CMAQ can incorporate output from different emission and meteorological modeling systems and other data sources through special interface processors into the CMAQ Chemical Transport Model (CCTM), which performs chemical transport modeling for multiple pollutants on multiple scales. Current



version of CMAQ uses the Fifth-Generation NCAR / Penn State Mesoscale Model (MM5) for meteorological simulation, and the Sparse Matrix Operator Kernel Emissions (SMOKE) modeling system for the emissions processing. The CCTM is also designed with a modular structure, allowing different science components to be interchanged. Gas-phase chemistry, for example, can be described with RADM2 (Stockwell et al., 1990; Gross and Stockwell, 2003), CB4 (Gery et al., 1989), or SAPRC99 chemical mechanisms (Carter 2000a; 2000b).

CMAQ can be used to study air quality issues nation-wide, region-wide or in smaller scales. In recent years, it has been used extensively to simulate ambient fine particle concentrations for both regulatory and research applications (Byun and Ching, 1999; Schere, 2002; Bailey et al., 2002; Eder et al., 2002; Yu et al., 2003; Godowitch, 2004). CMAQ's module structure allows it to incorporate latest scientific research findings into its different modules. The aerosol module in CMAQ has been frequently updated since CMAQ's first release in 1998 and its development is described in detail by Binkowski and Roselle (Binkowski and Roselle, 2003). In June 2002, the aerosol module in CMAQ, *aero3*, was updated with improved treatments of secondary organic aerosol formation. An absorption mechanism (Schell, 2001) was adopted to describe SOA partitioning. The most recent update of the aerosol module was released to the public in CMAQ Version 4.4 in Fall 2004 and will be described further below.

Like all air quality models, CMAQ uses a simplified representation of SOA formation in its aerosol module. The hydrocarbon precursors to SOA are defined by the specific gas-phase chemistry mechanism used in CMAQ. For the SAPRC99 mechanism (Carter 2000a; 2000b), the current aerosol module defines 6 classes of SOA hydrocarbon

precursors as shown in Table 5.1. It contains 1 biogenic and 5 anthropogenic precursors: monoterpenes (TRP1), three categories of aromatics (ARO1; ARO2; CRES), internal alkenes (OLE2), and long alkanes (ALK5). Each precursor is assumed to form 1 or 2 semivolatile products that condense to the aerosol phase, with a total of 10 SOA products.

The gas/particle partitioning parameters of the 10 condensable products currently in CMAQ are also shown in Table 5.1. These 10 products are not real chemical compounds but hypothetical model species. Their chemical formula and thermodynamic properties are unknown. The mass-based stoichiometric coefficient,  $\alpha_i$ , and the effective saturation concentration,  $C_{sat,i}^*$  are simply empirical evaluations based on smog chamber experimental data (Odum et al., 1997; Griffin et al., 1999; Kalberer et al., 2000), or from published estimates (Strader et al., 1999) where smog chamber data is unavailable, such as for alkanes and cresol.  $\alpha_i$  values are taken directly from the experimental data.  $C_{sat,i}^*$  is the reciprocal of experimental  $K_i$  values adjusted to 298 K using the Sheehan and Bowman method (Sheehan and Bowman, 2001), since most of the smog chamber experiments were carried out at a higher temperature. The molecular weights of anthropogenic reaction products are assumed to be an arbitrary 150 g/mol. The molecular weights of the biogenic products are assumed to be 177 g/mol, based on average of pinionaldehyde (168 g/mol) and pinonic acid (186 g/mol)

Table 5.1. Current SOA precursors and partitioning parameters in CMAQ (EPA, 2004).

Hydrocarbon Precursors	$MW_i$	$\alpha_i$	$C_{sat,i}^*$ ( $\mu\text{g}/\text{m}^3$ )
Monoterpenes (TRP1)	184	0.0864	0.865
		0.3857	11.804
Aromatics like toluene (ARO1)	150	0.071	1.716
		0.138	47.855
Aromatics like xylene (ARO2)	150	0.038	2.165
		0.167	64.946
Aromatics like cresol (CRES)	150	0.05	0.2611
Internal alkenes (cyclohexene, OLE2)	150	0.36	111.11
		0.32	1000.0
Long alkanes (ALK5)	150	0.0718	0.3103

In the current CMAQ aerosol module, the secondary organic aerosol formation process is represented using an absorptive partitioning mechanism with temperature-dependent partitioning coefficients. However, the effect of aerosol composition on SOA partitioning is not accounted for and the activity coefficient  $\zeta_i$  of all compounds is assumed to be unity. To better represent interactions between chemically dissimilar aerosol components, the aerosol module in CMAQ also needs to be updated to include composition dependence. Aerosol composition effects have only recently begun to be included in air quality models (Pun et al, 2002; Griffin et al., 2002).

#### Formulating New SOA Precursors and Products

In current CMAQ aerosol module, SOA partitioning is described with empirically assigned aerosol partitioning coefficients for up to two hypothetical reaction products from each hydrocarbon precursor. Although the yield data from smog chamber experiments can be fitted well using these empirical values, this approach provides

limited insight to the chemical structure of the SOA products. For a more detailed representation of SOA formation process, an updated set of SOA precursors, products, and partitioning parameters has been developed.

For the purpose of easy integration into current CMAQ aerosol module, the updated SOA representation retains the same basic structure as the current version. A small number of hydrocarbon compounds from the SAPRC99 gas phase chemistry mechanism are used as SOA precursors. Each precursor compound forms two lumped semivolatile products that are defined by the current parameters,  $\alpha_i$ ,  $C_{sat,i}^*$ ,  $MW_i$ , and new chemical structure parameters,  $s_{ji}$ .

The new aerosol module includes several important modifications. First, the classification of hydrocarbon compounds as SOA precursors has been reviewed and updated to better account for the contributions from individual precursors. Following the structure of the gas-phase chemistry mechanism, hydrocarbon precursors with similar chemical structure are grouped together into several major compound classes. Individual hydrocarbon precursors are weighted according to their significance of emission. The updated categorization reduces the number of SOA precursor classes from the original 6 to 5. One biogenic class (TRP1) represents monoterpene precursors such as  $\alpha$ -pinene,  $\beta$ -pinene, and limonene. Four anthropogenic classes (ARO1, ARO2, OLE2, ALK5) represent, respectively high-yield aromatics like toluene and ethylbenzene; low-yield aromatics like xylene and trimethylbenzene; internal alkenes such as cyclohexene; and long-chain alkanes. Cresol is a separate precursor class in the current CMAQ aerosol module, but is assumed to have the same products as the high-yield aromatics in the

updated version due to its relatively minor emission rate compared with other aromatic precursors.

Next, for each class of HC precursors, partitioning parameters of the two semivolatile products used in the model have been completely revised. Individual SOA products from each HC precursor are used to define the properties of the lumped products in the model. The selection of individual SOA products is based on specific species identified in smog chamber experiments or theoretically predicted to be able to condense to particle phase. The partitioning parameters of the lumped compounds are not simply an empirical fit from experimental results, but are directly derived from the parameters of the individual SOA components. Finally, chemical structure parameters for each species have been added to include the effects of aerosol composition on gas-aerosol partitioning. The parameter of a lumped group  $s_{ji}$  represents the number of UNIFAC functional groups  $j$  in the lumped compound.

The new SOA precursors, products, partitioning properties and the detailed chemical structure for each individual component are shown in Tables 5.2 – 5.10. The  $\alpha_i$  values were obtained from experimental data or estimated and adjusted by emissions-based weighting factors for the precursors.  $p_i^{0*}$  values were obtained from published predictions or calculated based on the thermodynamic and chemical structural properties of the compound (Joback and Reid, 1987; Myrdal and Yalkowsky, 1997), at a reference temperature of  $T = 308$  K. All compounds were assumed to have a temperature dependence of  $B_i = H_i / R = 10,000$  K (Sheehan and Bowman, 2001).

### *Biogenics (TRP1)*

For biogenic emissions, monoterpenes are expected to be the predominant SOA precursor compounds. Sesquiterpenes may also be biogenic emission contributors (Hoffmann et al., 1997; Bonn and Moortgat, 2003; Jaoui and Kamens, 2003a, 2003b), but they are emitted at much lower rates and much less is known about their SOA formation pathways. They are not included in this study due to these reasons and because of limitations in the emissions data used as input for CMAQ simulations. The major components of biogenic monoterpenes contributing to aerosol formation are  $\alpha$ -pinene,  $\beta$ -pinene,  $\Delta^3$ -carene, sabinene and limonene (Andersson-Sköld and Simpson, 2001). They have also been the most commonly studied species in smog chamber experiments (Yu et al., 1998, 1999; Hoffmann et al., 1998; Jang 1999, Glasius et al., 1999, 2000; Koch et al., 2000; Larsen et. al., 2001; Jaoui and Kamens, 2003). Most of the major semivolatile aerosol products from the oxidation reactions of these species have been identified, and many of their stoichiometric coefficients have been measured (Yu et al., 1999).

The identified products from these 5 monoterpenes were used to define a detailed mixture of semivolatile components produced by the biogenic hydrocarbon TRP1, as shown in Table 5.2. The stoichiometric coefficient  $\alpha_i$  for each component was obtained from reported experimental data (Yu et al., 1999; Pankow et al., 2001) and weighted by the emissions of the parent monoterpene. The emissions-based weighting factors are those currently used in CMAQ, 0.4, 0.25, 0.15, 0.1, and 0.1, respectively for  $\alpha$ -pinene,  $\beta$ -pinene,  $\Delta^3$ -carene, sabinene, and limonene. The vapor pressure  $p_i^{0*}$  for each component is obtained from predicted data (Pankow et al., 2001) and adjusted to the value at the

reference temperature (Sheehan and Bowman, 2001). The detailed chemical structure of each compound is shown in Table 5.3.

Table 5.2. SOA products and individual partitioning properties for monoterpenes (TRP1).

Precursor	SOA Components <sup>a</sup>	$\alpha_i^b$	$p_i^{o*a,c}$ (torr)	MW <sub>i</sub>
TRP1	pinonaldehyde	0.1458	1.07 x10 <sup>-4</sup>	168
	hydroxy pinonaldehyde	0.0762	2.29 x10 <sup>-4</sup>	184
	norpinonic acid	0.1129	8.17 x10 <sup>-6</sup>	170
	norpinic acid	0.0012	7.50 x10 <sup>-6</sup>	172
	pinonic acid	0.0568	2.22 x10 <sup>-6</sup>	184
	pinic acid	0.0661	2.10 x10 <sup>-6</sup>	186
	hydroxy pinonic acid	0.0397	2.03 x10 <sup>-6</sup>	200
	limonic acid	0.0661	1.10 x10 <sup>-4</sup>	186
	limononic acid	0.0568	3.37 x10 <sup>-3</sup>	184
	norlimonic acid	0.0012	2.28 x10 <sup>-4</sup>	172
	norlimononic acid	0.1129	3.40 x10 <sup>-3</sup>	170
	hydroxy norpinonic acid	0.0032	6.93 x10 <sup>-6</sup>	186
	3-caric acid	0.0039	2.10 x10 <sup>-6</sup>	186
	3-caronic acid	0.0085	1.46 x10 <sup>-3</sup>	184
	nor-3-caronic acid	0.0043	5.55 x10 <sup>-3</sup>	170
	caronaldehyde	0.0158	9.15 x10 <sup>-5</sup>	168
	hydroxy 3-caronic acid	0.0024	2.03 x10 <sup>-6</sup>	200
	sabinic acid	0.0016	2.10 x10 <sup>-6</sup>	186
	norsabinic acid	0.0003	7.50 x10 <sup>-6</sup>	172
	norsabinonic acid	0.0059	8.17 x10 <sup>-6</sup>	170
sabina ketone	0.0079	9.49 x10 <sup>-3</sup>	138	

<sup>a</sup> Pankow et al., 2001.

<sup>b</sup> values from Pankow et al., 2001 weighted by parent monoterpene emissions

<sup>c</sup> Sheehan and Bowman, 2001

Table 5.3. Chemical structure of individual SOA components for monoterpenes (TRP1).

SOA Components	Structure	SOA Components	Structure
pinonaldehyde		hydroxy norpinonic acid	
hydroxy pinonaldehyde		3-caric acid	
norpinonic acid		3-caronic acid	
norpinic acid		nor-3-caronic acid	
pinonic acid		caronaldehyde	
pinic acid		hydroxy 3-caronic acid	
hydroxy pinonic acid		sabinic acid	
limonic acid		norsabinic acid	
limononic acid		norsabinonic acid	
norlimonic acid		sabina ketone	
norlimononic acid			



### *High Yield Aromatics (ARO1)*

Aromatics are by far the most significant anthropogenic SOA precursors (Odum et al., 1996, 1997). Prevalent in gasoline, they are emitted by fuel combustion and evaporation and contribute significantly to air pollution in urban areas. Benzene, toluene, ethylbenzene, xylenes, and trimethylbenzenes are the greatest contributors to aromatic emissions. For this new SOA formulation, aromatics are grouped into two precursor classes: high-yield and low-yield aromatics, following the suggestion of Odum et al. (1997). In the gas-phase chemistry mechanism, high-yield aromatics are represented by ARO1 which includes major aromatic compounds such as toluene and ethylbenzene. Aromatics like cresol (CRES in current CMAQ) are minor contributors to aerosol formation due to relatively small emissions and are assumed to form the same semivolatile products as the high-yield aromatics. A variety of aerosol products have been identified from the photooxidation of toluene and ethylbenzene (Fostner et al., 1997; Smith, et al., 1998; Jang and Kamens, 2001; Kleindienst, 2004), but a complete characterization of all the major products, with quantitative stoichiometric coefficients, has not yet been achieved. For the other aromatics known to be high-yield aerosol precursors, there is relatively limited information regarding product identification.

Because product identification and quantification is incomplete, a few specific products, expected to be representative of the semivolatile components produced by ARO1, were selected from compounds identified in photooxidation experiments of toluene and ethylbenzene, as listed in Table 5.4. Their chemical structural information is shown in Table 5.5.

Table 5.4. SOA products and individual partitioning properties for high-yield aromatics (ARO1).

Precursor	SOA Components <sup>a</sup>	$\alpha_i$	$p_i^{o* d}$ (torr)	MW <sub>i</sub>
ARO1	phenol <sup>a</sup>	0.073	8.59 x10 <sup>-4</sup>	94
	2-hydroxybenzoic acid <sup>b</sup>	0.073	3.76 x10 <sup>-4</sup>	138
	p-cresol <sup>a</sup>	0.073	3.47 x10 <sup>-4</sup>	108
	4-ethylbenzaldehyde <sup>a</sup>	0.073	3.24 x10 <sup>-4</sup>	134
	sec-phenethyl alcohol <sup>b</sup>	0.073	3.30 x10 <sup>-4</sup>	122
	benzyl alcohol <sup>a</sup>	0.073	2.82 x10 <sup>-4</sup>	108
	3-hydroxy benzaldehyde <sup>b</sup>	0.073	5.13 x10 <sup>-5</sup>	122
	benzoic acid <sup>c</sup>	0.073	3.18 x10 <sup>-5</sup>	122
	4-oxo-2-butenoic acid <sup>c</sup>	0.073	2.14 x10 <sup>-5</sup>	100
	p-toluic acid <sup>a</sup>	0.073	9.07 x10 <sup>-6</sup>	136
	4-oxo-2-pentenoic acid <sup>c</sup>	0.073	8.92 x10 <sup>-6</sup>	114

<sup>a</sup> Forstner et al., 1997.

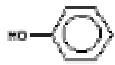
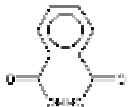





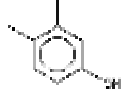
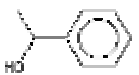
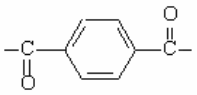
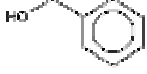
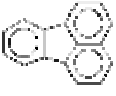


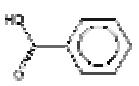

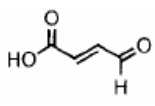
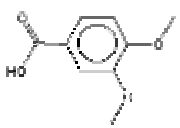
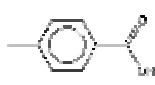

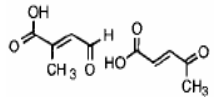
<sup>b</sup> Smith et al., 1998.

<sup>d</sup> Jang and Kamens, 2001.

<sup>d</sup> Joback and Reid, 1987; Myrdal and Yalkowsky, 1997.

Because experimentally derived stoichiometric yield data are not available, the stoichiometric coefficients for each aromatic product are assumed to be the same. The specific value of  $\alpha_i$  for these products was selected to provide a good agreement with experimental yield data. Although this representation of the aromatic products is only a rough estimate, considering the lack of detailed experimental product data, it is a reasonable initial step in describing the aerosol composition. Vapor pressures are calculated based on the thermodynamic and chemical structural properties of the compound (Joback and Reid, 1987; Myrdal and Yalkowsky, 1997).

Table 5.5. Chemical structure of individual SOA components for high-yield (ARO1) and low-yield (ARO2) aromatics.

SOA Components (ARO1)	Structure	SOA Components (ARO2)	Structure
phenol		phthalic acid	
2-hydroxybenzoic acid		m-tolualdehyde	
p-cresol		2,5-dimethylphenol	
4-ethylbenzaldehyde		3,4-dimethylphenol	
sec-phenethyl alcohol		1,2-benzenedicarboxyl	
benzyl alcohol		fluoranthene	
3-hydroxy benzaldehyde		pyrene	
benzoic acid		2,4,6-trimethylbenzoic acid	
4-oxo-2-butenoic acid		3,4-dimethoxybenzoic acid	
p-toluic acid		chrysene	
4-oxo-2-pentenoic acid			

### Low Yield Aromatics (ARO2)

The low-yield aromatic precursor compounds are represented by ARO2 which includes xylene, trimethylbenzene, and polycyclic aromatic hydrocarbons (PAHs). As with the high-yield aromatics, product information is incomplete. Representative semivolatile components were selected from identified products of xylene and trimethylbenzene (Forstner et al., 1997; Smith et al., 1999), as well as known aerosol phase PAHs (Harner and Bidleman, 1998.). These components were chosen based on their volatility and abundance in ambient aerosol phase. The properties of these compounds are listed in Table 5.6, and their structural information is shown in Table 5.5.

Table 5.6. SOA products and individual partitioning properties for low-yield aromatics (ARO2).

Precursor	SOA Components	$\alpha_i$	$p_i^{o*e}$ (torr)	MW <sub>i</sub>
ARO2	phthalic acid <sup>a</sup>	0.048	1.93 x10 <sup>-3</sup>	222
	m-tolualdehyde <sup>b</sup>	0.048	9.59 x10 <sup>-4</sup>	120
	2,5-dimethylphenol <sup>b</sup>	0.048	2.42 x10 <sup>-4</sup>	122
	3,4-dimethylphenol <sup>b</sup>	0.048	1.06 x10 <sup>-4</sup>	122
	1,2-benzenedicarboxyl <sup>b</sup>	0.048	2.17 x10 <sup>-4</sup>	166
	fluoranthene <sup>c</sup>	0.048	1.20 x10 <sup>-4</sup>	202
	pyrene <sup>c</sup>	0.048	7.94 x10 <sup>-5</sup>	202
	2,4,6-trimethylbenzoic acid <sup>d</sup>	0.048	1.64 x10 <sup>-5</sup>	164
	3,4-dimethoxybenzoic acid <sup>d</sup>	0.048	6.90 x10 <sup>-6</sup>	182
	chrysene <sup>c</sup>	0.048	4.57 x10 <sup>-6</sup>	228

<sup>a</sup> Zheng et al., 2002

<sup>b</sup> Smith et al., 1999.

<sup>c</sup> Harner and Bidleman, 1998.

<sup>d</sup> Forstner et al., 1997.

<sup>e</sup> Joback and Reid, 1987; Myrdal and Yalkowsky, 1997.

Same as the high-yield aromatics, their stoichiometric coefficients are set to agree with experimental yield data are assumed to be the same for each component. Vapor pressures

are theoretically estimated by the Joback and Reid (1987) method and Myrdal and Yalkowsky (1997) method.

### *Internal Alkenes (OLE2)*

Larger internal alkenes have also been shown to be SOA precursors (Pandis et al., 1992) and are represented in the gas-phase mechanism by OLE2, which includes C5 - C12 olefins such as cyclohexene. Cyclohexene is a compound that has been very well studied (Kalberer et al., 2000; Keywood et al., 2004) and in this study is chosen as a representative species of internal alkenes because it has detailed product information from smog chamber experimental work. The major identified SOA products from cyclohexene are dicarboxylic acids and hydroxylated dicarboxylic acids with low molecular weight, as shown in Tables 5.7 and 5.8. The values of the stoichiometric coefficients are taken from Pankow et al. (2001) who obtained them from experimental values (Kalberer et al., 2000). Vapor pressure values are theoretically predicted values by Pankow et al. (2001) and were adjusted to the reference temperature using the Sheehan and Bowman (2001) method. Product X represents unidentified aerosol mass in the chamber experiments with unknown structure and partitioning properties. In this study, product X is assumed to consist of a compound with 2 CH<sub>2</sub> and 2 COOH UNIFAC functional groups (Pankow et al., 2001) and is assigned a vapor pressure of  $1.00 \times 10^{-6}$  torr to match the experimental data.

Table 5.7. SOA products and individual partitioning properties for internal alkenes (OLE2).

Precursor	SOA Components <sup>a</sup>	$\alpha_i^a$	$p_i^{o^*a, b}$ (torr)	MW <sub>i</sub>
OLE2	2-hydroxy-pentanoic acid	0.0158	5.28 x10 <sup>-4</sup>	118
	4-hydroxy-butanaldehyde	0.0303	4.31 x10 <sup>-4</sup>	88
	oxalic acid	0.0703	7.05 x10 <sup>-5</sup>	90
	malonic acid	0.0969	5.53 x10 <sup>-5</sup>	104
	1,4-butanedial	0.0061	5.35 x10 <sup>-5</sup>	86
	4-oxo-butanoic acid	0.0963	5.04 x10 <sup>-5</sup>	102
	succinic acid	0.0096	3.35 x10 <sup>-5</sup>	118
	glutaraldehyde	0.006	2.72 x10 <sup>-5</sup>	100
	5-oxo-pentanoic acid	0.0688	2.60 x10 <sup>-5</sup>	116
	glutaric acid	0.1064	1.77 x10 <sup>-5</sup>	132
	adipaldehyde	0.0262	1.26 x10 <sup>-5</sup>	114
	6-oxo-hexanoic acid	0.0714	1.23 x10 <sup>-5</sup>	130
	adipic acid	0.0406	8.59 x10 <sup>-6</sup>	146
	2-hydroxy glutaric acid	0.0331	4.87 x10 <sup>-8</sup>	148
	2-hydroxy adipic acid	0.0187	2.70 x10 <sup>-8</sup>	162
	X (unidentified mass)	0.0505	1.00 x10 <sup>-6</sup>	118

<sup>a</sup> Pankow et al., 2001.

<sup>b</sup> Sheehan and Bowman, 2001.

Table 5.8. Chemical structure of individual SOA components for internal alkenes (OLE2).

SOA Components	Structure	SOA Components	Structure
2-hydroxy-pentanoic acid		5-oxo-pentanoic acid	
4-hydroxy-butanaldehyde		glutaric acid	
oxalic acid		adipaldehyde	
malonic acid		6-oxo-hexanoic acid	
1,4-butanedial		adipic acid	
4-oxo-butanoic acid		2-hydroxy glutaric acid	
succinic acid		2-hydroxy adipic acid	
glutaraldehyde		X	

### Long Alkanes (ALK5)

Long chain alkanes, with 7 or more carbons are represented in the gas-phase chemistry mechanism by ALK5. There is no detailed information on the composition and properties of experimentally identified SOA products from long alkanes. But products from long alkanes have large molecular weights and low vapor pressures, so they can be expected to partition to the aerosol phase. Those compounds with carbon number less than 7 are believed not to form SOA. For this study, SOA products of ALK5 are assumed to be long-chained acids and diacids with 7 to 30 carbons, as shown in Table 5.9 and Table 5.10.

Table 5.9. SOA products and individual partitioning properties for long alkanes (ALK5).

Precursor	SOA Components	$\alpha_i$	$p_i^{o*a}$ (torr)	MW <sub>i</sub>
ALK5	capric acid	0.0145	6.58 x10 <sup>-3</sup>	172
	undecanoic acid	0.0145	2.71 x10 <sup>-3</sup>	186
	dodecanoic acid	0.0145	9.40 x10 <sup>-4</sup>	200
	tridecanoic acid	0.0145	4.88 x10 <sup>-4</sup>	214
	pimelic acid	0.0145	3.19 x10 <sup>-4</sup>	160
	myristic acid	0.0145	2.15 x10 <sup>-4</sup>	228
	suberic acid	0.0145	1.53 x10 <sup>-4</sup>	174
	pentadecanoic acid	0.0145	9.72 x10 <sup>-5</sup>	242
	azelaic acid	0.0145	7.48 x10 <sup>-5</sup>	188
	palmitic acid	0.0145	4.49 x10 <sup>-5</sup>	256
	sebacic acid	0.0145	3.68 x10 <sup>-5</sup>	202
	heptadecanoic acid	0.0145	2.05 x10 <sup>-5</sup>	270
	stearic acid	0.0145	9.24 x10 <sup>-6</sup>	284
	eicosanoic acid	0.0145	1.77 x10 <sup>-6</sup>	312
	heneicosanoic acid	0.0145	7.53 x10 <sup>-7</sup>	326
	docosanoic acid	0.0145	3.15 x10 <sup>-7</sup>	340
	n-tricosanoic acid	0.0145	1.29 x10 <sup>-7</sup>	354
tetracosanoic acid	0.0145	5.21 x10 <sup>-8</sup>	368	
hexacosanoic acid	0.0145	8.02 x10 <sup>-9</sup>	396	
nonxacosanoic acid	0.0145	1.17 x10 <sup>-9</sup>	438	

<sup>a</sup> Joback and Reid, 1987; Myrdal and Yalkowsky, 1997

Table 5.10. Chemical structure of individual SOA components for long alkanes (ALK5).

SOA Components	Structure	SOA Components	Structure
capric acid		sebacic acid	
undecanoic acid		heptadecanoic acid	
dodecanoic acid		stearic acid	
tridecanoic acid		eicosanoic acid	
pimelic acid		heneicosanoic acid	
myristic acid		docosanoic acid	
suberic acid		n-tricosanoic acid	
pentadecanoic acid		tetracosanoic acid	
azelaic acid		hexacosanoic acid	
palmitic acid		nonacosanoic acid	

These compounds have large molecular weight and vapor pressures that are sufficiently low to condense to particle phase. Considering the limited SOA product information, although the selection of these components has some uncertainties, it is still a feasible representation of SOA products. The stoichiometric coefficients are assumed to be the



same for each compound and are assigned a value that roughly matches previous estimates of alkane aerosol yield (Strader et al., 1999). The vapor pressure for all the compounds are estimated based on their structural information using the Joback and Reid (1987) method and Myrdal and Yalkowsky (1997) method.

### *Lumped Groups*

After the individual SOA components within each precursor class were specified, they were lumped into 2 or more groups that represent SOA products for each precursor. Within each precursor class, vapor pressure is used as the criterion to lump individual components with similar volatility together according to the lumping method described in Chapter IV. Components were lumped into 2, 3 and 4 groups to determine the number of groups required to approximate the behavior of the detailed mixture. The group assignments are listed in Table 5.11, with 2a and 2b referring to the individual groups when 2 groups are used, 3a, 3b, and 3c when 3 groups are used, etc.

It is important to note that the lumped groups are not specific real compounds, but are imaginary model compounds that represent an entire mixture. In this respect they are similar to the products in the current CMAQ aerosol module. However, unlike the current partitioning parameters in CMAQ that are determined from experimental fits or estimates, the newly developed partitioning parameters are directly calculated from the properties of the individual SOA mixture components. As a result, the chemical structural information of these compounds is available. The UNIFAC functional groups of the lumped species are shown in Table 5.12. The number of each functional group within a compound may not be an integer, since the lumped species are not real compounds, but hypothetical

species with an average chemical structure. Because the lumped parameters are based on actual, albeit limited, product and property data, this approach provides a framework into which new SOA products can be incorporated once they are identified in experiments and additional product information is known.

Table 5.11. Partitioning properties of lumped groups

Lumped Group	$\alpha$	$p^{0*}$ (torr)	MW	B (K)
TRP1				
2a	0.2912	$3.36 \times 10^{-6}$	180	9379
2b	0.1490	$1.62 \times 10^{-4}$	172	9580
ARO1				
2a	0.365	$1.67 \times 10^{-5}$	119	9323
2b	0.438	$3.67 \times 10^{-4}$	117	9949
3a	0.146	$8.99 \times 10^{-6}$	125	10000
3b	0.219	$3.11 \times 10^{-5}$	115	9818
3c	0.438	$3.67 \times 10^{-4}$	117	9949
ARO2				
2a	0.192	$1.02 \times 10^{-5}$	194	8522
2b	0.288	$2.15 \times 10^{-4}$	159	9635
3a	0.096	$5.56 \times 10^{-6}$	205	9935
3b	0.096	$2.81 \times 10^{-5}$	183	9238
3c	0.288	$2.15 \times 10^{-4}$	159	9635
OLE2				
3a	0.0518	$4.08 \times 10^{-8}$	153	9989
3b	0.5788	$1.21 \times 10^{-5}$	119	8186
3c	0.1164	$1.07 \times 10^{-4}$	93	9595
4a	0.0518	$4.08 \times 10^{-8}$	153	9989
4b	0.0505	$1.10 \times 10^{-6}$	126	10000
4c	0.5283	$2.13 \times 10^{-5}$	118	9463
4a	0.1164	$1.07 \times 10^{-4}$	93	9595
ALK5				
2a	0.1015	$2.42 \times 10^{-7}$	362	7967
2b	0.1885	$5.40 \times 10^{-5}$	214	8861
3a	0.0580	$4.43 \times 10^{-8}$	389	9563
3b	0.0725	$1.56 \times 10^{-6}$	306	7245
3c	0.1595	$1.22 \times 10^{-4}$	202	9543
4a	0.0580	$4.43 \times 10^{-8}$	389	9563
4b	0.0435	$7.46 \times 10^{-7}$	326	9352
4c	0.0290	$1.28 \times 10^{-5}$	277	9799
4d	0.143	$1.22 \times 10^{-4}$	202	9543

Table 5.12. UNIFAC structural properties of lumped groups

Precursor	Lumped group	UNIFAC functional groups ID#												
		CH3	CH2	CH	C	ACH	AC	OH	ACOH	CH3CO	CH2CO	CHO	CH3O	COOH
TRP1	2a	1.99	1.63	2.01	1			0.08		0.39	0.07	0.37		1.18
	2b	2	1.69	2.21	1			0.20		0.77	0.05	0.83		0.26
ARO1	2a	0.2				1.2	0.8	0.2	0.8	0.2		0.2		1
	2b	0.5	0.17	0.17		2.67	1.33	0.83		0.17				0.17
	3a	0.5					1		2			0.5		1
	3b					2	0.67	0.33		0.33				1
	3c	0.5	0.17	0.17		2.67	1.33	0.83		0.17				0.17
ARO2	2a	0.75				6.75	4.75						0.5	0.5
	2b	0.83				4.67	3	0.33		0.17				0.67
	3a					7.5	4.5						1	0.5
	3b	1.5				6	5							0.5
	3c	0.83				4.67	3	0.33		0.17				0.67
OLE2	3a		2.36	1				1						2
	3b		2.62							0.41				1.46
	3c	0.40	0.53	0.40				0.40				0.13		1.34
	4a		2.36	1				1				0.26		2
	4b		2											2
	4c		2.68					1		0.45		0.15		1.40
	4d	0.40	0.53	0.40				0.40				0.26		1.34
ALK5	2a	1	21.6											1
	2b	0.69	10.3											1.31
	3a	1	23.5											1
	3b	1	17.6											1
	3c	0.64	9.36											1.36
	4a	1	23.5											1
	4b	1	19											1
	4c	1	15.5											1
4d	0.64	9.36											1.36	

## Evaluation of Updated SOA Parameters

The performance of the new SOA representations were evaluated by calculating the predicted aerosol yield of the SOA mixture within each hydrocarbon precursor class and comparing the results to the yield estimated from the partitioning parameters used in the current version of CMAQ, which are fits from smog chamber experiment data or published estimates. The results of the comparison for each hydrocarbon precursor class are shown in Figures 5.1 – 5.6. To approximate ambient aerosol conditions, the yield calculations were performed over a  $M_o$  range of 0 – 20  $\mu\text{g m}^{-3}$ , at  $T = 298 \text{ K}$ , using dry wood smoke particles (Chandramouli et al. 2003) as preexisting absorbing aerosols. The relatively polar wood smoke mixture is representative of aged atmospheric aerosols that contain components with high polarity. The composition of the wood smoke mixture is listed in Table 4.3. In all figures,  $Y_d$  is the yield predicted by the detailed SOA mixture components produced from each classified hydrocarbon precursor as listed in Tables 5.2 – 5.7.  $Y_2, Y_3, Y_4$  are the yields predicted when the mixtures are lumped into 2, 3, and 4 groups as listed in Table 5.11. As discussed in Chapter III and Chapter IV, when the number of lumped groups increases, the yield of the lumped group better approximates the yield of the detailed mixture.  $Y$  is the yield calculated from the current CMAQ module, which uses a 2-product model with two empirical parameters,  $\alpha_i$  and  $C_{\text{sat},i}^*$  (calculated at 298 K), for each product, as shown in Table 5.1. For long alkanes,  $Y$  is estimated with a single set of  $\alpha_i$  and  $C_{\text{sat},i}^*$ .

*Biogenics (TRP1)*

Figure 5.1 shows the comparison between the yield predictions for biogenic monoterpenes.

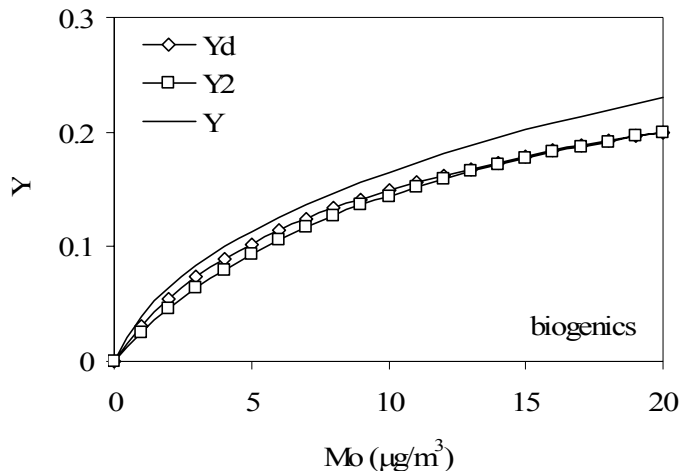


Figure 5.1. Comparison of predicted and measured organic aerosol yields as a function of organic aerosol mass for biogenic monoterpenes.

As shown in the figure, 2 groups approximate the detailed mixture quite well and are generally sufficient to represent the detailed SOA mixture. Compared with the yield estimated by empirical fits to experimental data,  $Y$ , the updated SOA representation,  $Y_2$ , results in a somewhat lower yield over the entire  $0 - 20 \mu\text{g m}^{-3} M_o$  range. Possible reasons for the difference include the composition of the absorbing aerosols, the selection of available identified SOA species, and uncertainty in the empirical parameters. Moreover, the empirical 2-product model was fit to experimental data over a much broader  $M_o$  range, up to  $200 \mu\text{g m}^{-3}$  (Griffin et al., 1999), with most yield measurements at an aerosol mass concentration much larger than  $20 \mu\text{g m}^{-3}$ . Therefore, at ambient conditions when  $M_o$  is low, there is even greater uncertainty in the empirical model. Overall, this updated SOA

representation for biogenic monoterpenes provides an excellent approximation with a more detailed description of SOA composition.

### *High Yield Aromatics (ARO1)*

Figure 5.2 compares the yield predictions for high-yield aromatic compounds. As shown in the figure,  $Y$  is the yield estimated by empirical fits to experimental data.  $Y_d$ ,  $Y_2$ ,  $Y_3$  are the yields predicted by the updated SOA representation, and  $Y_{exp}$  indicates the experimental data points.

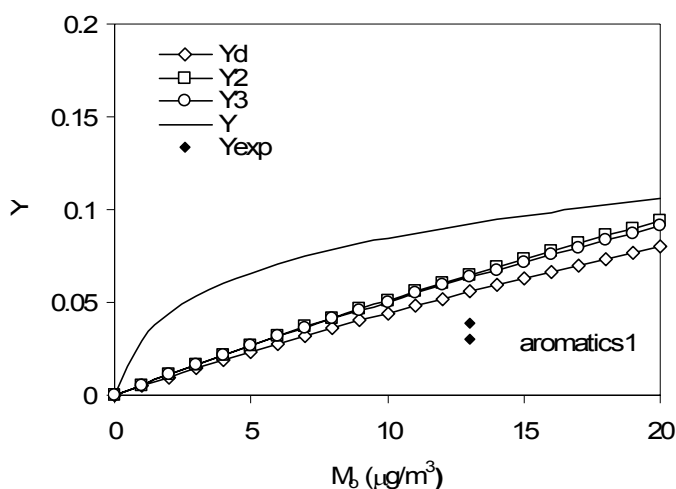


Figure 5.2. Comparison of predicted and measured organic aerosol yields as a function of organic aerosol mass for high-yield aromatics.

Compared with the empirical yield fit, the yield predicted by the updated SOA components is lower when  $M_o$  is in the range of  $0 - 20 \mu\text{g m}^{-3}$ . Because the selection of aromatic products for the updated SOA formulation is not based on complete detailed experimental product identification but is somewhat arbitrary, this difference is not unexpected. However, when compared with the experimentally measured yield data, this

theoretical prediction is more accurate than the empirical fit. At larger  $M_o$ , the updated SOA representation tends to overpredict the yield, but for typical ambient conditions with low  $M_o$  concentration it provides a good approximation. Considering the uncertainties in both aromatic product composition and empirical yield curves, this approximation is a feasible representation of SOA products from high yield aromatics. As additional aromatic SOA product information becomes available in the future, this approach will be able to incorporate more detailed product information and provide a better approximation. As shown in Figure 5.2, 2- and 3-group lumping both predict a higher yield than the detailed SOA mixture. Because the properties of the products are quite dissimilar from each other, lumping the compounds simply based on their volatility results in some error compared to the detailed mixture predictions.

#### *Low Yield Aromatics (ARO2)*

Figure 5.3 compares the yield predictions for low-yield aromatic compounds. Similar to the case of high-yield aromatics, 2- and 3-group lumping both predict a higher yield than the detailed SOA mixture. Compared with the yield fit with experimental data, the yield of the new SOA mixture generally underpredicts at the  $M_o$  range of interest, but is closer to the single experimental data point within the relevant  $M_o = 0 - 20 \mu\text{g m}^{-3}$  range. Overall this updated representation provides a reasonable approximation to low SOA yield aromatic products, considering the uncertainties related to limited product information.

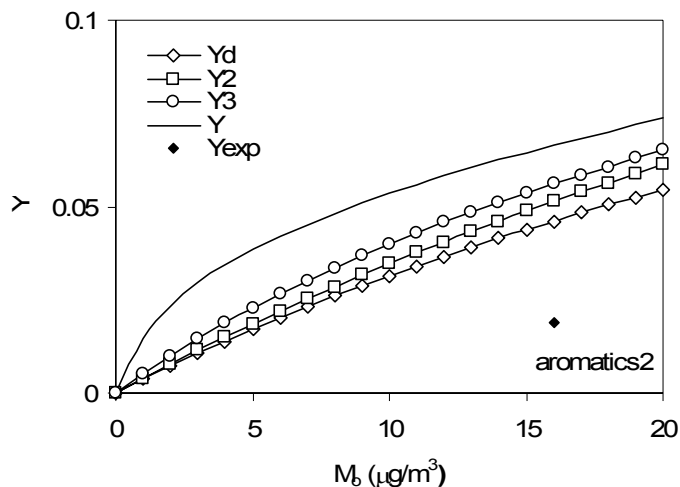


Figure 5.3. Comparison of predicted and measured organic aerosol yields as a function of organic aerosol mass for low-yield aromatics.

#### *Internal Alkenes (OLE2)*

Figures 5.4 and 5.5 show the comparison between the yield predictions for internal alkenes (as represented by cyclohexene), for a range of absorbing aerosol mass  $M_o$  at  $0 - 20 \mu\text{g}/\text{m}^3$  and  $0 - 140 \mu\text{g}/\text{m}^3$ , respectively.  $Y_d$  represents the yield predicted by the detailed SOA mixture, and  $Y_3, Y_4$  are the yields predicted using 3 and 4 groups. The scattered points indicated by  $Y_{\text{exp}}$  are the measured SOA yield values from individual smog chamber experiments (Kalberer et al., 2000). When comparing the predicted yields with the empirically fit values, for the  $M_o$  range of  $0 - 20 \mu\text{g}/\text{m}^3$ , predicted values are much larger than empirically fit values, but are closer to the single experimentally measured yield in this  $M_o$  range. For  $M_o = 0 - 140 \mu\text{g}/\text{m}^3$ , which is the range of aerosol mass in the chamber experiments, the new yield prediction is larger at low  $M_o$  and smaller at higher  $M_o$  when compared with the empirical fit.



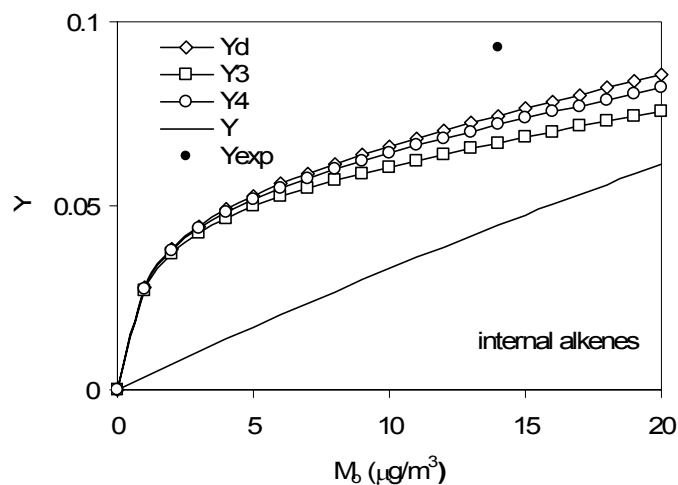


Figure 5.4. Comparison of predicted and measured organic aerosol yield predictions as a function of organic aerosol mass for internal alkenes, at  $M_o = 0 - 20 \mu\text{g}/\text{m}^3$ .

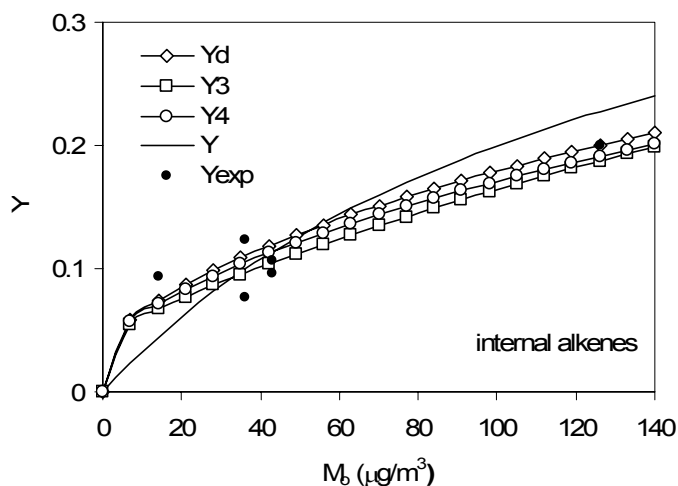


Figure 5.5. Comparison of predicted and measured organic aerosol yield predictions as a function of organic aerosol mass for internal alkenes, at  $M_o = 0 - 140 \mu\text{g}/\text{m}^3$ .

However, the new SOA presentation also provides a good fit to the experimental data points, suggesting that the differences between empirical and detailed yields in Figure 5.4

are due to limitations in fitting the empirical model to a few relatively scattered chamber data points. As shown in the figures, 3 and 4 lumped groups approximate the yield of the detailed mixture quite well at both smaller and larger  $M_o$  ranges.

### *Long-Chain Alkanes (ALK5)*

Figure 5.6 shows the comparison between the yield predictions for long alkanes.  $Y_d$  represents the yield predicted by the detailed SOA mixture, and  $Y_2$ ,  $Y_3$ ,  $Y_4$  are the yields predicted using 2, 3, and 4 groups. While 2-group lumping results in relatively larger errors, 3- and 4-group lumping both approximate the detailed mixture quite well.

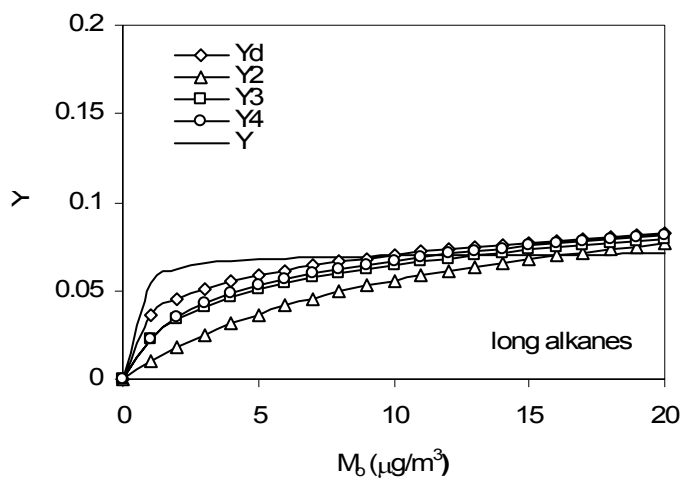


Figure 5.6. Comparison of predicted and measured organic aerosol yields as a function of organic aerosol mass for long alkanes.

Compared with results using the current CMAQ parameters,  $Y$ , the lumped groups predict lower yields at small  $M_o$  range, and larger yields as  $M_o$  increases. This difference in the shape of the yield curves occurs because the current CMAQ uses a single product of low volatility that partitions almost entirely to the aerosol phase even at low  $M_o$ .

Considering that there is very little information about identified products from long alkane oxidation reactions, and most of the SOA products specified in this study are only predicted species based on their ability to partition into particle phase, this is an acceptable estimate of alkane SOA formation. As with the other precursor classes, as additional information about identified products becomes available, the SOA representation can be updated to include more accurate parameters.

Overall, the newly formulated set of SOA precursors, products, and partitioning parameters provides a more detailed representation of SOA, that compares quite well with experimental data and estimates. This method provides a theoretical framework which is flexible for incorporating future updates in SOA representation in air quality models. The number and types of products appropriate for each gas phase precursor can be determined based on specific user requirements, and additional SOA products can be added as needed. In this sense, further experimental work will be very helpful in identifying more SOA products and their gas/particle partitioning parameters. Newly identified products can be added into this framework to provide more detailed and specific SOA species. Their structural and other properties can be applied to calculate more accurate properties for the lumped products.

## CHAPTER VI

### SUMMARY AND CONCLUSION

The principal goal of this research has been to develop and apply a theoretical model that can lump the multiple secondary organic aerosol components in an organic aerosol mixture into a few lumped compounds. The lumping model offers an original approach to simplify the incorporation of SOA in air quality models. The lumped compounds represent the detailed chemical structure and other partitioning properties of the individual components in the detailed aerosol mixture. It has been shown to predict the gas-particle partitioning behavior of the overall mixture quite well. This goal has been achieved in the following steps.

First, in Chapter III, a theoretical lumping model was developed that successfully converts SOA components into lumped compounds. The absorption partitioning properties of the lumped compounds are derived from those of the individual components through a set of equations. This stage of modeling work included only the temperature dependence of gas-to-particle partitioning and made the assumption of ideal mixture behavior among the aerosol components. Lumping criteria were based on the volatility of each component which was indicated by the partitioning coefficient. Modeling results demonstrate that the lumping model can effectively approximate the partitioning behavior over a range of temperature and organic aerosol mass conditions. Accuracy of the model improves with the number of lumped groups, but in general 2 or 3 groups are sufficient to represent partitioning behavior of the whole mixture.

In Chapter IV, the lumping model was improved to incorporate aerosol composition effects. The lumping equations were expanded to include more partitioning parameters including vapor pressure, molecular weight, and UNIFAC functional groups for each SOA component. Different lumping criteria such as vapor pressure, chemical structure, and activity coefficient in water were investigated to find the optimum lumping guidelines. Simulations results from several SOA systems show that aerosol mixture composition has a strong influence on gas/particle partitioning and lumping performance of the model. Comparisons of different lumping criteria show that lumping by vapor pressure is a feasible and efficient approach.

In Chapter V, the partitioning behavior of an aerosol mixture produced by multiple hydrocarbon precursors was studied. A new SOA formulation with an updated set of SOA precursors and products was developed for the aerosol module of the CMAQ air quality model. A new set of aerosol partitioning parameters that include composition effects was also formulated for each SOA component. 2 or more lumped species were developed for each precursor. The specific number of groups (products) can be flexibly determined based on required computational efficiency. The partitioning behavior predicted by the updated products was compared to experimental data from smog chambers and was shown to be a reasonable approximation. This new SOA formulation provides a framework that not only has been proved to work well in incorporating composition dependence, but is also very flexible, allowing future updates to include more SOA product information from experimental or field data.

Future work is planned to incorporate the presented lumping model into the aerosol module of CMAQ to account for the composition dependence of SOA

partitioning. The lumped SOA products and partitioning parameters presented here will be included in an updated version of the CMAQ aerosol module that includes composition dependent partitioning. Simulation tests will be run with the updated module with the improved partitioning parameters to determine the sensitivity of SOA predictions to temperature, compositional effects, and SOA product definition. The results will be compared with ambient measurements and the simulation results from the current CMAQ version to evaluate the accuracy of the new aerosol module, and to study the effects of temperature, composition and SOA product definition. The SOA formulation in the model can also be updated or expanded to include new identified SOA products when such information becomes available.

## REFERENCES

- Andersson-Sköld, Y. and Simpson, D., 2001. Secondary organic aerosol formation in Northern Europe: A model study. *Journal of Geophysical Research*, 106, 7357-7374.
- Ansari, A.A. and Pandis, S.N., 2000. Water absorption by secondary organic aerosol and its effect on inorganic aerosol behavior. *Environmental Science and Technology* 34, 71-77.
- Atkins, P.W., 1990. *Physical Chemistry*. Oxford University Press, Oxford.
- Bailey, E.M., Gautney, L.L., Condrey, J.W., Kelsoe, J.J., and Jacobs, M.E., 2002. An assessment of Models3 performance during the 1999 SOS Nashville study. 2002 Models-3 Users' Workshop, Research Triangle Park, N.C., October 21-23, 2002.
- Barthelmie, R.J. and Pryor, S.C., 1999. A model mechanism to describe oxidation of monoterpenes leading to secondary organic aerosol:  $\alpha$ -pinene and  $\beta$ -pinene. *Journal of Geophysical Research* 104, 23,657-23,669.
- Bian, F. and Bowman, F.M., 2002. Theoretical method for lumping multicomponent secondary organic aerosol mixtures. *Environmental Science and Technology* 36, 2491-2497.
- Bian, F. and Bowman, F.M., 2005. A lumping model for composition- and temperature-dependent partitioning of secondary organic aerosols. *Atmospheric Environment*, 39, 1263-1274.
- Bidleman, T.F., Billings, W.N. and Foreman, W.T., 1986. Vapor-particle partitioning of semivolatile organic compounds--Estimates from field collections. *Environmental Science and Technology*, 20, 1038-1043.
- Binkowski, F.S. and Roselle, S.J., 2003. Models-3 community multiscale air quality (CMAQ) model aerosol component, 1, Model description. *Journal of Geophysical Research* 108 (D6), 4183, doi:10.1029/2001JD001409.
- Binkowski, F.S., 1999. Aerosols in MODELS-3 CMAQ, in Science Algorithms of the EPA Models-3. Community Multiscale Air Quality (CMAQ) Modeling System, EPA 600/R-99-030, EPA.
- Blando, J.D., Porcja, R.J., Li, T-H, Bowman, D., Lioy, P.J. and Turpin, B.J., 1998. Secondary formation and the Smoky Mountain organic aerosol: an examination of aerosol polarity and functional group composition during SEAVS. *Environmental Science and Technology*, 32, 604-613.

- Bonn, B. and Moortgat, G.K., 2003. Sesquiterpene ozonolysis: Origin of atmospheric new particle formation from biogenic hydrocarbons. *Geophysical Research Letters*, 30 (11), 1585-1588.
- Bowman, F.M., Odum, J.R., Seinfeld, J.H. and Pandis, S.N., 1997. Mathematical model for gas-particle partitioning of secondary organic aerosols. *Atmospheric Environment*, 31, 3921-3931.
- Bowman, F. M. and Melton, J.A., 2003. Effect of activity coefficient models on predictions of secondary organic aerosol partitioning. *Journal of Aerosol Science*, 35, 1415-1438.
- Bowman, F.M, and Karamalegos, A.M., 2002. Estimated effects of composition on secondary organic aerosol mass concentrations. *Environmental Science and Technology* 36, 2701-2707.
- Brown, S.G., Herckes, P., Ashbaugh, L., Hannigan, M P., Kreidenweis, S.M. and Collett, Jr., J L., 2002. Characterization of organic aerosol present in Big Bend National Park, Texas during the Big Bend Regional Aerosol and Visibility Observational (BRAVO) Study. *Atmospheric Environment* 36, 5807-5818.
- Byun, D.W. and Ching, S., 1999. Science algorithms of the EPA Models-3 Community Multiscale Air Quality Model (CMAQ) modeling system. EPA/600/R-99/030, U.S.EPA, Research Triangle Park, NC.
- Carter, W.P.L., 1990. A detailed mechanism for the gas-phase atmospheric reactions of organic compounds. *Atmospheric Environment* 24A, 481-515.
- Carter, W.P.L., 2000a. Documentation of the SAPRC-99 chemical mechanism for VOC reactivity assessment. Report to California Air Resources Board. (<ftp://ftp.cert.ucr.edu/pub/carter/pubs/s99txt.pdf>)
- Carter, W.P.L., 2000b. Implementation of the SAPRC99 chemical mechanism into the models-3 frame work. Report to the United States Environmental Protection Agency. (<ftp://ftp.cert.ucr.edu/pub/carter/pubs/s99mod3.pdf>)
- Castro, L.M., Pio, C.A., Harrison, R.M. and Smith, D.J.T., 1999. Carbonaceous aerosol in urban and rural European atmospheres: estimation of secondary organic carbon concentrations. *Atmospheric Environment* 33, 2771-2781.
- Chandramouli, B., Jang, M. and Kamens, R.M., 2003. Gas-particle partitioning of semi-volatile organics on organic aerosols using a predictive activity coefficient model: analysis of the effects of parameter choices on model performance. *Atmospheric Environment* 37, 853-864.



- Claeys, M., Graham, B., Vas, G., Wang, W., Vermeylen, R., Pashynska, V., Cafmeyer, J., Guyon, P., Andreae, M.O., Artaxo, P. and Maenhaut, W., 2004. Formation of secondary organic aerosols through photooxidation of isoprene, *Science* 303: 1173-1176.
- Cocker III, D.R., Flagan, R.C. and Seinfeld, J.H., 2001a. State-of-the-Art chamber facility for studying atmospheric aerosol chemistry. *Environmental Science & Technology*, 35(12), 2594-2601.
- Cocker III, D.R., Clegg, S.L., Flagan, R.C. and Seinfeld, J.H., 2001b. The effect of water on gas-particle partitioning of secondary organic aerosol. Part I:  $\alpha$ -pinene/ozone system. *Atmospheric Environment* 35, 6049-6073.
- Cocker III, D.R., Mader, B.T., Kalberer, M., Flagan, R.C. and Seinfeld, J.H., 2001c. The effect of water on gas-particle partitioning of secondary organic aerosol: II. m-xylene and 1,3,5-trimethylbenzene photooxidation systems. *Atmospheric Environment* 35, 6073-6085.
- Cousins, I.T. and Mackay, D., 2001. A critical review of gas-particle partitioning of organic compounds and its interpretation using relative solubilities. *Environmental Science & Technology*, 35(4), 643-647.
- Day, D.E., Malm, W.C. and Kreidenweis, S.M., 1997. Seasonal variations in aerosol composition and acidity at Shenandoah and Great Smoky Mountains National Parks. *Journal of Air & Waste Management Association*, 47, 411-418.
- Donaldson, K., Li X.Y. and MacNee, W., 1998. Ultrafine (Nanometre) particle mediated lung injury. *Journal of Aerosol Science* 29, 553-560.
- Eder, B., Yu, S.-C., Dennis, R., Pleim, J., and Schere, K., 2002. Preliminary evaluation of the June 2002 version of CMAQ. 2002 Models-3 Users' Workshop, Research Triangle Park, N.C., October 21-23, 2002.
- Edney, E.O., Driscoll, D.J., Speer, R.E., Weather, W.S., Kleindienst, T.E., Li, W. and Smith, D.F., 2000. Impact of aerosol liquid water on secondary organic aerosol yields of irradiated toluene/propylene/ $\text{NO}_x$ / $(\text{NH}_4)_2\text{SO}_4$ /air mixtures. *Atmospheric environment* 34, 3907-3919.
- Edney, E.O., Kleindienst, T.E., Conner, T.S., McIver, C.D., Corse, E.W. and W.S. Weathers, 2003. Polar organic oxygenates in  $\text{PM}_{2.5}$  at a southeastern site in the United States. *Atmospheric environment* 37, 3947-3965.
- Eldering, A. and Cass, G.R., 1996. Source-oriented model for air pollutant effects on visibility. *Journal of Geophysical Research*, 101 (D14), 19, 343-19, 369.

- Environ, 2003. Development of an advanced photochemical model for particulate matter: PMCAMx. Final Report CRC project A-30, Environ.
- EPA, 1988. Compendium of method for the determination of toxic organic compounds in ambient air. EPA/600/4-89-017, U.S. Environmental Protection Agency, Research Triangle Park, NC
- EPA, 1999. Science algorithms of the EPA Models-3 Community Multiscale Air Quality (CMAQ) modeling system. EPA/600/R-99/030.
- EPA, 2004. Source code documentation with CMAQ.
- Forstner, H.J.L., Flagan, R.C. and Seinfeld, J.H., 1997a. Secondary organic aerosol from the photooxidation of aromatic hydrocarbons: molecular composition. *Environmental Science and Technology* 31, 1346-1358.
- Forstner, H.J.L., Flagan, R.C. and Seinfeld, J.H., 1997b. Molecular speciation of secondary organic aerosols from photooxidation of the higher alkenes: 1-Octene and 1-Decene. *Atmospheric Environment* 31(13), 1953-1964.
- Gery, M.W., Whitten, G.Z., Killus, J.P. and Dodge, M.C., 1989. A photochemical kinetics mechanism for urban and regional scale computer modeling. *Journal of Geophysical Research* 94, 12,925-12,956.
- Glasius, M., Duane, M. and Larsen, B.R., 1999. Determination of polar terpene oxidation products in aerosols by liquid chromatography-ion trap mass spectrometry. *Journal of Chromatography A* 833, 121-135.
- Glasius, M., Lahaniati, M., Calogirou, A., Bella, D.D., Jensen, N.R., Hjorth, J., Kotzias, D. and Larsen, B.R., 2000. Carboxylic acids in secondary aerosols from oxidation of cyclic monoterpenes by ozone. *Environ. Sci. Technol.* 34, 1001-1010.
- Godowitch, J.M., 2004. Simulations of aerosols and photochemical species with the CMAQ plume-in-grid modeling system. 2004 Models-3 Conference, Chapel Hill, NC, October 18-20, 2004.
- Goss, K.-U. and Schwarzenbach, R.P., 1998. Empirical prediction of heats of vaporization and heats of adsorption of organic compounds. *Environmental Science & Technology*, 32(14), 2025-2032.
- Griffin, R.J., Cocker III, D.R., Flagan, R.C. and Seinfeld, J.H., 1999. Organic aerosol formation from the oxidation of biogenic hydrocarbons. *Journal of Geophysical Research* 104, 3555-3567.

- Griffin, R.J., Dabdub, D. and Seinfeld, J.H., 2002a. Secondary organic aerosol 1. Atmospheric chemical mechanism for production of molecular constituents. *Journal of Geophysical Research* 107 (D17), 4332, doi:10.1029/2001JD000541.
- Griffin, R.J., Dabdub, D., Kleeman, M.J., Fraser, M.P., Cass, G.R. and Seinfeld, J.H., 2002b. Secondary organic aerosol 3. Urban/regional scale model of size-and composition-resolved aerosol. *Journal of Geophysical Research* 107 (D17), 4334, doi:10.1029/2001JD000544.
- Griffin, R.J., Nguyen, K., Dabdub, D. and Seinfeld, J.H., 2003. A coupled hydrophobic-hydrophilic model for predicting secondary organic aerosol formation. *Journal of atmospheric chemistry* 44, 171-190.
- Gross, A. and Stockwell, W.R., 2003. Comparison of the EMEP, RADM2 and RACM mechanisms. *Journal of Atmospheric Chemistry* 44, 151-170.
- Grosjean, D. and Seinfeld, J.H., 1989. Parametrization of the formation potential of secondary organic aerosols. *Atmospheric Environment*, 23, 1733-1747.
- Guenther, A., Geron, C., Pierce, T., Lamb, B., Harley, P. and Fall, R., 2000. Natural emission of non-methane volatile organic compounds, carbon monoxide, and oxides of nitrogen from North America. *Atmospheric Environment* 34, 2205-2230.
- Hallquist, M., Wänbberg, I. and Ljungström, E., 1997. Atmospheric fate of carbonyl oxidation products originating from  $\alpha$ -pinene and  $\Delta^3$ -carene: determination of rate of reaction with OH and NO<sub>3</sub> radicals, UV absorption cross sections, and vapor pressures. *Environ. Sci. Technol.* 31, 3166-3172.
- Harner, T. and Bidleman, T.F., 1998. Octanol-air partition coefficient for describing particle/gas partitioning of aromatic compounds in urban air. *Environmental Science and Technology*, 32, 1494-4502.
- Hemming, B.L. and Seinfeld, J.H., 2001. On the hygroscopic behavior of atmospheric organic aerosols. *Industrial and Engineering Chemistry Research*, 40, 4162-4171.
- Hinds, W.C., 1999. *Aerosol technology*, Wiley-Interscience, New York.
- Hoffmann, T., Bandur, R., Marggraf, U. and Linscheid, M., 1998. Molecular composition of organic aerosols formed in the  $\alpha$ -pinene/O<sub>3</sub> reaction: Implication for new particle formation processes. *Journal of Geophysical Research* 103, 25569-25578.
- Hoffmann, T.P.W., Odum, J.R., Bowman, F., Collins, D.R., Klockow, D., Flagan, R.C. and Seinfeld, J.H., 1997. Formation of organic aerosols from the oxidation of biogenic hydrocarbons. *Journal of Atmospheric Chemistry* 26, 189-222.

- Hurley, M.D., Sokolov, O., Wallington, T.J., Takekawa, H., Karasawa, M., Klotz, B., Barnes, I. and Becker, K.H., 2001. Organic aerosol formation during the atmospheric degradation of toluene. *Environmental Science and Technology* 35, 1358-1366.
- IMSL Math/Library Volumes 1 and 2*; Visual Numerics, Inc.: Houston, TX, 1997; Chapter 10.
- Izumi, K. and Fukuyama, T., 1990. Photochemical aerosol formation from aromatic hydrocarbons in the presence of NO<sub>x</sub>. *Atmospheric Environment* 24A, 1433-1441.
- Jacobson, M.Z., 1998. Fundamentals of Atmospheric Modeling
- Jacobson, M.C., Hansson, H.C., Noone, K.J. and Charlson, R.J. 2000. Organic atmospheric aerosols: Review and state of the science. *Reviews of Geophysics*, 38, 267-294
- Jang M., Kamens, R.M., Leach, K.B. and Strommen, M.R., 1997. A thermodynamic approach using group contribution methods to model the partitioning of semivolatile organic compounds on atmospheric particulate matter. *Environmental Science and Technology* 31, 2805-2811.
- Jang, M., Czoschke, N.M., Lee, S. and Kamens, R.M., 2002. Heterogeneous atmospheric aerosol formation by acid-catalyzed particle phase reactions. *Science* 298, 814-817.
- Jang, M. and Kamens, R.M., 1998. A thermodynamic approach for modeling partitioning of semi-volatile organic compounds on atmospheric particulate matter: humidity effects. *Environmental Science and Technology* 32, 1237-1243.
- Jang, M. and Kamens, R.M., 1999. Newly characterized products and composition of secondary aerosols from the reaction of  $\alpha$ -pinene with ozone. *Atmospheric Environment* 33, 459-474.
- Jang, M. and Kamens, R.M., 2001. Characterization of secondary aerosol from the photooxidation of toluene in the presence of NO<sub>x</sub> and 1-propene. *Environmental Science and Technology*, 35, 3626-3639.
- Jang, M., Lee, S. and Kamens, R.M., 2003. Organic aerosol growth by acid-catalyzed heterogeneous reactions of octanal in a flow reactor. *Atmospheric Environment* 37, 2125-2138.
- Jaoui, M. and Kamens, R.M., 2001. Mass balance of gaseous and particulate product analysis from  $\alpha$ -pinene/NO<sub>x</sub>/air in the presence of natural sunlight. *Journal of Geophysical Research* 106 (D12), 12,541-12,558.

- Jaoui, M. and Kamens R.M., 2003a. Gaseous and particulate oxidation products analysis of a mixture of  $\alpha$ -pinene +  $\beta$ -pinene/O<sub>3</sub>/air in the absence of light and  $\alpha$ -pinene +  $\beta$ -pinene/NO<sub>x</sub>/air in the presence of natural sunlight. *Journal of Atmospheric Chemistry*, 44, 259-297.
- Jaoui, M. and Kamens, R.M., 2003b. Mass balance of gaseous and particulate products from  $\beta$ -pinene/O<sub>3</sub>/air in the absence of light and  $\beta$ -pinene/NO<sub>x</sub>/air in the presence of natural light. *Journal of Atmospheric Chemistry* 43, 101-141.
- Jaoui, M. and Kamens, R.M., 2003c. Gas and particulate distribution from the photooxidation of  $\alpha$ -humulene in the presence of NO<sub>x</sub>, natural atmospheric air and sunlight. *Journal of Atmospheric Chemistry* 46, 29-54.
- Jaoui, M., Leungsakul, S. and Kamens, R.M., 2003. Gas and particle products distribution from the reaction of  $\beta$ -caryophyllene with ozone. *Journal of Atmospheric Chemistry* 45, 261-287.
- Joback, K.G. and Reid, R.C., 1987. Estimation of pure-component properties from group-contributions. *Chemical Engineering Communications*, 57, 233–243.
- Kalberer, M., Yu, J., Cocker, D.R., Flagan, R.C. and Seinfeld, J.H., 2000. Aerosol formation in the cyclohexene-ozone system. *Environmental Science and Technology* 34, 4894-4901.
- Kalberer, M., Paulsen, D., Sax, M., Steinbacher, M., Dommen, J., Prevot, A.S., Fisseha, R., Weingartner, E., Frankevich, V., Zenobi, R. and Baltensperger, U., 2004. Identification of polymers as major components of atmospheric organic aerosols. *Science*, 303, 1659-1662.
- Kamens, R., Jang, M., Chien, C-J. and Leach, K., 1999. Aerosol formation from the reaction of  $\alpha$ -pinene and ozone using a gas-phase kinetics-aerosol partitioning model. *Environmental Science and Technology* 33, 1430-1438.
- Kamens, R.M. and Jaoui, M., 2001. Modeling aerosol formation from  $\alpha$ -pinene +NO<sub>x</sub> in the presence of natural sunlight using gas-phase kinetics and gas-particle partitioning theory. *Environmental Science and Technology* 35, 1394-1405.
- Kanakidou, M., Seinfeld, J.H., Pandis, S. N., Barnes, I., Dentener, F.J., Facchini, M.C., van Dingenen, R., Ervens, B., Nenes, A., Nielsen, C.J., Swietlicki, E., Putaud, J.P., Balkanski, Y., Fuzzi, S, Horth, J., Moortgat, G.K., Winterhalter, R., Myhre, C.E.L., Tsigaridis, K., Vignati, E., Stephanou, E.G. and Wilson, J., 2004. Organic aerosol and global climate modelling: a review. *Atmospheric Chemistry and Physics Discussions (SMOCC Special Issue)* 4, 5855-6024.
- Kaupp, H. and McLachlan, M.S., 1999. Gas/particle partitioning of PCDD/Fs, PCBs, PCNs and PAHs. *Chemosphere*, 38(14), 3411-3421.

- Keywood, M.D., Kroll, J.H., Varutbangkul, V., Bahreini, R., Flagan, R.C. and Seinfeld, J.H., 2004. Secondary organic aerosol formation from cyclohexene ozonolysis: Effect of OH scavenger and the role of radical chemistry. *Environmental Science & Technology*, 38, 3343-3350.
- Kleeman, M.J., Eldering, A., Hall, J.R. and Cass, G.R., 2001. Effect of emissions control programs on visibility in southern California. *Environmental Science and Technology* 35, 4668 – 4674.
- Kleindienst, T.E., Smith, D.F., Li, W., Edney, E.O., Driscoll, D.J., Speer, R.E. and Weathers, W.S., 1999. Secondary organic aerosol formation from the oxidation of aromatic hydrocarbons in the presence of dry submicron ammonium sulfate aerosol. *Atmospheric Environment* 33, 3669-3681.
- Kleindienst, T.E., Conner, T.S., McIver, C.D. and Edney, E.O., 2004. Determination of secondary organic aerosol products from the photooxidation of toluene and their implications in ambient PM<sub>2.5</sub>. *Journal of Atmospheric Chemistry* 47, 79 – 100.
- Koch, S., Winterhalter, R., Uherek, E., Koloff, A., Neeb, P. and Moortgat, G.K., 2000. Formation of new particles in the gas-phase ozonolysis of monoterpenes. *Atmospheric Environment*, 34, 4031-4042.
- Kourtidis, K. and Ziomas, I., 1999. Estimation of secondary organic aerosol (SOA) production from traffic emissions in the city of Athens. *Global NEST: The International Journal* 1(1): 33-39.
- Kunzli, N., Kaiser, R., Medina, S., Studnicka, M., Chanel, O., Filliger, P., Herry, M. and Horak, F., 2000. Public Impact of Outdoor and Traffic-Related Air Pollution: A European Assessment. *The Lancet*, 356, 795-801.
- Larsen, B.R., Bella, D.D., Glasius, M., Winterhalter, R., Jensen, N.R. and Hjorth, J., 2001. Gas-phase OH oxidation of monoterpenes: gaseous and particulate products. *Journal of Atmospheric Chemistry* 38, 231-276.
- Lazaridis, M., 1999. Gas-particle partitioning of organic compounds in the atmosphere. *Journal of Aerosol Science*, 30(9), 1165-1170.
- Leach, K.B., Kamens, R.M., Strommen, M.R. and Jang, M., 1999. Partitioning of semivolatile organic compounds in the presence of a secondary organic aerosol in a controlled atmosphere. *Journal of Atmospheric Chemistry*, 33, 241-264.
- Leitch, W.R., Bottenheim, J.W., Biesenthal, T.A., Li, S.M., Liu, S.M., Asalien, K., Dryfhout-Clark, H., Hopper, F. and Brechtel, F., 1999. A case study of gas-to-particle conversion in an eastern Canadian forest, *Journal of Geophysical Research* 104, 8095-8111.

- Liang, C., Pankow, J.F., Odum, J.R. and Seinfeld, J.H., 1997. Gas/particle partitioning of semivolatile organic compounds to model inorganic, organic, and ambient smog aerosols. *Environmental Science and Technology*, 31, 3086-3092.
- Lim, H-J. and Turpin, B.J., 2002. Origins of primary and secondary organic aerosols in Atlanta: results of time-resolved measurements during the Atlanta supersite experiment. *Environmental Science and Technology* 36, 4489-4496.
- Limbeck, A., Kulmala, M. and Puxbaum, H., 2003. Secondary organic aerosol formation in the atmosphere via heterogeneous reaction of gaseous isoprene on acidic particles. *Geophysical Research Letters*, 30(19), ASC6/1-ASC6/4.
- Mader, B.T. and Pankow, J.F., 2003. Study of the effects of particle-phase carbon on the gas/particle partitioning of semivolatile organic compounds in the atmosphere using controlled field experiments. *Environmental Science and Technology* 36, 5218-5228.
- Maria, S.F., Russell, L.M., Gilles, M.K. and Myneni, S.C.B., 2004. Organic aerosol growth mechanisms and their climate-forcing implications. *Science*, 306, 1921-1924.
- Meng, Z.Y., Dabdub, D. and Seinfeld, J.H., 1998. Size-Resolved and chemically resolved model of atmospheric aerosol dynamics. *Journal of Geophysical Research*, 103, 3419-3435
- Myrdal, P.B. and Yalkowsky, S.H., 1997. Estimating pure component vapor pressure of complex organic molecules, *Industrial and Engineering Chemistry Research*, 36, 2494-2499.
- Mebust, M.R., Eder, B.K., Binkowski, F.S. and Roselle, S.J., 2003. Models-3 community multiscale air quality (CMAQ) model aerosol component, 2, Model evaluation. *J. Geophys. Res.* 108(D6), 4184, doi:10.1029/2001JD001410.
- Odum, J.R., Hoffmann, T., Bowman, F., Collins, D., Flagan, R.C. and Seinfeld, J.H., 1996. Gas/particle partitioning and secondary organic aerosol yields. *Environmental Science and Technology* 30, 2580-2585.
- Odum, J.R., Jungkamp, T.P.W., Griffin, R.J., Flagan, R.C. and Seinfeld, J.H., 1997a. The atmospheric aerosol-forming potential of whole gasoline vapor. *Science* 276, 96-99.
- Odum, J.R., Jungkamp, T.P.W., Griffin, R.J., Forstner, H.J.L., Flagan, R.C. and Seinfeld, J.H. 1997b. Aromatics, reformulated gasoline, and atmospheric organic aerosol formation. *Environmental Science and Technology* 31, 1890-1897.

- Pandis, S.N., Paulson, S.E., Seinfeld, J.H. and Flagan, R.C., 1991. Aerosol formation in the photooxidation of isoprene and  $\beta$ -pinene. *Atmospheric Environment*, 25, 997-1008.
- Pandis, S.N., Harley, R.A., Cass, G.R. and Seinfeld, J.H., 1992. Secondary organic aerosol formation and transport. *Atmospheric Environment*, 26A, 2269-2282.
- Pankow, J.F., 1991. Common y-intercept and single compound regressions of gas-particle partitioning data vs  $1/T$ . *Atmospheric Environment* 25A, 2229-2239.
- Pankow, J.F., 1994a. An absorption model of gas-particle partitioning of organic compounds in the atmosphere. *Atmospheric Environment* 28, 185-188.
- Pankow, J.F., 1994b. An absorption model of the gas/aerosol partitioning involved in the formation of the secondary organic aerosol. *Atmospheric Environment* 28, 189-193.
- Pankow, J.F., Seinfeld, J.H., Asher, W.E. and Erdakos, G.B., 2001. Modeling the formation of secondary organic aerosol. 1. Application of theoretical principles to measurements obtained in the  $\alpha$ -pinene/,  $\beta$ -pinene/, sabinene/,  $\Delta^3$ -carene/, and cyclohexene/ozone systems. *Environmental Science and Technology* 35, 1164-1172.
- Phalen, R.F., 1998. Uncertainties relating to the health effects of particulate air pollution: The US EPA's particle standard. *Toxicology Letters*, 96-97: 263-267.
- Pilinis, C., Pandis, S. and Seinfeld, J.H., 1995. Sensitivity of direct climate forcing by atmospheric aerosols to aerosol size and composition, *Journal of Geophysical Research* 100, 18,739-18,754.
- Pope, C.A. III, Thun, M.J., Namboodiri, M.M., Dockery, D.W., Evans, J.S., Speizer, F.E. and Heath Jr., C.W., 1995. Particulate air pollution as a predictor of mortality in a prospective study of U.S. adults. *American Journal of Respiratory and Critical Care Medicine* 151, 669-674.
- Pope, C.A. III, 2000. Epidemiological basis for particulate air pollution health standards. *Aerosol Science and Technology*. 32, 4-14
- Pun, B.K., Griffin, R.J., Seigneur, C. and Seinfeld, J.H., 2002. Secondary organic aerosol 2. Thermodynamic model for gas/particle partitioning of molecular constituents. *Journal of Geophysical Research* 107(D17), 4333, doi:10.1029/2001JD000542.
- Pun, B.K., Wu, S.-Y. and Seigneur, C., 2002. Contribution of biogenic emissions to the formation of ozone and particulate matter in the eastern United States. *Environmental Science and Technology* 36, 3586-3596.



- Pun, B.K., Wu, S.Y., Seigneur, C., Seinfeld, J.H., Griffin, R.J. and Pandis, S.N., 2003. Uncertainties in modeling secondary organic aerosols: Three-dimensional modeling studies in Nashville/Western Tennessee. *Environmental Science and Technology* 37, 3647-3661.
- Rogge, W.F., Mazurek, M.A., Hildemann, L.M., Cass, G.R. and Simoneit, B.R.T., 1993. Quantification of urban organic aerosols at a molecular level: Identification, abundance and seasonal variation. *Atmospheric Environment*, 27, 1309-1330.
- Saathoff, H., Linke, C., Naumann, K.-H., Wagner, R., Weingartner, E. and Schurath, U., 2004. Temperature dependence of the yield of secondary organic aerosol from the ozonolysis of  $\alpha$ -pinene and limonene. EAC 2004, Budapest, Hungary, September 6-10, 2004, S151-S152.
- Saxena, P. and Hildemann, L.M., 1997. Water absorption by organics: A survey of laboratory evidence and evaluation of UNIFAC for estimating water activity. *Environmental Science and Technology*, 31, 3318-3324.
- Schauer, J.J., Rogge, W.F. and Hildemann, L.M., Mazurek, M.A. and Cass, G.R., 1996. Source apportionment of airborne particulate matter using organic compounds as tracers. *Atmospheric Environment*, 30(22), 3837-3855.
- Schauer, J.J., Kleeman, M.J., Cass, G.R. and Simoneit, B.R.T., 1999. Measurement of emissions from air pollution sources. 1. C1-C29 organic compounds from meat charbroiling. *Environmental Science Technology* 33, 1566-1577.
- Schauer, J.J., Kleeman, M.J., Cass, G.R. and Simoneit, B.R.T., 1999. Measurement of Emissions from Air Pollution Sources. 2. C1-C29 Organic Compounds from Medium Duty Diesel Trucks. *Environmental Science and Technology* 33, 1578-1587.
- Schell, B., Ackermann, I.J., Hass, H., Binkowski, F.S. and Ebel, A., 2001. Modeling the formation of secondary organic aerosol within a comprehensive air quality model system. *Journal of geophysical research* 106(D22), 28,275-28,293.
- Schere, K.L., 2002. The Models-3/CMAQ model: 2002 release – new features. 2002 Models-3 Users' Workshop, Research Triangle Park, N.C., October 21-23, 2002.
- Schwarzenbach, R.P., Gschwend, P.M. and Imboden, D.M., 1993. *Environmental Organic Chemistry*, John Wiley, New York.
- Seigneur C., 2001. Current status of air quality models for particulate matter. *Journal of the Air & Waste Management Association*, 51, 1508-1521.
- Seinfeld, J.H. and Pandis, S.N., 1998. *Atmospheric Chemistry and Physics: From Air Pollution to Climate Change*. John Wiley, New York

- Seinfeld, J.H., Erdakos, G.B., Asher, W.E. and Pankow, J.F., 2001. Modeling the formation of secondary organic aerosol. 2. The predicted effects of relative humidity on aerosol formation in the  $\alpha$ -pinene-,  $\beta$ -pinene-, sabinene-,  $\Delta^3$ -carene-, and cyclohexene-ozone systems. *Environmental Science and Technology* 35, 1806-1817.
- Seinfeld, J.H., Griffin, R.J., Pun, P.K., Seigneur, C. and Dabdub, D., 2002. Thermodynamics of organic atmospheric aerosols. Final Report to California Air Resources Board, Contract No. 98-314. (<ftp://ftp.arb.ca.gov/carbis/research/apr/past/98-314.pdf>)
- Seinfeld, J.H. and Pankow, J.F., 2003. Organic atmospheric particulate material. *Annual Review of Physical Chemistry* 54, 121-140.
- Sheehan, P.E. and Bowman, F.M., 2001. Estimated effects of temperature on secondary organic aerosol concentrations. *Environmental Science and Technology*, 35, 2129-2135.
- Sillman, S., 1999. The relation between ozone, NO<sub>x</sub> and hydrocarbons in urban and polluted rural environments. *Atmospheric Environment*, 33, 1821-1845.
- Smith, D.F., McIver, C.D. and Kleindienst, T.E., 1998. Primary product distribution from the reaction of hydroxyl radicals with toluene at ppb NO<sub>x</sub> mixing ratios. *Atmospheric Environment*, 30, 209-228.
- Smith, D.F., Kleindienst, T.E. and McIver, C.D., 1999. Primary product distributions from the reaction of OH with m-, p-xylene, 1,2,4- and 1,3,5-trimethylbenzene. *Journal of Atmospheric Chemistry* 34, 339-364.
- Stockwell, W.R., Middleton, P. and Chang, J.S., 1990. The second generation regional acid deposition model chemical mechanism for regional air quality modeling. *Journal of Geophysical Research* 95, 16,343-16,367.
- Stockwell, W.R., Kirchner, F., Kuhn, M. and Seefeld, S., 1997. A new mechanism for regional atmospheric chemistry modeling. *Journal of Geophysical Research* 102, 25,847-25,879.
- Strader, R., Lurmann, F. and Pandis, S.N., 1999. Evaluation of secondary organic aerosol formation in winter. *Atmospheric Environment* 33, 4849-4863.
- Takekawa, H., Minoura, H. and Yamazaki, S., 2003. Temperature dependence of secondary organic aerosol formation by photo-oxidation of hydrocarbons. *Atmospheric Environment* 37, 3413-3424.

- Tanner, R.L., Parkhurst, W.J., Valente, M.L. and Philips, W.D., 2004. Regional composition of PM<sub>2.5</sub> aerosols measured at urban, rural and "background" sites in the Tennessee valley. *Atmospheric Environment*, 38, 3143-3153
- Tobias, H.J., Docherty, K.S., Beving, D.E. and Ziemann, P.J., 2000. Effect of relative humidity on the chemical composition of secondary organic aerosol formed from reactions of 1-tetradecene and O<sub>3</sub>. *Environmental Science and Technology* 34, 2116-2125.
- Tobias, H.J. and Ziemann, P.J., 2000. Thermal desorption mass spectrometric analysis of organic aerosol formed from reactions of 1-tetradecene and O<sub>3</sub> in the presence of alcohols and carboxylic acids. *Environmental Science and Technology* 34, 2105-2115.
- Turpin, B.J. and Huntzicker, J.J., 1995. Identification of secondary organic aerosol episodes and quantitation of primary and secondary organic aerosol concentrations during SCAQS. *Atmospheric Environment* 29, 3527-3544.
- Turpin, B.J., Saxena, P. and Andrews, E., 2000. Measuring and simulating particulate organics in the atmosphere: problems and prospects. *Atmospheric Environment* 34, 2983-3013.
- Virkkula, A., Dingenen, R.V., Raes, F. and Hjorth, J., 1999. Hygroscopic properties of aerosol formed by oxidation of limonene,  $\alpha$ -pinene, and  $\beta$ -pinene. *Journal of Geophysical Research* 104(D3), 3569-3579.
- Xia, A.G., Michelangeli, D.V. and Makar, P., 2004, Modeling the secondary organic aerosol within a 3-dimensional air quality model. AAAR 2004 Annual Conference, Atlanta, Georgia.
- Yamasaki H., Kuwata K. and Miyamoto H., 1982. Effects of temperature on aspects of airborne polycyclic aromatic hydrocarbons. *Environmental Science and Technology* 16, 189-194.
- Yu, J., Cocker III, D.R., Griffin, R.J., Flagan R.C. and Seinfeld, J.H., 1999a. Gas-phase oxidation of monoterpenes: gaseous and particulate products. *Journal of Atmospheric Chemistry* 34, 207-258.
- Yu, J.-Z., Griffin, R.J., Cocker III, D.R., Flagan, R.C. and Seinfeld, J.H., 1999b. Observation of gaseous and particulate products of monoterpenes in forest atmosphere. *Geophysical Research Letter* 26 (8), 1145-1148.
- Yu, S., Dennis, R., Eder, B., Lewis, C., Gipson, G., Binkowski, F., Bhawe, P., Pleim, J., Schere, K., Klouda, G. and Pouliot, G., 2003. Simulation of primary and secondary (biogenic and anthropogenic) organic aerosols over the United States

by US EPA Models-3/ CMAQ: evaluation and regional analysis. 2003 Models-3 Users' Workshop, Research Triangle Park, N.C., October 27-29, 2003.

- Zhang, S.H., Shaw, M., Seinfeld, J.H. and Flagan, R.C., 1992. Photochemical aerosol formation from  $\alpha$ -pinene and  $\beta$ -pinene. *Journal of Geophysical Research*, 97, 20,717-20,729.
- Zhang, Y., Pun, B., Vijayaraghavan, K., Wu, S.-Y., Seigneur, C., Pandis, S., Jacobson, M., Nenes, A. and Seinfeld, J.H., 2004. Development and application of the Model of Aerosol Dynamics, Reaction, Ionization and Dissolution (MADRID). *Journal of Geophysical Research*, 109, D01202, doi:10.1029/2003JD003501.
- Zheng, M., Cass, G., Schauer, J.J. and Edgerton, E., 2002. Source apportionment of PM<sub>2.5</sub> in the southeastern United States using solvent-extractable organic compounds as tracers. *Environmental Science and Technology* 36, 2361-2371.